Universidade De São Paulo
Faculdade De Medicina De Ribeirão Preto
Departamento De Genética

Thiago Vidotto

Caracterização do Genoma e da Resposta Imune no Microambiente Tumoral de Neoplasias *PTEN*-Deficientes

Characterization of the Genome and Immune Response in the Tumor Microenvironment of *PTEN*-Deficient Cancers

Ribeirão Preto - SP
2019

Thiago Vidotto

Caracterização do Genoma e da Resposta Imune no Microambiente Tumoral de Neoplasias *PTEN*-Deficientes

Characterization of the Genome and Immune Response in the Tumor Microenvironment of *PTEN*-Deficient Cancers

Tese apresentada à Faculdade de Medicina de Ribeirão Preto da Universidade de São Paulo, como requisito para obtenção do título de Doutora em Ciências, área de concentração: Genética

Orientador: Prof. Dr. Jeremy A. Squire

Ribeirão Preto - SP

2019

FICHA CATALOGRÁFICA

Vidotto, Thiago

Caracterização do genoma e da resposta imune no microambiente tumoral de neoplasias *PTEN*-deficientes. Ribeirão Preto, São Paulo, 2019.

181p.: il.; 30cm.

Tese de Doutorado apresentada à Faculdade de Medicina de Ribeirão Preto, Universidade de São Paulo. Área de concentração: Genética.

Orientador: Squire, Jeremy A.

1. Resposta imune; 2. PTEN; 3. PanCancer; 4. Instabilidade genômica; 5. Aneuploidia. 6. Bioinformática.

Vidotto, Thiago

Characterization of the Genome and immune response in the tumor microenvironment of *PTEN*-deficient cancers. Ribeirão Preto, São Paulo, 2019.

181p.: il.; 30cm.

Ph.D. thesis presented to the Medical School of Ribeirão Preto, University of São Paulo. Area of concentration: Genetics.

Supervisor: Squire, Jeremy A.

1. Immune response; 2. PTEN; 3. PanCancer; 4. Genomic instability; 5. Aneuploidy. 6. Bioinformatics.

FOLHA DE APROVAÇÃO

Thiago Vidotto

Caracterização do genoma e da resposta imune no microambiente tumoral de neoplasias *PTEN*-deficientes

Tese apresentada à Faculdade de Medicina de Ribeirão Preto da Universidade de São Paulo, como requisito para obtenção do título de Doutora em Ciências, área de concentração: Genética

Orientador: Prof. Dr. Jeremy A. Squire

Aprovada em: _____|_____|_____

BANCA EXAMINADORA

Prof. Dr _____

Instituição:_____ Assinatura: _____

Prof. Dr _____

Instituição:_____ Assinatura: _____

Prof. Dr _____

Instituição:_____ Assinatura: _____

Prof. Dr _____

Instituição:_____ Assinatura: _____

Prof. Dr _____

Instituição:_____ Assinatura: _____

Para José Carlos Vidotto e Cleusa Truiz Vidotto.

Agradecimentos

I would like to thank my supervisor **Dr. Jeremy A. Squire** for providing me such an astonishing opportunity for being his PhD student for the past few years. Dr. Jeremy is extremely sincere, practical and smart, and his qualifications as a supervisor contributed to an exceptional guidance during my PhD. In the same manner, Dr. Jeremy always encouraged my ideas and was very helpful when I needed personal guidance. Moreover, my aim during the past few years was not only to conduct my research but also understand a bit more about the English language, culture, and everything the experienced life of Dr. Jeremy could teach me. Thank you, Professor, for being such an inspiration to me.

Dr. Madhuri Koti is my second PhD supervisor. By virtue of her inspiration, this study now touches both immunology and genetic fields. During my 8-months stay in Kingston, Dr. Madhuri was extraordinary kind and open to discuss the several - and sometimes too many - questions I had. During my internship with her, I was also able to learn a bit more about her culture and how similar Brazilian and Indians can be. In addition, she gave me several opportunities for bioinformatics training, which was crucial for the development of this thesis and other future partnerships. Dr. Madhuri, thank you for being so kind and helpful during the three years of my PhD.

Aos grandes colaboradores e mentes inspiradoras por trás de grandes aprendizados: **Dr. Fabiano Saggioro**, por ter trabalhado duro comigo durante sábados, domingos e feriados e por partilhar comigo a sua visão de mundo descontraída e humilde. Dr. Fabiano também foi peça chave na seleção e análise dos pacientes desse estudo; ao **Dr. Rodolfo B. Reis**, por ter contribuído para a obtenção dos casos desse estudo e por ser extremamente motivado em mudar a realidade da ciência e medicina no Brasil; ao **Dr. Daniel Tiezzi,** por prontamente responder meus e-mails inadequados durante fins de semana e feriados e por sempre me ajudar em alguma questão de bioinformática que eu tinha. Dr. Daniel me inspirou a sempre aprender cada vez mais. Tê-lo como colaborador nesse estudo é um orgulho! Agradeço também a **Dra. Lúcia Martelli**, que fez parte da minha rotina de aprendizado e que sempre transmitiu extrema sabedoria para lidar com problemas que, para mim, pareciam complicados demais. A agradeço, além de tudo, por sempre dar sua opinião prática sobre como eu deveria apresentar meus resultados para uma banca.

To **Dr. Tamara Jamaspishvili** for helping me with TMA and pathological analyses and for also being an inspiring and helpful person during my entire stay in Canada. To **Dr. Nicki Peterson**, who made my visit at Dr. Madhuri's lab more pleasant and funny. Dr. Nicki helped me with important issues I had in Canada but, most importantly, she was there during my long periods of browsing Amazon's website. Thank you for everything, Nicki!

I would also like to thank **Dr. Charles Graham** for being an amazingly helpful person to me during my stay in Canada. Dr. Charles and I share many life principles, and I am extremely grateful for having him as a collaborator in this research. Also, special thanks to **Dr. Robert Siemens** and **Dr. David Berman** for improving my view on clinical research and English writing. Lastly, **Lee Boudreau** and **Shakeel Virk**, for helping me with immunohistochemistry experiments, analysis and for being helpful during my entire stay in Canada. Last but not least, to **Catherine Brewster**, for showing me the essence of a Canadian heart on being extremely helpful and kind.

Às grandes amigas que terei pela vida toda, **Lívia Verzola**, **Victoria Cortez**, **Dra. Alexandra Galvão, Dra. Juliana Dourado, Juliana Josahkian, Dra. Flávia Gaona** e **Dra. Clarissa G. Picanço de Albuquerque**: muito obrigado por partilharem tantos momentos especiais comigo. Cada uma de vocês me ensinou muito sobre as mais variadas formas de se ver o mundo. Cada uma me inspira de um jeito diferente, e eu me sinto extremamente grato por tê-las comigo para o resto da minha vida.

À **Dra. Tathiane Malta**, pois, sem você, os caminhos poderiam não existir. Ou, se existissem, seriam um pouco mais tortuosos. Você é um exemplo de humildade, bom humor e honestidade. Foi um prazer enorme poder contar com você em tantas dúvidas e angústias que tive.

Agradeço também minha amiga **Maritza Salas**, que se tornou uma grande companheira nesses últimos anos, que colaborou para a realização dessa tese e que esteve sempre aberta para ajudar em tudo que eu precisava; o amigo **Dr. Tiago Silva**, por ter contribuído com essa pesquisa sempre com bom humor e com interesse em ajudar. Agradeço também a minha nova amiga **Dra. Camila M. Melo** por ter contribuído com a formulação, escrita e revisão dessa tese.

Ao amigo **Dr. Vinícius Kannen** por sempre estar aberto a discussão de manuscritos e ideias científicas e por revisar essa tese; **Dr. Edson Z. Martinez** pelo imenso aprendizado em bioestatística e programação em R; **Bia**, **Dr. Luciano Neder** e **Dr. Rui Reis** pela ajuda com a construção dos TMAs no Hospital de Amor; e, em especial, agradeço a **Deise Chesca** por partilhar tantos conhecimentos comigo, por ter tanto bom humor e por sempre estar disposta a fazer o possível para atingir um nível altíssimo de excelência em tudo que faz.

Aos funcionários da Genética e Bloco C, **Dona Maria, Gi, Regis, Marli, Susie, Paulo** e **Luís** pela ajuda em todas as solicitações que fiz ao longo desses anos.

À agencia de fomento **FAPESP**, por confiar em minha pesquisa e por ter me dado a oportunidade de vivenciar outras culturas. Obrigado pela seriedade com que vocês lidam com a pesquisa no Brasil.

Aos amigos **Pedro Lorenzo, Gabriel Pagotto e Hikaru Fukae** por sempre me fazerem rir sobre as coisas da vida e também por me atentarem sobre alguns assuntos pertinentes sobre o mundo.

À amiga **Dra. Sabrina** por ter me ajudado nos primeiros passos da minha bolsa FAPESP.

Aos amigos **Rafael Cazuza, Richard Spinelli, Malina Vaz, Guta da Fonte, Ricardo, Paula, Vivien Rissato** e **Marcela Marega** por serem grandes amigos e por partilharem suas experiências sobre a pós-graduação e sobre sua visão de mundo.

To my great friend and discovery from 2017, **Sean O. Matthew**. Sean made possible what I could never imagine happening: meeting and making a new best friend in a different country. Sean contributed to an amazingly smooth stay in Canada, filled with fun, amazing conversations, and exceptional food. Sean was there when I needed most and was able to teach me values I had lost during my lifetime. Thank you, my friend, for having such an inspiring, beautiful heart and the patience to hear me rant about politics, science, life, and business.

Aos amigos ribeirão-pretanos **Ge, Taís, Janine, Carol, Gui, Dra. Carla, Joina, Paula, Vinícius** e **Dra. Carol** por todos os momentos de descontração regados a vinhos, queijos e bons jantares que compartilhamos nos últimos anos.

Aos meus grandes amigos de coração **Karen Gomes, Rafaela Mie**, **Lucas Hirata** e **Josiane Scarpassa** por terem sempre ouvido minhas reclamações e por me fazerem ter cada vez mais vontade de superar minhas falhas. Vocês são meus irmãos!

Às minhas irmãs **Dr. Ana Paula Vidotto** e **Tatiana Vidotto**, por sempre acreditarem nos meus sonhos. Vocês são uma inspiração para mim!

Aos meus pais **Cleusa Truiz Vidotto** e **José Carlos Vidotto**, por acreditarem que a educação pode mover montanhas e por sempre me estimularem a ser cada vez melhor no que faço. Vocês são a minha fonte de vida para crescer e me tornar um grande homem. Obrigado pelos ensinamentos e por confiarem em mim. Eu vou mostrar ao mundo que tudo que vocês me ensinaram valeu a pena!

Ao meu amigo felino, companheiro de análise de dados, e atualmente residente do céu dos bichos, **Mob**. Nunca pensei que eu desenvolveria amor por um animal de estimação. Pois bem, Mob veio e quebrou mais uma certeza que eu tinha. Não só por ser um companheiro, ele me ensinou a ver tudo, absolutamente tudo, de forma diferente. Tenho certeza que seu sofrimento no mundo foi infinitamente menor que o amor que eu pude te dar. Descanse em paz, grande amigo.

Ao meu segundo e não menos importante amigo egípcio, **Bóris**, por literalmente acompanhar todos os processos desse doutorado enquanto se lambia e soltava pelos no meu colo. É inacreditável pensar que a paz e calma que tive nos últimos anos se devem em grande parte à sua existência. Sua beleza me faz feliz, meu amiguinho!

Ao meu grande parceiro de vida, **Marcelo Estevam Ferreira**. Marcelo é a representação física e mental do meu oposto. Enquanto eu enxergo branco, ele vê preto – e isso faz com que, todos os dias, eu pense: "Será que fui claro? Será que estou dando o meu melhor? Será que não há outra forma de fazer isso?". É como viver com um treinador dentro da cabeça, me obrigando a superar algo a cada dia que passa. Marcelo me deu forças para escrever o que eu considerei a melhor tese de doutorado possível. E, muito provavelmente, ele nem sabe disso. Obrigado por me inspirar a lutar para ser cada dia melhor. Obrigado por me ouvir, aconselhar e partilhar dos melhores momentos da minha vida. O futuro é nosso!

Por último, agradeço a **Deus**. Alguém que redescobri depois de muitos anos, durante um turbilhão de pensamentos e situações inusitadas. Deus me deu forças ao me acalmar e mostrar que o caminho não era assim tão complicado quanto eu imaginava. Nesse período, percebi que a admiração que tenho pela natureza e pela forma com que ela se desenvolve é similar à minha admiração por Deus. É como se, de fato, as leis do universo não tivessem sido criadas, mas que fossem parte do que chamo de Deus. Talvez essa seja a razão d'Ele estar em todos os lugares.

À todos, muito obrigado.
Nada disso seria possível sem a colaboração de cada um de vocês.

Down to their innate molecular core, cancer cells are hyperactive, survival-endowed, scrappy, fecund, inventive copies of ourselves.

Siddhartha Mukherjee

Resumo

VIDOTTO, T. **Caracterização do genoma e da resposta imune no microambiente tumoral de neoplasias *PTEN*-deficientes.** 2019, 181p. Tese de Doutorado. Faculdade de Medicina de Ribeirão Preto. Universidade de São Paulo.

Alterações no genoma de células tumorais são eventos comuns durante a carcinogênese. Tais aberrações genômicas – como mutações e variações estruturais - são diretamente relacionadas a detecção e morte de células neoplásicas pelo sistema imune. Além da contribuição da perda de função de genes supressores tumorais (GSTs) no desenvolvimento neoplásico, GSTs também influenciam a resposta imune no câncer. Por exemplo, o GST *PTEN* afeta diretamente a via interferon através da desfosforilação do fator regulador de interferon 3 (IRF3). No entanto, se mantém inconclusivo se a inativação de *PTEN* diretamente influencia a resposta imune através de IRF3 ou por provocar altos níveis de instabilidade genômica. Para responder essa questão, conduzimos uma análise PanCancer de 33 tipos tumorais da coorte The Cancer Genome Atlas para identificar se existem associações entre a inativação do gene *PTEN* e alterações genômicas específicas que podem suprimir ou ativar a resposta imune antitumoral. O *status* de inativação de *PTEN* foi determinado a partir de dados de variação no número de cópias e presença de mutações de ponto. Nesse estudo, investigamos o efeito da inativação de *PTEN* nas alterações genômicas de tumores e na abundância de 22 células do sistema imune derivadas do algoritmo CIBERSORT. Observamos que a inativação de *PTEN* foi significantemente associada com níveis elevados de aneuploidia, mutações, e heterogeneidade intratumoral. Além disso, nossos achados mostraram que a inativação de *PTEN* é altamente específica para cada tipo tumoral. Da mesma maneira, observamos que pacientes com tumores *PTEN*-inativos podem apresentar variações na resposta a imunoterapia. Tal observação deriva da correlação significativa entre a inativação de *PTEN* e a expressão dos alvos terapêuticos proteína programada 1 da morte celular (*PD1*), seu ligante (*PDL1*), e indoleamina 2,3 dioxigenase (*IDO1*). Na análise PanCancer, a inativação de *PTEN* também foi significativamente associada à composição de células do sistema imune no microambiente tumoral, incluindo células T regulatórias (Treg) e células CD8+. A partir desses achados, conduzimos uma análise aprofundada de tumores de próstata primários e metastáticos com a perda de PTEN. Através de uma análise *in* silico, nós observamos que tumores primários e metastáticos apresentam maiores densidades de Treg quando há perda da proteína PTEN. Nós também observamos que, dependendo do local de metástase prostática, a deficiência de PTEN é associada a um perfil de células imunes supressivas no microambiente tumoral. A partir da análise de uma coorte brasileira composta por 94 tumores primários de próstata, observamos que a perda de PTEN se associa a uma maior densidade de Tregs e uma maior expressão da proteína imunossupressora IDO1. Além disso, tumores PTEN-deficientes com altas densidades de Tregs apresentaram o pior prognóstico entre pacientes. Coletivamente, nós demonstramos que a inativação de *PTEN* é associada a um estado imunossuprimido no microambiente tumoral. Ademais, a perda de *PTEN* possivelmente se associa a resposta imune antitumoral através da combinação de duas diferentes vias – uma dependente de IRF3 e outra relacionada ao efeito no genoma de células cancerosas. Ensaios funcionais são necessários para validar os achados desse estudo; porém, sugerimos que a avaliação do *status* de inativação de *PTEN* pode ter alto potencial para discernir pacientes que responderão à imunoterapia.

Palavras-chave: PTEN. Resposta imune. Gene supressor tumoral. Checkpoint imune. Instabilidade genômica. Aneuploidia. PanCancer.

Abstract

VIDOTTO, T. **Characterization of the genome and immune response in the tumor microenvironment of *PTEN*-deficient cancers.** 2019, 181p. Ph.D. Thesis. Medicine School of Ribeirão Preto, University of São Paulo.

Cancer-cell genomes undergo several abnormalities during carcinogenesis. Indeed, many of the tumor-specific genomic changes, such as mutations and chromosomal aberrations, are related to how the host immune system responds to detect and kill tumor cells. In addition to these general effects, loss of function of specific tumor suppressor genes (TSG) contributes to tumor development and progression and at the same time also regulates several facets of the immune response in cancer. For instance, the TSG phosphatase and tensin homolog (*PTEN*) was shown to directly regulate the anti-viral interferon response by licensing the interferon regulatory factor 3 (IRF3). However, it is still unclear whether *PTEN* directly influences the immune response through the interferon network or by provoking higher levels of genomic instability. To address this question, we conducted a PanCancer analysis of 33 tumor types from The Cancer Genome Atlas to determine whether there were associations between *PTEN* inactivation and specific genomic features that are linked to immunosuppressive states in cancer. PTEN inactivation status was determined by combining copy number and point mutation data. Then, we performed a parallel analysis of genomic instability and immune-cell abundances derived from the CIBERSORT algorithm comparing PTEN deficient to intact tumors. We found that *PTEN* inactivation was strongly associated with enhanced levels of aneuploidy, mutation load, immunogenic mutations, and tumor heterogeneity. Furthermore, we found that the outcome of *PTEN* inactivation status was highly specific to each tumor type and the induced changes appeared to lead to variation in immune responses in different cancers. Response to current immunotherapeutic approaches depends on the expression of targeted immune checkpoints, and we found that tumors with *PTEN* deficiency had altered expression of programmed death protein 1 (*PD1*), its ligand (*PDL1*), and the immunosuppressive protein indoleamine 2,3-dioxygenase (*IDO1*). We also found that *PTEN* inactivation led to a distinct immune-cell composition in the tumor microenvironment, including regulatory T cells and CD8+ T cells. Lastly, we performed an in-depth analysis of the immune-cell content of prostate tumors that harbored *PTEN* protein loss. Through an *in silico* analysis of 622 tumors, we found that both primary and metastatic lesions had higher densities of regulatory T cells when PTEN was lost. Then, the analysis of 94 primary prostate tumors from Brazil demonstrated that PTEN protein loss was significantly associated with high Treg density and IDO1 protein expression. Moreover, PTEN-null tumors with high Treg density exhibited the worse outcome among patients. We also found that, depending on the prostate cancer metastatic site, PTEN deficiency was linked to variation in the immunosuppressive immune cell landscape. Collectively, we show that *PTEN* inactivation associates with the anti-tumor immune response likely through direct avenues (via licensing of IRF3) and indirectly by influencing the genome of cancer cells. Functional studies are required to validate our *in silico* findings; however, we speculate that determining *PTEN* inactivation status may allow clinicians to distinguish patients that are more likely to respond to current immunotherapies.

Keywords: PTEN. Immune response. Tumor suppressor genes. Immune checkpoint. Genomic instability. Aneuploidy. PanCancer.

List of figures

recurrence of prostate cancer. **B** – PDL1 was not associated with biochemical recurrence. **C** – PTEN-deficient tumors with high IDO1 protein expression are more likely to have earlier biochemical recurrence. **D** – PTEN deficiency tumors with high PDL1 protein expression were not significantly associated with biochemical recurrence. FoxP3+ Treg cell density and IDO1 and PDL1 protein. 131

List of tables

List of abbreviations

The Cancer Genome Atlas malignancy types

ACC – Adrenocortical carcinoma

BLCA – Bla dder Urothelial Carcinoma

BRCA – Breast invasive carcinoma

CESC – Cervical squamous cell carcinoma and endocervical adenocarcinoma

CHOL – Cholangiocarcinoma

COAD – Colon adenocarcinoma

DLBC – Lymphoid Neoplasm Diffuse Large B-cell Lymphoma

ESCA – Esophageal carcinoma

GBM – Glioblastoma multiforme

HNSC – Head and Neck squamous cell carcinoma

KICH – Kidney Chromophobe

KIRC – Kidney renal clear cell carcinoma

KIRP – Kidney renal papillary cell carcinoma

LAML – Acute Myeloid Leukemia

LGG – Brain Lower Grade Glioma

LIHC – Liver hepatocellular carcinoma

LUAD – Lung adenocarcinoma

LUSC – Lung squamous cell carcinoma

MESO – Mesothelioma

OV – Ovarian serous cystadenocarcinoma

PAAD – Pancreatic adenocarcinoma

PCPG – Pheochromocytoma and Paraganglioma

PRAD – Prostate adenocarcinoma

READ – Rectum adenocarcinoma

SARC – Sarcoma

SKCM – Skin Cutaneous Melanoma

STAD – Stomach adenocarcinoma

TGCT – Testicular Germ Cell Tumors

THCA – Thyroid carcinoma

THYM – Thymoma

UCEC – Uterine Corpus Endometrial Carcinoma

UCS – Uterine Carcinosarcoma

UVM – Uveal Melanoma

Genes and Proteins

AKT – Protein kinase B

CHD1 – Chromodomain-helicase-DNA-binding protein 1

CKH1 – Checkpoint kinase 1

CTLA4 – Cytotoxic T-lymphocyte associated protein 4

CXCL12 – CXC motif chemokine ligand 12

CXCR4 – CXC chemokine receptor 4

IDO1 – Indoleamine-pyrrole 2,3-dioxygenase

IL-1RA – Interleukin-1 receptor antagonist

IRF3 – Interferon regulatory factor 3

KRAS – Kirsten rat sarcoma viral oncogene homolog

LKB1 – Serine/Threonine Kinase 11

MAPK – Mitogen-activated protein kinase

MCM2 – Minichromosome maintenance complex component 2

mTOR – Mammalian target of rapamycin

MYC – BHLH Transcription Factor

NF-kB – Factor nuclear kappa B

NF-Kb – Nuclear factor kappa B

PD1 – Programmed cell death 1 protein

PDL1– Programmed cell death ligand 1 protein

PI3K – Phosphoinositide 3-kinase

PIP2 – Phosphoinositol-4,5-biphosphate

PIP3 – Phosphoinositol-3,4,5-trisphosphate

PML – Promyelocytic leukemia protein

PTEN – Phosphatase and tensin homolog

PTEN-L – Long-PTEN isoform

TNF – Tumor necrosis factor

TP53 – Transformation-related protein 53

UPS – Ubiquitin-proteasome system

General

aCGH – Array comparative genomic hibridization

CI – Confidence interval

DBS – Double strand breaks

DC – Dendritic cell

DDR – DNA damage repair

DNA – Desoxiribonucleic acid

EMT – Epithelial-to-mesenchymal transition

H&E – Hemaetoxilyn and eosin

HCRP – Clinics Hospital of Ribeirão Preto

HR – Hazard ratio

HRD – Homologous repair defect

IFN – Interferon

IFNI – Type I interferon response

LCNC – Large-cell neuroendocrine cancer

LM22 – CIBERSORT leukocyte signature matrix 22

LSCC – lung squamous cell carcinoma

M0 – M0 macrophage

M1 – M1 macrophage

M2 – M2 macrophage

mCRPC – Metastatic castrate resistant prostate cancer

MDSC – Myeloid-derived suppressor cells

MSKCC – Memorial Sloan Kettering Cancer Center

NK – Natural killer cell

OG – Oncogene

PSA – Prostate-specific antigen

RNAseq – RNA sequencing

SCC – Squamous cell carcinoma

SCLC – Small-cell lung cancer

SCNA – Somatic copy number alteration

SNV – Single nucleotide variation

T – Pathological T staging

TAM – Tumor infiltrating macrophages

TCGA – The Cancer Genome Atlas

TMA – Tissue microarray

TME – Tumor microenvironment

Treg – Regulatory T cell

TSG – Tumor suppressor gene

Software, R packages, and algorithms

ABSOLUTE v1.0.6 – Algorithm employed to determine ploidy, tumor heterogeneity, and tumor purity.

CIBERSORT – *In silico* flow-cytometry analysis method.

ClueGO – Cytoscape-dependent pathway enrichment visualization.

ComplexHeatmap – R package for heatmap plotting.

Corrplot – R package for correlation analysis and plots.

Cytoscape - Software for visualizing complex networks.

DESeq2 – R package for defining mean-variance dependence in raw RNAseq count data plus test for differential expression analysis through a negative binomial distribution.

Ggplot2 – R package for data visualization.

Ggpubr – R package for boxplot plotting.

GSEA – Gene Set Enrichment Analysis is a software used for pathway analysis of differentially expressed genes.

Maftools – R package for Mutation Annotation Format (MAF) Analysis and visualization

Survival 2.43-3 – R package for Cox regression and log-rank analyses; Kaplan-Meier plots.

Survminer – R package for Kaplan Meier plotting using ggplot2.

Summary

1. INTRODUCTION

During tumorigenesis, normal cells undergo genomic changes that grant them abnormal proliferation rates[1]. As a consequence of increased mitosis ratios, chromosomal aberrations – such as losses, amplifications, and translocations of chromosome arms or regions – are more likely to occur[2,3]. The loss of a tumor suppressor gene that in normal conditions prevent cells from dividing continuously, drives a series of events that favors cell survival and multiplication[4].

Tumor suppressors not only determine cell fate, but increasing evidence has shown that these genes can shape the crosstalk between cancer cells and the surrounding environment – referred to as tumor microenvironment[5]. Solid tumors are composed of cancer cells and normal cells, being normal cells primarily those derived from the immune system and the extracellular matrix[6]. Several reports have evidenced that the inactivation of a tumor suppressor gene may influence how cancer cells are recognized as abnormal and killed by specific cytolytic immune cells[7]. These events are triggered as a result of the highly diverse and intricate manner by which tumor suppressor act in regulating distinct cell signaling pathways[8].

The phosphatase and tensin homolog (*PTEN*) gene undergoes somatic inactivation events in several malignancies and has shown to regulate a plethora of critical networks, including those related to the adaptive immune response[9,10]. Recently published studies allow us to speculate that there is fine-tuning of cancer-intrinsic expression – including *PTEN* inactivation – that leads to regulation of neoantigens development and immune checkpoint activities[11,12]. However, little is known on how PTEN inactivation in tumor cells shape the tumor microenvironment. Therefore, this thesis focused on how PTEN loss of function determines tumor-cell fate and disease progression by influencing the genome of cancer cells. Since neoplastic cells undergo several genomic abnormalities, we also aimed to verify how PTEN inactivation and the associated genomic instability drives the immune response in cancer.

We first performed a literature review to summarize the emerging roles of *PTEN* in shaping tumor-intrinsic genomic events, and how such mechanisms allow an in-depth understanding of the anti-tumor immune response in cancers. Further, we conducted a PanCancer study aiming to determine if *PTEN* inactivation is crucial for the anti-tumor immune response in 33 types of tumors (**Chapter 1**). Lastly, based on our findings from the PanCancer analysis, we verified the impacts of PTEN protein loss by immunohistochemistry in the most relevant immune cells within the TME of prostate tumors (**Chapter 2**).

2. LITERATURE REVIEW

2.1 Background

In the past few years, immunotherapeutic approaches for cancer treatment have shown significant favorable long-lasting outcomes in a subset of patients[13]. Immune checkpoint blockade is the primary immunotherapy approach currently available. The principle of the treatment consists of blocking the suppressive interactions between cancer and the patient's immune system. The blocking negatively regulates immune checkpoints and usually restores the capacity of the exhausted immune system to start killing the tumor cells again. However, the majority of individuals treated with immune checkpoint blockade therapies exhibit relapse as consequence of the development of resistance to treatment[14]. Most mechanisms of tolerance during treatment rely on changes in the tumor microenvironment (TME) (tumor cell extrinsic) and in cancer cells (tumor cell intrinsic)[15]. However, the lack of response to therapy and the protection of tumor cells from the immune attack may also be derived from properties of tumor or immune cells[16,17].

Immune and tumor cells often communicate through cell surface receptor binding and paracrine cell signaling mediated by chemokines and interleukins[18]. The inactivation of T-cell by cell-to-cell contact with regulatory T cells (Treg) and other immunosuppressive cells is one of the primary mechanisms by which cancers evade the anti-tumor immune cell response[19]. Immunogenicity, defined as the ability in provoking adaptive immune responses is influenced by the crosstalk between tumor and immune cells in the TME[20]. For instance, the presence of high mutation load in tumor cells is often associated with increased immunogenicity, higher immune-cell abundance in the TME, improved patient survival, and a better response to immune checkpoint blockade therapies[21,22]. The presence of tumor mutations (neoantigens) in one of the cancer-intrinsic changes that shapes the interplay between cancers and immune-cells[16,23].

Higher levels of expressed neoantigens trigger the immune response and favor immune-cell recruitment in the TME[21]. For instance, tumors with highly unstable genomes (*e.g.*, melanoma, non-small cell lung cancer, and colorectal cancer) present increased number of neoantigens, which can be expressed and thus promote anti-tumor immune-cell response[24]. CD8+ T-cells and antigen presenting cells constitute the first line host immune response against tumor cells. Conversely, tumor cells may exhibit abnormal antigen presentation, which can be derived from chromosomal deletions of critical genes that regulate epitope processing and presentation[25,26]. The reduced expression or genomic copy number loss of T-cell-recognized neoantigens may result in a reduced anti-tumor immune response in the TME[27]. In addition,

oncogenic alterations in tumor cells may lead to genetic T-cell exclusion through the expression of inactivating transmembrane ligands in addition to dysregulated immune pathways[8,16].

The presence of activating mutations in oncogenes (e.g. *MYC, LKB1, KRAS*) and loss of function of tumor suppressor genes (e.g. *TP53, PTEN*) have been described as critical for cancer development[28]. The inactivating mutation or deletion of a tumor suppressor gene can facilitate tumor development and progression by conferring a continuous cell proliferation state to cancer cells[29,30]. However, emerging evidence has demonstrated that tumor suppressor genes may influence the immune response as part of their role in regulating tumor-cell intracellular responses[10,11]. For instance, the inactivation of the p53 tumor suppressor is associated with antiviral defense, cytokine production, immune checkpoint regulation, and induction of type I interferon response[31]. In addition, it has been shown that these tumor-intrinsic changes are also related to resistance to immunotherapy in several different types of cancer[17]. In summary, tumor-intrinsic genomic changes, such as somatic point mutations and copy number alterations, may profoundly alter the interactions between immune and cancer cells.

The somatic inactivation of the tumor suppressor gene *PTEN* is associated with earlier cancer development, as seen in pre-neoplastic prostate lesions[32–34], and has also been widely linked to aggressive cancer phenotypes[35]. An overview of the recently published PanCancer data from The Cancer Genome Atlas shows that *PTEN* hemi- and homozygous deletions are high across tumor types. In prostate cancer, melanoma, breast, ovarian, and lung adenocarcinoma, *PTEN* deficiency is observed in 32% (159/490), 63% (227/359), 30% (318/1038), 41% (168/401), and 27% (142/512), respectively (manuscript in preparation). The techniques for detecting *PTEN* deficiency are highly reproducible, which increases its potential use as a biomarker for disease stratification[36] and, currently, for being a potential biomarker for immunotherapy response. In this review, we discuss the most recent findings on the roles of PTEN in the immune response across cancers.

2.2 PTEN functions in the cytoplasm and nucleus

PTEN is one of the most common somatically mutated and deleted gene in cancer[37]. *PTEN* is located on 10q23.31 region and consists of nine exons that encode 403 amino acids[38]. PTEN protein acts as a dual-specificity phosphatase and a direct antagonist of phosphatidylinositide 3-kinases (PI3K) signaling by reverting the second messenger phosphoinositol-3,4,5-trisphosphate (PIP3) into PIP2, which inhibits downstream signaling pathways[39]. In the cytoplasm, the loss or inactivating point mutation of the *PTEN* gene triggers the activation of the PI3K signaling pathway[39] and consequently the downstream activation of

the AKT protein. Phospho-AKT then activates different substrates, such as the mammalian target of rapamycin (mTOR)[40], which is a serine/threonine kinase that regulates cell growth, survival, and proliferation. More recently, it was shown that the simultaneous activation of the mitogen-activated protein kinase (MAPK) and PI3K/AKT pathways occurs in co-deleted *PTEN* and promyelocytic leukemia protein (*PML*) human metastatic prostate cancer[41].

In addition to its cytoplasmic functions in regulating cell growth and proliferation, PTEN regulates genome integrity and DNA replication stability in the nucleus[42]. *Pten*-null mice show increased genomic and chromosomal instability, leading to extensive centromere breakage, chromosomal translocations, and spontaneous DNA double-strand breaks through an AKT/PI3K/mTOR independent manner. Moreover, PTEN189 mutation (lacking C-terminus region) leads to significant increase in chromosomal aberrations, with transfected *PTEN189* cells showing a high levels of aneuploidy. This mechanism of centromere stability is directly regulated by PTEN interactions with the centromere protein, together with Rad51 regulation of double-strand break repair machinery[43] through homologous recombination[44].

Recently, PTEN was described to modulate the DNA-binding factor chromodomain-helicase-DNA-binding protein 1 (CHD1) degradation by suppressing cell proliferation, survival and tumorigenic potential in *PTEN*-deficient prostate and breast cancers. Furthermore, the authors demonstrated that PTEN deficiency stabilizes CHD1, which promotes the activation of the TNF-NFKB network[45]. In addition to this function, PTEN regulates the minichromosome maintenance complex component 2 (MCM2), which is critical for DNA replication. Consequently, tumors harboring *PTEN* loss undergo unrestrained fork progression, suggesting that this protein is essential for preventing chromosomal aberrations in cells under replicative stress. Indeed, the replication stress mediated by DNA damage repair signaling is enhanced in PTEN-deficient prostate cancer[46].

PTEN has also been linked to cell autophagy, which refers to the intracellular degradation of molecules or organelles by lysosomes[17]. In breast cell lines and mice treated with trastuzumab, PTEN loss was associated with decreased expression of the LC3I/II, LAMP, p62, and cathepsin B autophagic proteins[47]. In pancreatic cancer murine models, the presence of PTEN hemizygous deletions led to loss of autophagy and caused earlier pancreatic-cancer specific-death when compared to autophagy-competent animals[48]. When PTEN continues to be expressed in glioblastoma, there is enhanced autophagy flux in a PTEN lipid-phosphatase-independent manner[49]. In this study the authors demonstrated lipid-phosphatase-independent activation of mTOR that could inhibit autophagy whilst repressing the ubiquitin-proteasome

system (UPS). These findings illustrate the diversity of functions of PTEN in regulating a major catabolic pathways in cells.

PTEN functions have also been linked to cell senescence mechanisms, which refers to cells that no longer proliferate (reviewed in Collado, Blasco, & Serrano, 2007). Interestingly, the presence of GR-1^{+} myeloid cells in the tumor microenvironment were shown to antagonize PTEN loss induced-senescence by secreting interleukin-1 receptor antagonist (IL-1RA) in prostate cancer[51]. Moreover, the inhibition of AKT protein in PTEN-intact patient-derived prostate tumors led to the activation of the Ras/MEK/ERK pathway[52], suggesting that the PI3K/AKT/mTOR pathway regulated by PTEN may play a role in cell senescence. PTEN inactivation in prostate cancer epithelial cells of adult mice stimulated cell proliferation, which was then followed by a senescence-like growth arrest[46]. Mechanistic studies have found that PTEN deficiency promotes cell senescence through the p53-p21 signaling network. Both mTORC1 and mTORC2 complexes bind and phosphorylate p53 at serine 15, which then promotes the accumulation of p21 in the cytoplasm of cells. Consequently, p21 inhibits cell cycle and leads to cell senescence[53].

Interestingly, emerging evidence has shown that cancers with monoallelic *PTEN* inactivation are more aggressive than tumors with complete loss of the gene[54]. This occurs because complete loss of the PTEN protein activates p53-dependent cell senescence mechanism, triggering tumor-cell death. In contrast, tumors that retain one functional *PTEN* allele continue to proliferate but the haploinsufficiency of the PTEN protein increases the rate of chromosomal instability and somatic mutations leading to poorer outcomes[55]. *PTEN* haploinsufficiency has also been referred to as "quasi-inactivation" – which means that a subtle downregulation of this tumor suppressor can have distinct effects on cancer cells (Reviewed in [56]). Indeed, mice showing a 20% decrease on PTEN expression had tumor phenotypes similar to animals presenting *PTEN* hemizygous loss[57]. These observations indicate that the fine adjustment of cellular PTEN levels may have 1) significant effects on cancer-cell aggressiveness and 2) presumably drive other genomic changes as consequence of greater genomic instability. PTEN functions are summarized in **Figure 1**.

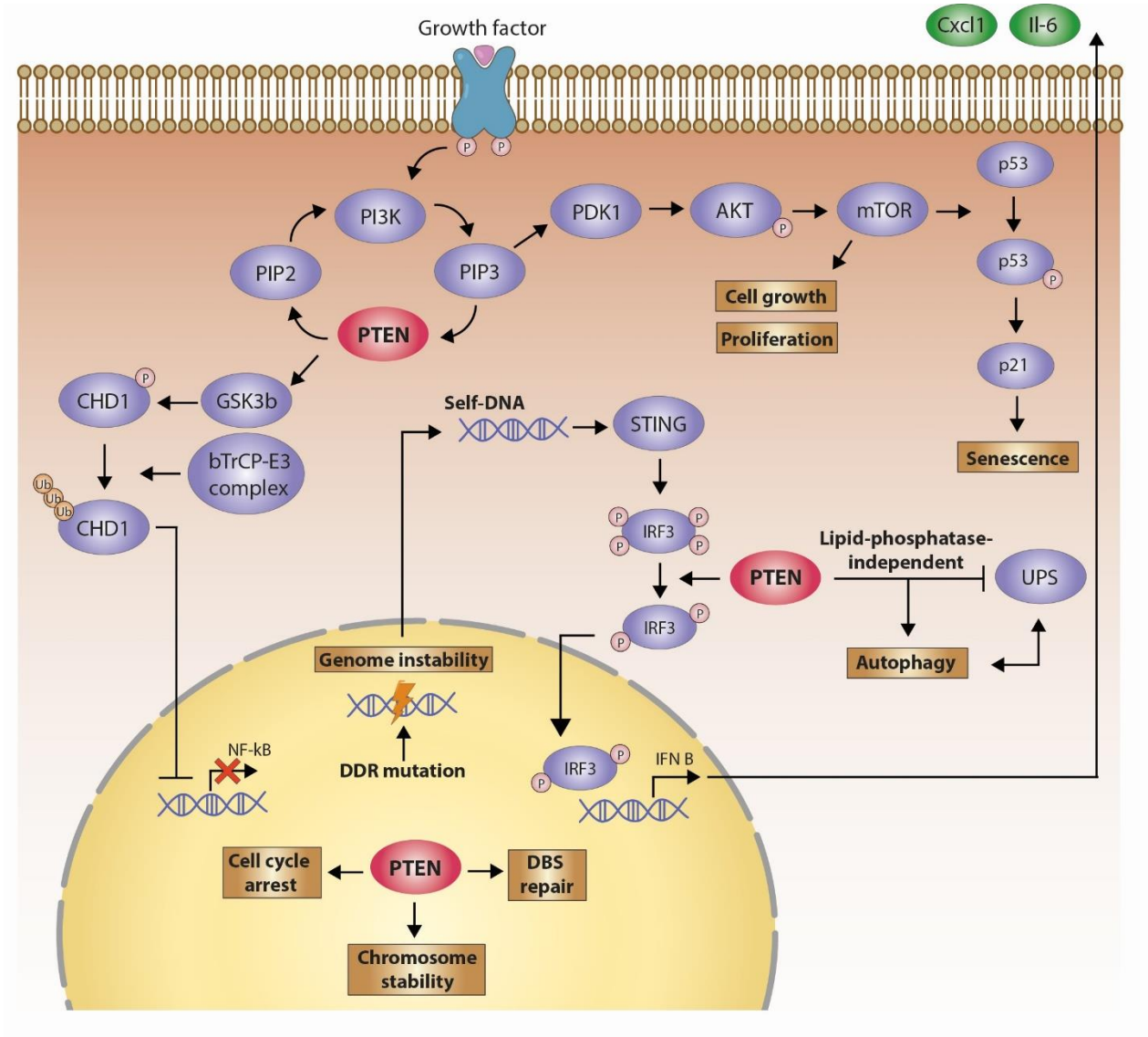

Figure 1. PTEN functions in the cytoplasm and nucleus of cells. The PI3K/AKT/mTOR pathway is negatively regulated by PTEN in the cytoplasm through the dephosphorylation of PIP3 in PIP2. mTOR complex directly phosphorylates p53, which promotes the accumulation of p21 in the cytoplasm that consequently promotes cell senescence. PTEN also negatively regulates NF-kB signaling pathway through CHD1, which is ubiquitinated in the presence of PTEN and thus is not able to promote the transcription of NK-kB genes in the nucleus. The concomitant presence of DDR gene mutations or genome instability leads to double strand breaks (DBS) in the DNA, which often causes self-DNA to migrate to the cytoplasm. The presence of cytoplasmic DNA activates the STING pathway, which phosphorylates IRF3. PTEN is required for IRF3 nucleus migration where this transcription factor will promote the expression of type I IFN genes. Moreover, PTEN controls several mechanisms during DNA replication, such as cell cycle, chromosome stability and DBS repair. More recently, PTEN was shown to regulate the activation of UPS and to directly promote cell autophagy via an independent lipid-phosphatase function.

2.3 Associations between genomic instability driven by PTEN inactivation and cancer immunogenicity

Since PTEN normally regulates several mechanisms that maintain chromosome stability in the nucleus, it is expected that PTEN-deficient cancers may exhibit high rates of chromosome rearrangements and mutational load. A study conducted with murine models demonstrated the heterozygous nonsense mutation resulting in the loss of the PTEN C-terminal led to genomic instability and fragile site rearrangements[58]. The authors showed that PTEN C-terminal-null metaphases had high levels of aneuploidy and polyploidy, with several acentric chromosome fragments, premature centromere separation, and Robertsonian chromosomal fusions. PTEN-null primary breast carcinomas exhibited increased cytoplasmic checkpoint kinase 1 (CKH1) and aneuploidy. As consequence of PTEN deficiency, AKT phosphorylation impaired CHK1 through phosphorylation and ubiquitination[59]. The same study group performed functional studies with murine embryonic stem cells and showed that PTEN deficiency promotes DNA damage due to aberrant inactivation of the kinase CHK1[60].

The investigation of >10,000 tumors from The Cancer Genome Atlas demonstrated that higher levels of aneuploidy (defined as whole chromosome or chromosome-arm imbalances) were associated with a significant decrease in the immune response levels due to lower leukocyte infiltration[26]. Although the observation that tumors with high aneuploidy levels are less immune-cell infiltrated is conflicting with the concept of tumor immunogenicity derived from genomic changes, the mechanisms by which these tumors evade the immune response is still under discussion. A recently published pan-cancer study demonstrated that the expression of HLA genes presented a significant negative correlation with chromosome instability scores[61]. However, it is well established that acquisition of genomic instability and aneuploidy in tumors leads to cell cycle arrest, senescence, and the production of pro-inflammatory signals that normally lead to clearance of abnormal cells[62].

Concomitant structural genomic changes and somatic mutations may provoke enhanced anti-tumor immune responses in the TME. For instance, as consequence of double strand breaks in the DNA concomitantly with the presence of inactivating mutations in DNA damage repair (DDR) genes, DNA fragments may be present in the cytoplasm of tumor cells[63]. These events may lead the activation of the cytosolic double-stranded DNA sensing cGAS-STING pathway, which promotes the phosphorylation of the transcription factor interferon regulator 3 (IRF3). It has been shown that PTEN and PTEN-L impact transcription of type I interferon (IFN) related genes by regulating IRF3 activation[10,11]. In this manner, PTEN deficiency in DDR

mutated tumors may provoke reduced levels of immune response activation due to the lack of transcription of interferon related genes by IRF3[64].

Since PTEN loss promotes higher rates of genomic instability, it is expected that PTEN-deficient tumors may exhibit increased immunogenicity. However, few studies have investigated the role of PTEN inactivation in promoting an immunogenic tumor microenvironment. Our group has demonstrated that *PTEN*-deficient prostate tumors exhibit higher levels of mutation and aneuploidy than tumors with an intact *PTEN* gene[65], suggesting that PTEN loss may elicit different anti-tumor immune responses in the TME. However, PTEN loss has been linked to an immunosuppressive tumor state that favors cancer progression[66–69], suggesting that more complex interactions with the immune system may take place in the TME. In this manner, the avenues of PTEN functions in maintaining the genome and regulating the immune response are still under debate (**Figure 2**).

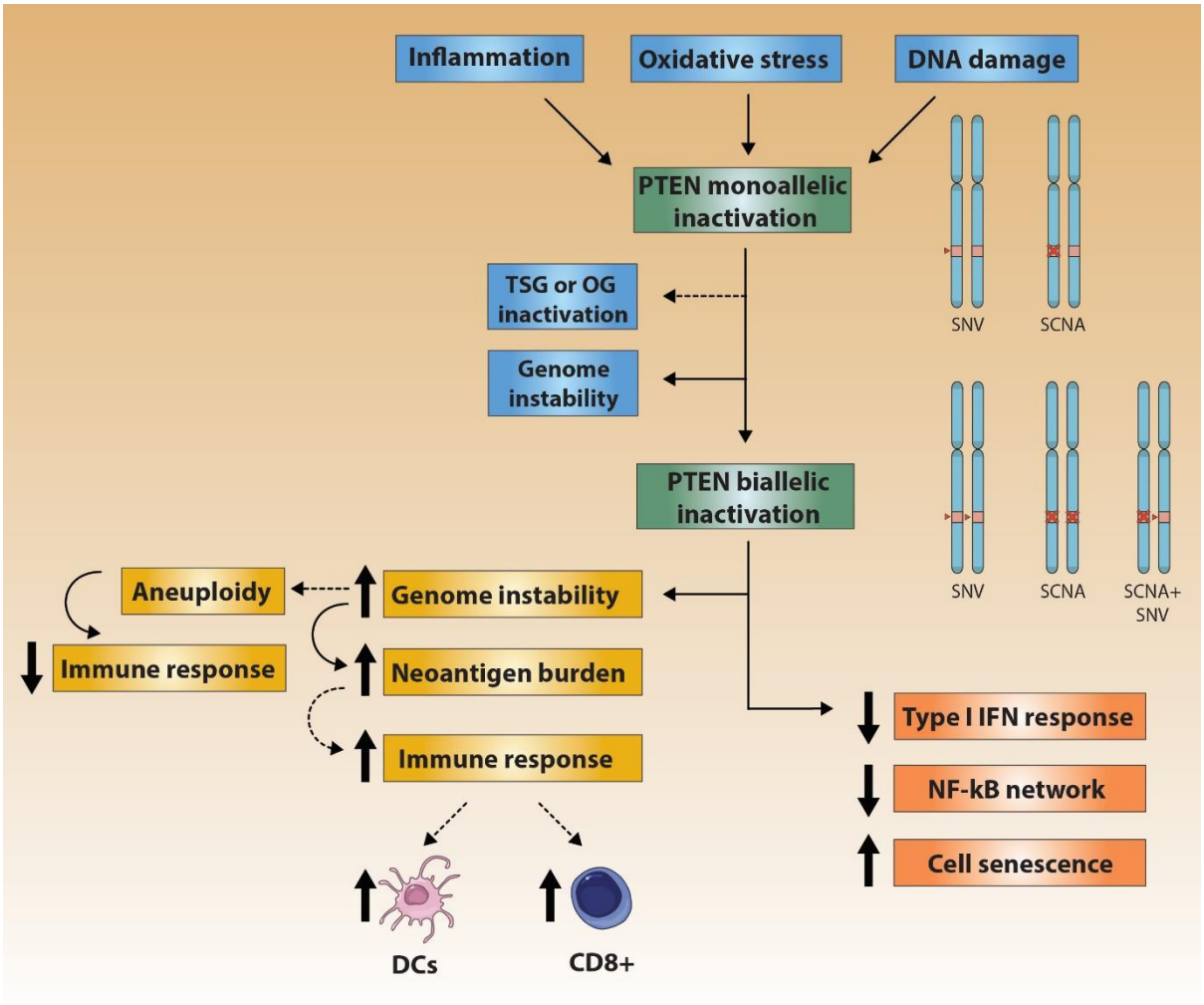

Figure 2. Effect of *PTEN* inactivation in the immune response of cancer. The presence of recurrent inflammation and DNA damage as consequence of metabolic stress may lead to somatic mutations (SNVs) or somatic copy number alterations (SCNA) of *PTEN*. The presence of other concomitant genomic changes in tumor suppressor genes (TSG) and oncogenes (OG) in addition to increased levels of genomic instability may drive the complete loss of function of *PTEN*. The lack of *PTEN* in the tumor cells may lead to reduced levels of type I IFN response and NF-kB pathway in the TME. Moreover, higher levels of instability of the genome triggers higher levels of mutations and consequently presence of neoantigens, which activate the immune-cell response in the TME. However, high levels of aneuploidy as consequence of genomic instability may inhibit the immune response.

2.4 Implications of PTEN deficiency in the immune response of cancer

Several reports have shown that oncogenes and tumor suppressor genes have secondary functions in regulating the immune response in the TME in addition to their role on cell proliferation and survival (reviewed in Wellenstein & de Visser, 2018). In addition to the regulatory effect of PTEN on AKT pathway and the genomic and chromosomal instability, PTEN influences the innate immune response by dephosphorylating Ser97 and thus enabling the nuclear migration IRF3. When in the nucleus, IRF3 promotes the transcription of type I IFN response genes[11]. Concordantly, PTEN-L, a secreted protein isoform of PTEN with 576 amino acids, regulates IRF3 and p65 nuclear import, where both factors trigger the transcription of type I IFN response and nuclear factor-kappa-B (NF-kB)-related genes, respectively[10]. Additionally, Cao and colleagues (2018) demonstrated that cells expressing only PTEN-L synthesized the highest levels of Cxcl10 and the proinflammatory cytokines Il-6 and Cxcl1.

The type I IFN response promotes the recruitment and activation of anti-tumor T-cell and natural killer (NK) cell in addition to stimulating antigen presentation by dendritic cells[70]. It is known that the overactivation of type I IFN responses are strongly linked to better response to immunotherapy and to an increased activation of antigen presentation by tumor cells (reviewed in Parker, Rautela, & Hertzog, 2016). On the other hand, NF-kB pathway regulates both immune and inflammatory responses and tumor-cell proliferation and apoptosis[72]. As a result, PTEN-deficient tumors may have impaired activation of type I IFN and NF-kB pathways, which favors tumor progression as consequence of an immunosuppressed TME.

In melanoma, PTEN deficiency was associated with reduced CD8+ T-cell density in the TME, which diminished the response to immune checkpoint blockade therapies with anti-PDL1 and anti-cytotoxic T-lymphocyte associated protein 4 (CTLA4)[17]. The authors demonstrated that PDL1 and MHC class I expression are not the primary mechanism of immunosuppression mediated by PTEN loss. Their further analysis suggested lack of response could be because PTEN-silenced xenografts exhibited higher VEGF protein expression and increased expression of inhibitory cytokines.

In a study conducted with 28 radical prostatectomy-derived specimens, PTEN loss was significantly associated with high macrophage density and CXCL8 expression[73]. In mice, the haploinsufficiency of *Pten* combined with oncogenic *Kras* mutations in pancreatic ductal adenocarcinoma was associated with NF-kB pathway activation. Moreover, the authors showed that the NF-kB network stimulation led to TME remodeling through the infiltration of immune-cell with pro-tumorigenic properties[74]. In prostate cancer murine models, tumors with *Pten* deletions exhibit high expression rates of *Csf1* and *Il1b*, which lead to an expansion of

myeloid-derived suppressor cells (MDSCs). In turn, the presence of MDSCs triggered the suppression of T cells in the TME of the prostate tumors[68,75].

In prostate cancer, *Pten*-null tumors are strongly immunosuppressed as a consequence of the upregulation of PTPN11 and Jak2-Stat3 pathway activation[76]. In a study conducted with *Pten*-deficient mice, the ablation of the growth regulatory kinase promoted T-cell recruitment through *Ccl5* and *Cxcl10* production[77]. This may explain why prostate tumors do not benefit from current immunotherapeutic approaches in result of a lack of T-cell infiltration.

PTEN loss has also linked to changes in the secretome (*i.e.*, cell-secreted molecules, such as chemokines and interleukins) so that its role in mediating immune responses in the TME may also be indirect. In non-small lung cancer, it was shown that the CXC chemokine receptor 4 (CXCR4) expression is dependent on the PI3K/PTEN/AKT/mTOR signaling pathway[78]. A study conducted with murine prostate epithelial cells and human prostate cancer cell lines demonstrated that loss of PTEN enhanced the expression of CXCR4 and CXC motif chemokine ligand 12 (CXCL12)[79]. Moreover, in prostate cancer cell lines and prostatic tissue, Maxwell and colleagues (2013) demonstrated that the expression and secretion of the pro-inflammatory chemokine CXCL8 was associated with PTEN inactivation[80].

It is now accepted that the interactions and coevolution of tumor cells and the surrounding cellular and non-cellular components of the TME can have a profound effect on all aspects of tumorigenesis and can contribute to therapeutic resistance. Structural TME remodeling driven by oncogenic alterations has been reported in several tumor types. For instance, in a murine model of T-cell acute lymphoblastic leukemia, *Pten* deficiency was reported to promote cell survival in a previously unsupportive TME. This finding suggests that PTEN inactivation not only promotes intrinsic tumor cell expansion, but also elicits extrinsic effects on the immediate microenvironment by altering the tumor niche in favor of tumor progression.

2.5 PTEN loss and immune cell infiltration

The immune-cell landscape of tumors that harbor *PTEN* somatic mutations is complex and highly heterogeneous, with studies showing that PTEN deficiency is linked to high CD8+ T-cell density[66,81] while others exhibit inverse correlations with this cell type[82–84] (**Table 1**). High degrees of tumor infiltration by CD8+ T cells are strongly linked to better prognosis in several types of cancer[85,86]. It is known that immune-cell recruitment and activation relies on tissue-specific mechanisms, which varies across different tumor types[87], and may even present immune-cell contents that are distinct for different lesions from a single patient[23]. Thus, it is

expected that PTEN deficiency in tumor cells may elicit effects in the TME that are tumor-type or even lesion specific. Interestingly, several reports have shown that tumors harboring PTEN deficiency are more likely to present increased M2 macrophage cell density (**Table 1**). The presence of M2 macrophage in tumors is linked to favorable growth and invasive features of cancer cells. Indeed, tumors with high M2 macrophage density are significantly associated with worse outcome[88,89].

Table 1. Associations between PTEN deficiency, immune-cell composition, and immune checkpoint expression in cancer.

Tumor type	CD8+	Treg	MDSC	TAM	PDL1	PD1	Sample size	Studies in murine models	Studies with human patients
Breast cancer	↑						836 patients		[66]
Breast cancer cell lines					↑		836 patients		[66]
Colorectal cancer					↑		404 patients		[90]
Endometrial	NA						382 patients		[91]
Endometrial				↑			3 mice per group		[92]
Glioblastoma	↑ Apoptosis						26 patients		[93]
Glioma					↑		10 cell lines		[69]
Gastric and Breast cancer				↑ M2			12 patients		[94]
HNSCC	↓	↑					5 mice per group	[82]	
LCNC, SCLC					NA		189 patients		[95]
LSCC					↑		5 mice per group	[96]	
LSCC					↓		102 patients		[97]
LUAD					↑		ND	[98]	
LUAD[#]				↑ M2			13 mice	[99]	
Melanoma	↓	↑					3 mice per group	[83]	
Melanoma	↓						135 patients		[84]
Melanoma*	↑			↑ M2			4 mice per group	[100]	
Melanoma cell lines					↑		33 patients		[101]
Prostate cancer				↑			70 patients		[73]
Prostate cancer	↑	↑					312 patients		[81]
Prostate cancer			↑				3 mice per group	[68]	
Prostate cancer			↑				3 mice per group	[75]	
Prostate cancer			↑				3 mice per group	[51]	
Prostate cancer					NA		20 patients		[102]
Thyroid		↑	↑	↑ M2			8 mice per group	[103]	
Uterine Leiomyosarcoma						↓	1 patient		[16]

LUAD – lung adenocarcinoma, SCC – squamous cell carcinoma, LSCC – lung squamous cell carcinoma, LCNC – Large-cell neuroendocrine cancer, SCLC – small-cell lung cancer, TAM – tumor associated macrophage, NA – No significant association observed, ND – Not described. HNSCC – Head and neck squamous cell carcinoma. CD8+ - CD8+ T cell, Treg – Regulatory T cell, MDSC – Myeloid-derived suppressor cell, TAM – tumor infiltrating macrophage, PDL1 – programmed death ligand 1, PD1 – programmed death protein 1. $^{\#}Pten^{D5/}$D5;$Kras^{Lox/+}$;$CCSP^{Cre/+}$ mice. *$BRAF^{V600E}$;$PTEN^{-/-}$ mice.

Interestingly, PTEN-deficient tumors often exhibit high densities of regulatory T-cell (Treg) in the TME (**Table 1**). Tregs have an immunosuppressive impact in the TME by inactivating the priming and effector activities of CD4+ and CD8+ T cells[104]. Indeed, high CD8+/Treg ratio is associated with favorable prognosis in ovarian[105], gastric[106], and cervival tumors[107]. Moreover, several reports have confirmed the associations between Treg density and poor outcome in several tumor types[108–110]. Studies have demonstrated that normal functioning PTEN is crucial for Treg development and maturation[111]; however, little is known on the mechanisms by which PTEN loss in tumor cells may have extrinsic effects leading to an increase in Tregs infiltration into the TME.

Studies with mice have shown that PTEN deficiency can increase tumor-infiltrating MDSC densities in TME (**Table 1**). The role of MDSCs in mediating immune responses may explain why PTEN can have complex interactions with the TME. MDSCs are a heterogeneous population of myeloid progenitors and immature granulocytes, macrophages, and dendritic cells. Mechanistically, MDSCs are highly immunosuppressive cells that suppress CD8+ T cell activity through the secretion of reactive oxygen species, peroxynitrite, and nitric oxide (reviewed in Gabrilovich & Nagaraj, 2009). Due to the modulating effect on the anti-tumor immune response, the presence of high densities of MDSCs correlates with worse outcome in several tumors [113,114]. In addition, the development of castration resistant prostate cancer – a condition on which tumors are insensitive to androgen-deprivation therapy – was found associated with the presence of high densities of tumor-infiltrating MDSCs and IL-23 concentration[75]. Since PTEN loss is present in >70% of castrate resistant prostate cancers it is important to understand how an immunosuppressive and tumor-tolerant TME is imposed by infiltrating MDSCs in such advanced cancers.

2.6 PTEN loss associations with immune checkpoint expression

The most effective current immunotherapeutic interventions include blockade of programmed death protein 1 (PD1) and programmed death ligand 1 (PDL1) proteins. Unfortunately, several patients relapse after benefiting from immune blockade therapies, suggesting that tumor-specific alterations may trigger drug resistance. In this context, mutations and pathway dysregulation of tumors lead to an altered immune cell composition in the TME, which is key to therapy response. It is known that responsiveness to immune checkpoint blockade requires the infiltration of CD8+ T-cell

in the TME. However, the presence of an immunosuppressive signature in tumors may thus negatively impact the response to immunotherapies.

During innate immune resistance, the constitutive activation of oncogenic pathways can promote the synthesis of PDL1 in tumor cells independently of the immune-cell state in the TME. For instance, in murine models of lung cancer, the activation of the AKT-mTOR pathway promoted the expression of the immune checkpoint PDL[115]. Functional studies with lung cancer cell lines also demonstrated that tumor infiltrating macrophages may promote PDL1 synthesis by secreting IFN-gamma in an JAK/STAT3-dependent manner[116]. On the other hand, in the adaptive immune resistance, the stimulation of tumor cells by immune-cell secreted IFN-gamma triggered the synthesis of PDL1 through JAK/STAT pathway[117]. Since PTEN ablation promotes low IFN pathway activation, it is expected that PTEN-deficient tumors may exhibit low levels of cancer cells expressing PDL1.

Overall, most studies show that PTEN loss is significantly associated with high PDL1 expression levels (**Table 1**). In uterine leiomyosarcoma, PTEN deficiency was linked to resistance to anti-PD1 therapy[16]. This study showed that the presence of a biallelic inactivation PTEN in a metastatic lesion was associated with reduced PD1 expression in tumor infiltrating immune cells. Through *in silico* analyses of TCGA sarcoma specimens, the authors also demonstrated that the presence of an oncogenic mutation and a heterozygous deletion of PTEN in had lower expression of CD8+ T cell markers (*GZMA*, *PRF1*, and *CD8A*) and *PD1* and *IFNG* genes. In murine lung cancer models, the activation of the PTEN/AKT/mTOR cascade in consequence of PTEN deficiency was associated with the overexpression of PDL1. The authors also showed that tumor growth was inhibited, tumor-infiltrating T-cells was increased, and Treg density decreased with the combined treatment with mTOR inhibition and anti-PD1[115]. In *PTEN*-deficient breast cancer cell lines, Mittendorf and colleagues (2014) observed overexpression of PD1 and PDL1, which were downregulated after PI3K pathway inhibition. Moreover, PTEN loss-induced PDL1 overexpression in tumor cells was associated with low T-cell proliferation rates[66]. Concordantly, the absence of PTEN expression in melanoma cell lines was associated with the upregulation of PDL1 expression[101]. In gliomas, PTEN loss was significantly associated with PDL1 overexpression[69]. In a castrate resistant prostate cancer murine model, the concomitant

deletion of *Pten*, *p53*, and *Smad4* led to resistance to immune checkpoint blockade therapies with anti-PD1 and anti-CTLA4 antibodies[118].

Interestingly, PTEN-deficiency was not associated with PDL1 expression in prostate cancer. Indeed, PDL1 expression in radical prostatectomy-derived prostate tumors is rare[102]. Taken together, these observations demonstrate that PTEN deficiency may be useful in distinguishing patients with specific tumor types that may benefit from current immunotherapeutic approaches.

2.7 Clinical trials investigating the impact of PTEN in the response to immunotherapy

Since PTEN functions are linked to how tumor cells interact with the immune response, this gene may be a useful biomarker in determining how patients will respond to therapy. There are a limited number of clinical trials that directly measure PTEN status and the response of the tumor to immune checkpoint blockade therapies (more details on **Table 2**). However, several downstream factors of PTEN signaling pathway, such as AKT and PI3K, have been investigated in conjunction of checkpoint blockade therapies. Indeed, PI3K and AKT inhibitors are under investigation in combinatory approaches with anti-PD1 and anti-PDL1 therapies in several tumor types.

Several reports have determined the effects of inhibiting downstream PTEN pathways on the anti-tumor immune response of cancer. Interestingly, the inhibition of the PI3K/AKT/mTOR network in *PTEN*-deficient primary cultures of gliomas led to a diminished T-cell death[93]. Concordantly, the ablation of PI3K pathway remarkably enhanced the anti-tumor functions of toll-like receptors ligands in murine models[119]. Thus, it is expected that several of the trials investigating PTEN-related genomic alterations and its links to immune checkpoint blockade response (**Table 2**) may provide promising results. The trials (NCT03206203 and NCT02299999) have ongoing whole transcriptome analysis, giving the opportunity to determine if other genomic changes occurring in conjunction with PTEN loss are linked to immunotherapy response. In this manner, determining PTEN deficiency in tumors may be useful for determining biomarker-guided combinatory drug approaches.

Table 2. Clinical trials investigating the effect of PTEN loss or activation of downstream effectors of PI3K/AKT/mTOR pathway.

PTEN-associated mechanism	Tumor type	Drug	Study details	Trial number
PTEN loss	Triple Negative Breast Cancer Stage IV Breast Cancer HER2 Negative Invasive Breast Cancer	Atezolizumab (Anti-PDL1) Carboplatin Atezolizumab + Carboplatin	Phase II Trial of Atezolizumab (Anti-PDL1) in combination with carboplatin in metastatic triple negative breast cancer (TNBC). Tumor infiltrating lymphocyte density and phenotype (TILs) will be measured. PD-L1 expression will be determined by IHC. RNA-seq will be performed for classifying tumors as TNBC. IHC will be performed with markers of T cell subsets (CD4, CD8, FoxP3, CD25, Glut1) and exhaustion proteins (PD1, CTLA4).	NCT03206203
PTEN loss and phospho-AKT	Non-Small Cell Lung Carcinoma (NSCLC)	AZD6244 (KRAS mutant patients) Erlotinib (wild-type KRAS patients) AZD6244 + Erlotinib	Phospho-ERK (p-ERK), Phospho Protein Kinase B (p-AKt) and PTEN expression will be determined. PD-1 expression will be investigated in Tregs and CD8+ T cells. Change in T Cell Immunoglobulin Mucin 3 (TIM-3) on Tregs. Change in CTLA-4 expression on Tregs. Change in PD-1 expression on Tregs.	NCT01229150
Phospho-AKT	Stage I-IV Oral Cavity Squamous Cell Carcinoma Stage I-IV Oropharyngeal Squamous Cell Carcinoma	Metformide Hydrochloride/Pioglitazone Hydrochloride Extended-Release Tablet	PD1 and PDL1 expression will be compared between patients before and after treatment. IHC will be performed with apoptosis biomarker cleaved caspase 3, cyclin D1, p21, PPAR gamma, (p)AKT, pAMPK, pS6 and tumor infiltrating immune cells (CD8, IFNg, Treg, CD68).	NCT02917629
Phospho-AKT	NSCLC Squamous Cell Adenocarcinoma	AZD5363 (AKT Inhibitor) Durvalumab (Anti-PDL1) Other drugs (ZD4547; Vistusertib; Palbociclib; Crizotinib; Selumetinib; Docetaxel; Osimertinib; Sitravatinib)	Multi-drug and genetic testing in a multi-arm phase II trial. No genomic or expression tests.	NCT02664935
Phospho-AKT	Metastatic Breast Cancer	MEDI4736 (Anti-PDL1) AZD5363 (AKT Inhibitor) Other drugs (AZD2014, AZD4547, AZD8931,	DNA will be investigated by NGS and microarray.	NCT02299999

		Selumetinib, Vandetanib, Bicalutamide, Olaparib, Anthracyclines, Taxanes, Cyclophosphamide, DNA intercalators, Methotrexate, Vinca alkaloids, Platinum based chemotherapies, Bevacizumab, Mitomycine C, Eribuline		
Phospho-AKT	NSCLC	MEDI4736 (Anti-PDL1) AZD5363 (AKT Inhibitor) Other drugs (AZD2014, AZD4547, AZD8931, Selumetinib, Vandetanib, Standard maintenance for squamous NSCLC, Pemetrexed.	DNA will be investigated by NGS and microarray.	NCT02117167
PI3K inhibition	Unresectable or Metastatic Microsatellite Stable Solid Tumor Along With Microsatellite Stable Colon Cancer Colon Cancer	Copanlisib (PI3K Inhibitor) Nivolumab (anti-PD1)	Phase I/II study of PI3K inhibition (Copanlisib) and anti-PD-1 (Nivolumab) in refractory mismatch-repair proficient (MSS) colorectal tumors. No genomic or expression tests.	NCT03711058
PI3K inhibition	Classical Hodgkin Lymphoma	Tenalisib Pembrolizumab	Phase I/II study to investigating the safety and eddicacy of RP6530 (PI3K δ/γ dual inhibitor) in combination with an anti-PD1 therapy (pembrolizumab). No genomic or expression tests.	NCT03471351
PI3K inhibition	Metastatic NSCLC	Abemaciclib	NGS for 245 genes, Nanostring nCounter including immune signature, and IHC with PD-L1 in patients treated with PI3K Inhibitor and PD1/PD-L1 inhibitors.	NCT03356587
PI3K inhibition	Advanced Solid Tumors	Itacitinib Epacadostat INCB050465	JAK inhibitor with JAK1 selectivity (Itacitinib) in combination with an IDO1 inhibitor (epacadostat; INCB024360; Group A) and Itacitinib in combination with a PI3K delta inhibitor (INCB050465; Group B)	NCT02559492

2.8 Concluding remarks

PTEN has a major role in regulating both cell-intrinsic and extrinsic mechanisms of the immune response. In this literature review, we described that PTEN inactivation status may determine the fate of tumors as consequence of anti-tumor-driven immune responses. However, the associations between secreted signaling proteins, immune cells, and immune checkpoint expression with PTEN status are complex and highly variable across tumor types. Indeed, it is unclear whether there are indirect effects of PTEN on the anti-tumor immune response that are driven by genomic instability in each cancer type. Thus, we conducted a PanCancer study of 33 tumor types aiming to investigate the genomic landscape of PTEN inactive tumors and to show how these genomic features interact with the immune response in human cancer. Lastly, based on our findings from the PanCancer study, we chose to perform a more in-depth study on prostate cancer focusing of PTEN protein loss. Since prostate tumors present high rates of PTEN homozygous losses and that PTEN immunohistochemistry assays in prostate are highly reproducible, we investigated 94 prostate tumor specimens from a Brazilian cohort.

Since most patients experience relapse after immunotherapy, it is critical to characterize tumor-specific genomic biomarkers of response that will be informative for immune-based treatments. Moreover, understanding how DNA mutations and copy number changes that impact the immune response may provide evidence for developing new treatment approaches.

3. OBJECTIVES

3.1 General objectives

3.1.1 To perform a cross-cancer investigation on how *PTEN* loss of function shapes the immune response of cancer.

3.2 Specific objectives

3.2.1 Characterize the frequency and distribution of *PTEN* point mutations, somatic copy number alterations, and mRNA expression loss across cancers.

3.2.2 Investigate the associations between *PTEN* inactivation and the genome landscape of cancer cells.

3.2.3 Determine the influence of *PTEN* inactivation in the anti-tumor immune response driven by immune checkpoint expression and immune-cell content within the tumor microenvironment.

3.2.4 Investigate whether *PTEN* loss indirectly provokes the activation of immune response against tumor cells by affecting tumor aneuploidy and mutational burden.

3.2.5 Compare the immune-cell composition of primary and metastatic prostate tumors harboring *PTEN* loss vs. those with retained *PTEN* expression.

3.2.6 Determine the prognostic impact of *PTEN* inactivation across cancers.

4. HYPOTHESIS

4.1 General hypothesis

4.1.1 As a result of the genetic diversity of cancer, we speculate that interactions between *PTEN* loss in a tumor and the immune system in its immediate microenvironment are specific for each type of cancer.

4.2 Specific hypotheses

4.2.1 We hypothesize that *PTEN* mutations and copy number alterations may vary according to each cancer type.

4.2.2 We expect that *PTEN*-null tumors may exhibit higher levels of genomic instability and chromosomal aberrations, since PTEN regulates genome integrity through various mechanisms in the nucleus of cells.

3.2.3 As PTEN regulates the anti-viral response through IRF3 transcription factor, we speculate that *PTEN*-inactive cancers will be highly immunosuppressive as consequence of the downregulation of type I interferon response genes. Moreover, we hypothesize that immunosuppression will also be observed in the immune-cell profile of tumors harboring *PTEN* loss.

4.2.4. Highly unstable genomes are linked to higher immune response activation in the tumor microenvironment. Thus, we speculate that *PTEN* inactivation may drive an immunosuppressive condition that can be reverted when the genome of cancer cells are more unstable.

4.2.5 Since immune-cell composition of cancers reflect how tumors interact with the tumor microenvironment, we speculate that metastatic prostate cancer will also be highly immunosuppressive when *PTEN* is lost.

4.2.6 We speculate that the biallelic inactivation and homozygous loss of *PTEN* is linked to a worse outcome of tumors.

5. CHAPTER 1

PAN-CANCER STUDY REVEALS THE DIVERSITY OF GENOMIC AND TRANSCRIPTOMIC ALTERATIONS OF *PTEN*-DEFICIENT TUMORS

5.1 Background

Tumor-specific DNA alterations, such as loss of tumor suppressor genes (TSGs) and activation of oncogenes, trigger numerous changes on how malignant cells are recognized and killed by immune cells[8]. The inactivation of the *PTEN* tumor suppressor gene is a remarkably common genomic event in human cancers that has a profound effect on predicting patient outcome across tumor types[36,120–122]. The PTEN protein functions in the cytoplasm and in the nucleus, playing a significant role in regulating cell proliferation and growth[37], chromosome stability[123,124], DNA repair[46], cell senescence and autophagy[49,52], and, as recently reported, in the anti-viral immune response[10,11].

The complete or partial inactivation of TSGs have distinct outcomes on cancer development and progression[4]. The classical "two-hit" hypothesis accounts for an effect being observed exclusively when there is complete loss of function of a TSG. However, partial loss of function by monoallelic inactivation may actually confer a greater selective advantage than complete loss of TSG function (reviewed in [56]). It follows that single-copy inactivation may be selected during tumor evolution, since biallelic inactivation may lead to senescence or cell death. This indicates that, during cancer development, partial inactivation is favored, as observed for TSGs such as *PTEN*, *ARF*, *p53*, and *NF1* (reviewed in [4]).

Regarding the direct and indirect effects of PTEN on the immune response, several studies have shown links between *PTEN* loss and immune-cell composition of the tumor microenvironment (TME) (reviewed in **Chapter 1**). *PTEN* deficiency has also been linked to the expression of immunosuppressive molecules, such as the programmed cell death ligand 1 (PDL1) and proinflammatory chemokines and cytokines.

Our group has demonstrated that primary prostate tumors harboring *PTEN* deletions have enhanced levels of aneuploidy and non-synonymous mutations[65] (**Attachment 1**). However, it is unclear whether the genomic instability generated by *PTEN* inactivation may drive the suppression or activation of anti-tumor immune mechanisms. A recently published PanCancer study showed that an increased frequency of chromosome arm and whole arm chromosome aberrations in tumor cells is strongly associated with a reduction in leukocyte fractions in the TME[26]. However, in contrast, several reports have indicated that tumors with higher genomic instability rates are more like to express neoantigens[125], and thus be more immunogenic.

There are a limited number of studies that have investigated the impact of the *PTEN*-dependent genomic changes on the immune response in the TME. *PTEN*-deficient cancer cells are likely to undergo abnormal mitosis and thus exhibit higher rates of chromosome aberrations that could trigger cell-specific anti-tumor responses independent of established downstream effects of PTEN on interferon regulatory factor 3 (IRF3) and PI3K/AKT/mTOR signaling pathways. Therefore in this chapter, we investigated genomic datasets to evaluate the impact of *PTEN* loss on the genomic alterations in different cancers, and explored the links between tumor-specific DNA changes and the immune response in the TME.

5.2 Methods

5.2.1 Data download and processing

We downloaded level 3 PanCancer normalized RNAseq, array-CGH, SNV, and methylation array of 10,713 samples from 33 tumor types from The Cancer Genome Atlas (TCGA) cohort (www.gdc.cancer.gov). Raw RNAseq experiments were performed through Illumina HiSeq 2000 RNA Sequencing platform. Copy number data were obtained from array-CGH experiments performed with the Affymetrix Genome-Wide Human SNP Array 6.0. DNA sequencing was performed in Illumina Genome Analyzer DNA sequencing.

Clinical data regarding progression-free survival and overall survival were obtained for all patients from the TCGA cohort. Raw RNAseq data of all investigated tumors were downloaded through *TCGAbiolinks* package in R[126]. Additional data on immunogenomic features of tumors were downloaded from the TCGA database[127,128]. All analyses were conducted with data derived from primary tumors.

5.2.2 Defining *PTEN* deletions and inactivation status

PTEN deletions were characterized by using GISTIC-derived categorical somatic copy number alterations (SCNA). Tumors had *PTEN* gene status ranging from homozygous deletions, hemizygous deletions, and the presence of both alleles or duplication. *PTEN* duplications consisted of the presence of gain of an extra copy of the entire gene or regions at 10q23.31 that include *PTEN*. Since *PTEN* deletions and somatic point mutations lead to loss of function of PTEN protein, our method was designed to verify the impacts of *PTEN* inactivation by either deletion or point mutation on the

genomic and immunogenic features of tumors. SNV data including missense, splice-site, inframe, indel, and truncating inactivating variants were analyzed to determine *PTEN* mutational status and SCNA data were used to determine the deletion status of the *PTEN* gene.

To determine which tumors had *PTEN* inactivation, we combined data on mutations and SCNA of *PTEN* gene. Since *PTEN* loss by promoter methylation is a rare event in tumors[129], we did not use methylation data to infer *PTEN* inactivation status. Tumors harboring *PTEN* hemizygous deletions or with a single somatic point mutation were classified as having *PTEN* monoallelic inactivation. The presence of *PTEN* homozygous deletions or the presence of concomitant hemizygous deletion plus a somatic point mutation determined tumors with *PTEN* biallelic inactivation status. Cases with both copies of *PTEN* and those with duplication were grouped as *PTEN* intact. Cases with a single point mutation and *PTEN* duplication were classified as *PTEN* intact, as we did not investigate if the duplication events that included the entire *PTEN* gene. A summary of our classification method of *PTEN* inactivation is summarized on **Figure 3**.

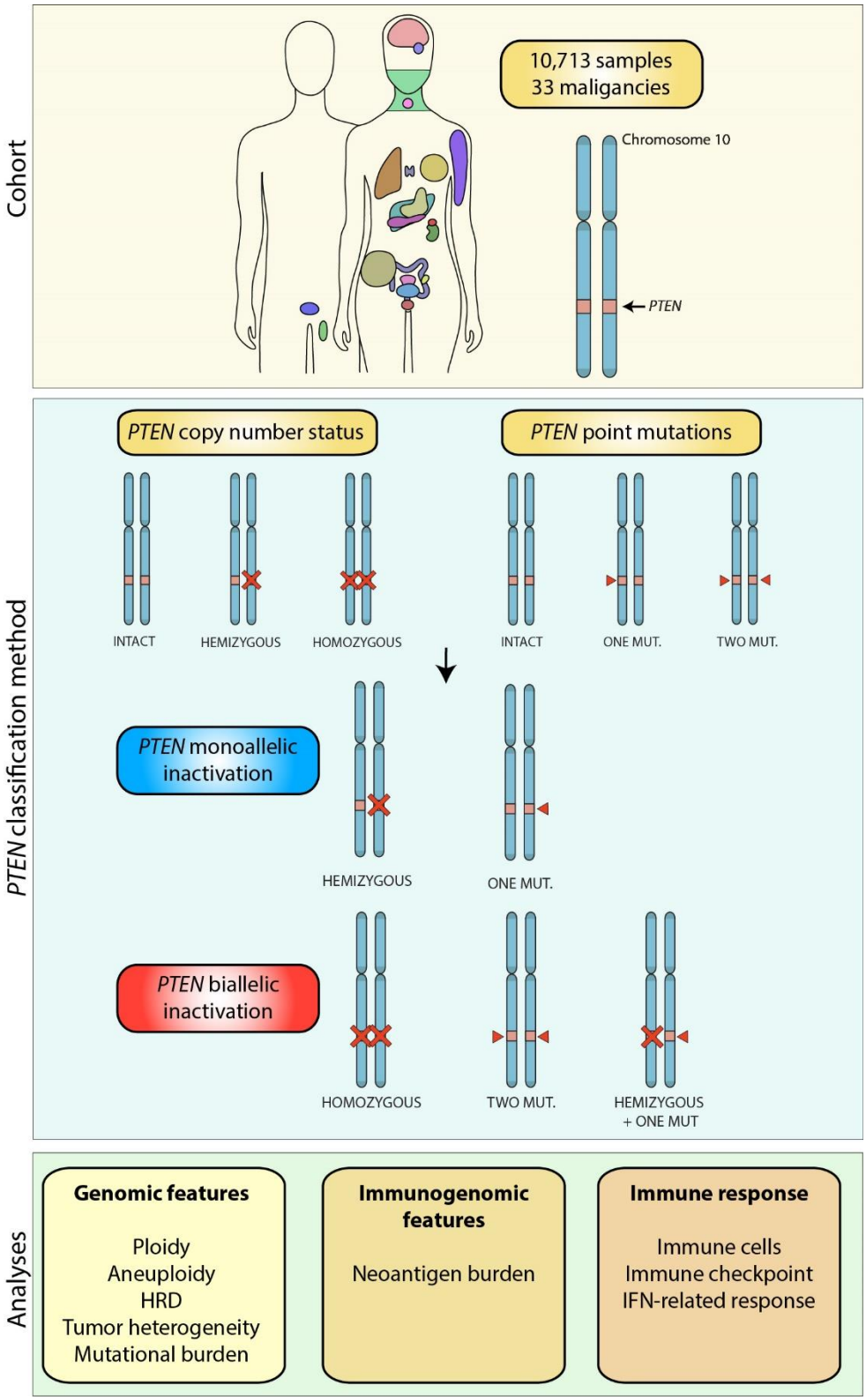

Figure 3. Summary of *PTEN* inactivation criteria utilized in our study. We investigated a total of 10,713 samples from 33 different tumor types. *PTEN* inactivation status was determined based on somatic copy number alterations and point mutations in *PTEN* gene. Tumors with both inactive alleles were characterized as undergoing biallelic inactivation. Concordantly, tumors harboring one allele inactivation were defined as monoallelic inactive tumors. These inactivation groups were compared regarding the anti-tumor immune response and genomic changes.

5.2.3 Differential expression analysis

To compare the transcriptome of *PTEN* intact tumors to those presenting monoallelic or biallelic *PTEN* inactivation, we conducted a differential expression analysis by employing raw RNAseq counts in *DESeq2* package in R. P-values were adjusted with the Benjamini Hochberg method and genes presenting P-adjusted values below 0.05 were considered as differentially expressed between groups. Gene Set Enrichment Analysis (GSEA) enrichment analysis was conducted to identify the most significantly altered pathways in *PTEN*-deficient tumors. The top differentially expressed genes were visualized through ClueGO package for Cytoscape 3.7.0 (https://cytoscape.org/).

5.2.4 Methylation, copy number and mutational profiling

Since *PTEN*-deficiency may be linked to other significant genomic changes, we aimed to characterize the methylation, mutational, and copy number landscape of primary tumors harboring *PTEN* loss. Copy number analysis was conducted by investigating the frequencies of SCNAs across all 10,713 primary tumors through Fisher Exact test with a significant P-value set to <0.05. We then stratified the PanCancer cohort by tumor type to identify recurrent SCNA calls in tumors harboring *PTEN* monoallelic and biallelic inactivation for each histology. The mutational signatures of *PTEN*-deficient primary cancer were also compared through Fisher Exact test in R. *Maftools* package was used to investigate .maf files and to select loss of function genomic variants for further comparisons. Each gene mutation frequency was compared between *PTEN* intact and deficient groups.

The DNA methylation preprocessed files of Illumina HumanMethylation450 bead array platform (450K) and Illumina HumanMethylation27 (27K) were retrieved through TCGAbiolinks package[126]. The TCGA PanCancer tumoral primary samples were selected (n=9,728) and both platforms were merged for the common probes (n=22,601). Supervised analysis among the deletion groups were performed by nonparametric Wilcoxon test followed by false discovery rate (FDR) correction in a two-step pairwise model: 1) Intact vs. biallelic inactivation; and 2) Intact vs. monoallelic inactivation. The DNA methylation data is given by beta (β) value score that ranges from 0 to 1 and results from the total DNA signal (β=(M/M+U) - M refers to the mean of methylated sites and U to the mean of unmethylated signals. Values close to 1 indicate increased methylation

levels on a particular CpG site. Our copy number, mutational, and methylation analyses are still under development.

5.2.5 Immunogenic and genomic effects of *PTEN* deficiency

To determine the association between *PTEN* inactivation and acquired DNA changes in tumors, we investigated the presence of genome doublings, homologous recombination defects (HRD), aneuploidy levels, tumor mutational burden, and intratumoral heterogeneity. Genome doubling status was determined through ABSOLUTE algorithm, which measures tumor ploidy and purity based on copy number and mutational signatures. Ploidy levels are determined by the actual quantity of DNA that each cancer cell presents after undergoing several numerical and structural chromosome aberrations. Clonality calls were employed to determine intratumor heterogeneity scores, which determines tumor copy number and point mutations as aggregates of clonal and subclonal components having varying ploidy levels. Tumor purity is a measurement which considers the fractions of normal cells within the bulk mass of tumor cells. Aneuploidy levels were calculated based on the total length of gained and deleted chromosome arms divided by the size of the genome[26]. Similarly, HRDs were calculated based on the copy number calls in with large (>15 Mb) non-arm-level chromosome imbalances with loss of heterozygosity, breaks between genes larger than >10 Mb, and subtelomeric regions harboring allelic imbalances. Groups with distinct *PTEN* inactivation status were compared by employing Kruskal-Wallis test in R.

In addition, we investigated the impact of *PTEN* inactivation in the immune-cell-based response of tumors using CIBERSORT. The transcriptome of all investigated samples was imputed in CIBERSORT platform and relative scores for 22 immune-cell types was obtained. Since immune-cell abundance is linked to the presence of neoantigens, we also investigated the relationship between *PTEN* status and immunogenic mutations. Lastly, to identify potential targets in *PTEN*-deficient tumors for immunotherapy, we characterized the expression of the immune checkpoints *PD1*, *PDL1*, *CTLA4* and *IDO1* in the context of *PTEN* inactivation status. Since we are interested in investigating markers of cross-talk between tumor and immune cells, we investigated immune checkpoint expression that is exclusive to immune cells (*PD1* and *CTLA4*), and two checkpoints found in tumor cells (*PDL1* and *IDO1*).

5.2.6 Prognostic effect of *PTEN*-deficiency

To determine if *PTEN* mono- and biallelic inactivation status has a significant impact in predicting recurrence and death events, we performed survival analysis using *Survival* package in R. Log-rank tests and Kaplan Meier curves were generated through the *Survival* and *Survminer* packages in R. In addition, Cox Regression univariate models were obtained for all tumors, grouped and separately by tumor type.

5.3 Results

5.3.1 Frequency of *PTEN* somatic copy number alterations and point mutations

Our PanCancer analysis of inactivating variants in 10,713 tumors revealed that 5.7% and 2.4% of tumors presented one and both mutated *PTEN* alleles, respectively (**Figure 4a**). Copy number analysis showed that *PTEN* was homozygously deleted in 4.2% of the primary tumors. We also observed that *PTEN* had hemizygous in 24.8% of tumors. *PTEN* duplication events or 10q23.31 chromosomal gains spanning *PTEN* were found in 7.1% of tumors (**Figure 4b**). By combining *PTEN* copy number and somatic point mutations data, we classified tumors as having monoallelic and biallelic inactivation. We found that *PTEN* had biallelic inactivation in 16.7% and monoallelic inactivation in 25.9% of primary tumors (**Figure 4c**).

When each tumor type was studied individually, we found that gynecological tumors - uterine corpus endometrial cancer (UCEC) and uterine carcinosarcoma (UCS) – had high frequencies of point mutations in *PTEN* (**Figure 5a**). Glioblastomas (GBM) were found as having the second most significant percentage of one allele *PTEN* point mutations. When we investigated the copy number alterations of *PTEN*, we found that GBM had the most significant presence of *PTEN* hemizygous deletions, followed by kidney (KICH), and melanoma (SKCM) (**Figure 5b**). Moreover, as expected[120], prostate tumors showed a high percentage of *PTEN* homozygous deletions. The combination of *PTEN* point mutations and copy number data confirmed that both UCEC and UCS had the most significant percentages of *PTEN* biallelic inactivation (**Figure 5c**). In addition, this classification also demonstrated that GBM also had high frequencies of *PTEN* mono- and biallelic inactivation.

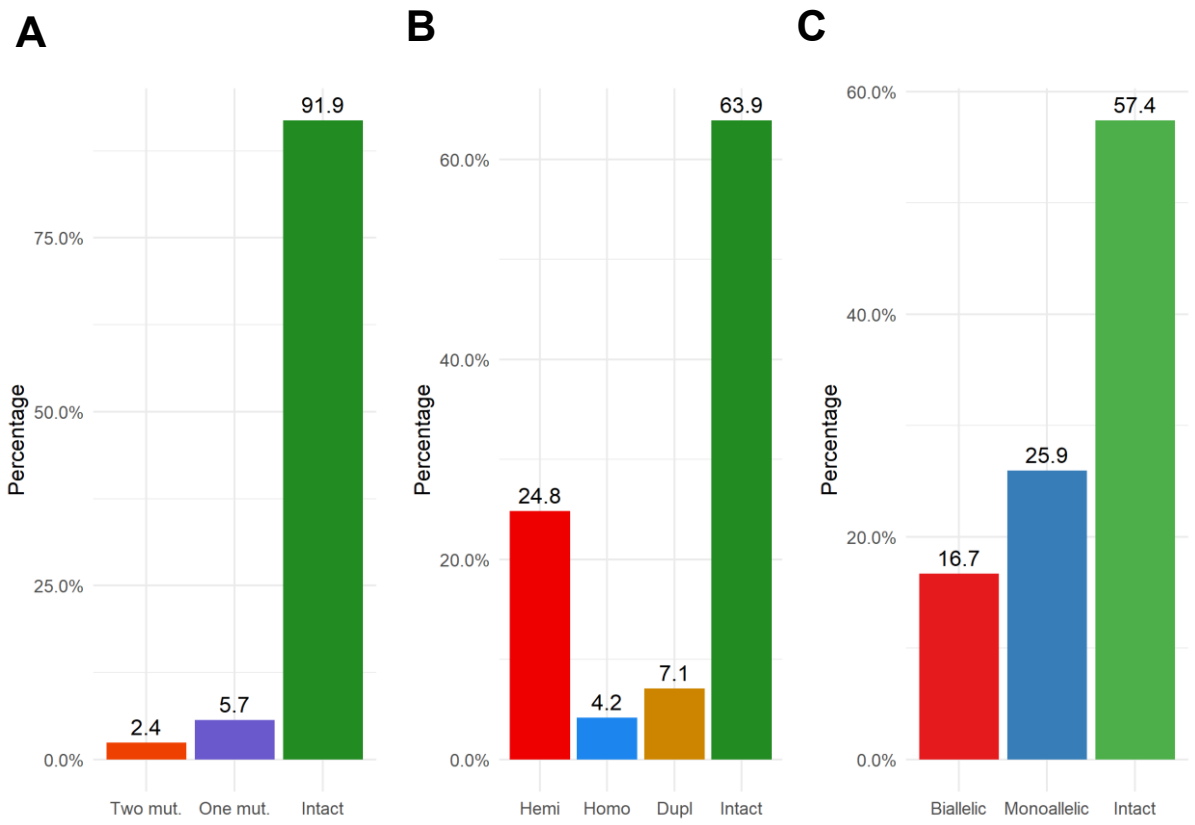

Figure 4. Percentage of *PTEN* mutation, copy number alteration, and inactivation among 33 TCGA tumor types. A – Percentage of one and two *PTEN* allele point mutations. *PTEN* biallelic somatic mutations are rare in tumors. **B** – Overall percentage of *PTEN* copy number alterations showing that *PTEN* hemizygous deletions (Hemi) are more common than *PTEN* amplifications (Dupl) and *PTEN* homozygous deletions (Homo). **C** – After combining *PTEN* somatic point mutations and *PTEN* copy number data, we classified tumors as having monoallelic and biallelic inactivation status. Monoallelic inactivation refers to tumors harboring one copy of *PTEN* mutated or lost. Biallelic inactivation was determined when tumors exhibited homozygous deletions or hemizygous deletions plus another allele with a somatic point mutation. *PTEN* amplification was considered as intact in keeping with the normal levels of *PTEN* being expressed.

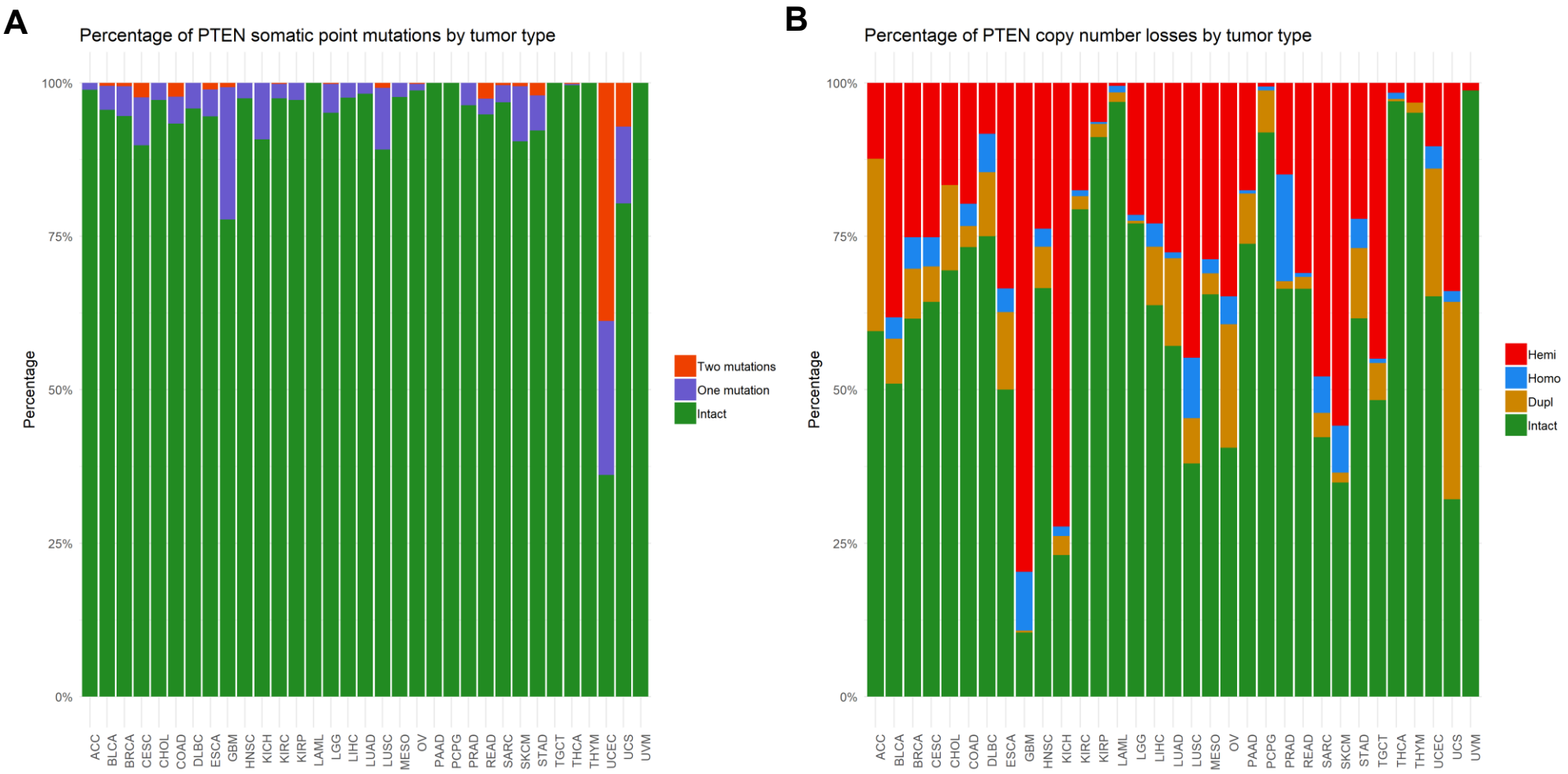
A
Percentage of PTEN somatic point mutations by tumor type
Percentage
100%
75%
50%
25%
0%
Two mutations
One mutation
Intact
ACC BLCA BRCA CESC CHOL COAD DLBC ESCA GBM HNSC KICH KIRC KIRP LAML LGG LIHC LUAD LUSC MESO OV PAAD PCPG PRAD READ SARC SKCM STAD TGCT THCA THYM UCEC UCS UVM
B
Percentage of PTEN copy number losses by tumor type
Percentage
100%
75%
50%
25%
0%
Hemi
Homo
Dupl
Intact
ACC BLCA BRCA CESC CHOL COAD DLBC ESCA GBM HNSC KICH KIRC KIRP LAML LGG LIHC LUAD LUSC MESO OV PAAD PCPG PRAD READ SARC SKCM STAD TGCT THCA THYM UCEC UCS UVM

C

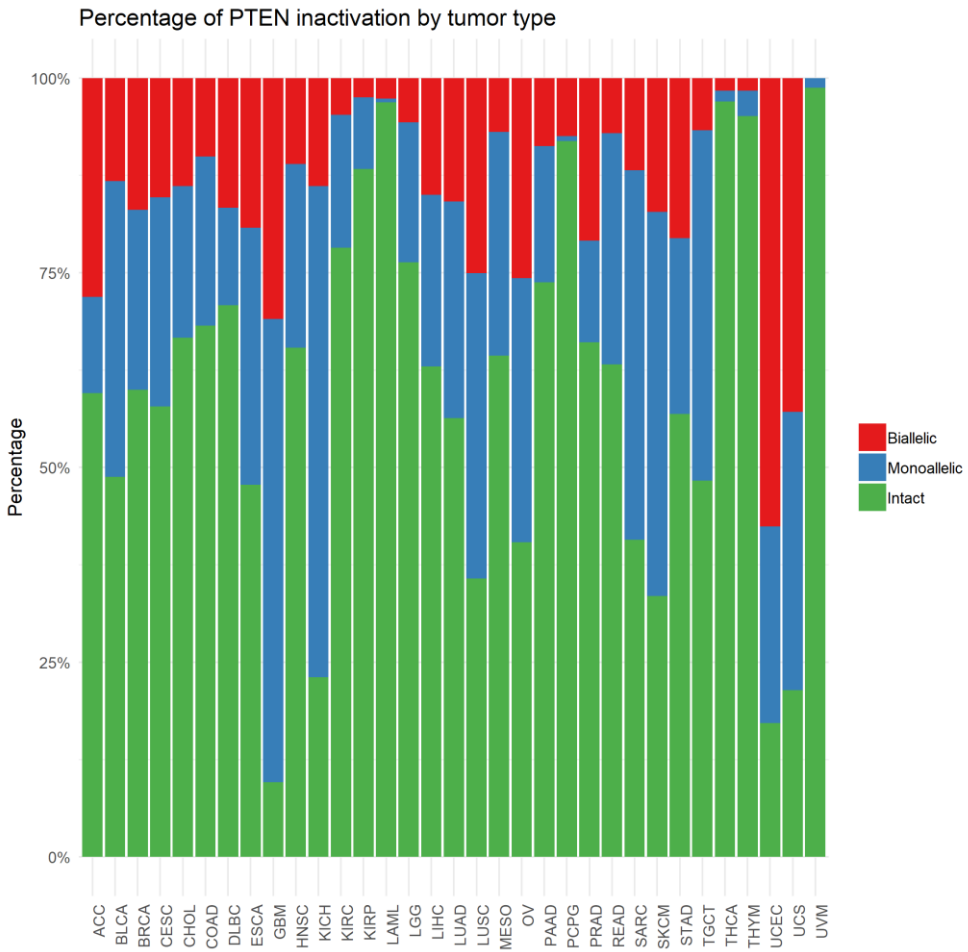
Percentage of PTEN inactivation by tumor type
Percentage
100%
75%
50%
25%
0%
ACC
BLCA
BRCA
CESC
CHOL
COAD
DLBC
ESCA
GBM
HNSC
KICH
KIRC
KIRP
LAML
LGG
LIHC
LUAD
LUSC
MESO
OV
PAAD
PCPG
PRAD
READ
SARC
SKCM
STAD
TGCT
THCA
THYM
UCEC
UCS
UVM
Biallelic
Monoallelic
Intact

Figure 5. Percentage of *PTEN* point mutations, copy number alterations and inactivation status in different types of cancer. A – Biallelic somatic mutation events are less common than monoallelic point mutations. Endometrial carcinomas (UCEC) presented the most increased percentage of *PTEN* point mutations followed by uterine carcinosarcoma (UCS). Glioblastoma (GBM) also showed high levels of *PTEN* point mutations. **B** – *PTEN* copy number analysis showed that GBM and kidney chromophobe (KICH) presented the highest levels of hemizygous deletions. Prostate cancer (PRAD) presented the most proeminent *PTEN* homozygous deletion percentage, followed by lung squamous cell carcinoma (LUSC) and GBM. **C** – The combination of *PTEN* point mutations and *PTEN* copy number status provides an overall incidence plot that shows that the majority of tumor types harbor *PTEN* monoallelic inactivation. ACC - Adrenocortical carcinoma, BLCA - Bladder Urothelial Carcinoma, LGG - Brain Lower Grade Glioma, BRCA - Breast invasive carcinoma, CESC - Cervical squamous cell carcinoma and endocervical adenocarcinoma, CHOL - Cholangiocarcinoma, LCML - Chronic Myelogenous Leukemia, COAD - Colon adenocarcinoma, ESCA - Esophageal carcinoma, HNSC - Head and Neck squamous cell carcinoma, KIRC - Kidney renal clear cell carcinoma, KIRP - Kidney renal papillary cell carcinoma, LAML - Acute Myeloid Leukemia, LIHC - Liver hepatocellular carcinoma, LUAD - Lung adenocarcinoma, DLBC - Lymphoid Neoplasm Diffuse Large B - cell Lymphoma, MESO - Mesothelioma, OV - Ovarian serous cystadenocarcinoma, PAAD - Pancreatic adenocarcinoma, PCPG - Pheochromocytoma and Paraganglioma, READ - Rectum adenocarcinoma, SARC - Sarcoma, SKCM - Skin Cutaneous Melanoma, STAD - Stomach adenocarcinoma, TGCT - Testicular Germ Cell Tumors, THYM - Thymoma, THCA - Thyroid carcinoma, UCEC - Uterine Corpus Endometrial Carcinoma, UVM - Uveal Melanoma.

5.3.2 Genome landscape of PTEN-deficient tumors

PTEN has been shown to regulate several mechanisms of chromosome stability and cell proliferation. Thus, we characterized the differential SCNA profile of tumors by comparing tumors with monoallelic and biallelic *PTEN* inactivation to those that were *PTEN* intact. The SCNA and mutational burden analyses are still under development.

To identify associations between *PTEN* inactivation status and genomic features of 33 tumor types, we compared the presence of genome doublings (ploidy) and aneuploidy levels in tumors previously characterized as having monoallelic or biallelic *PTEN* inactivation or having *PTEN* intact status (**Figure 4c** and **5c**). Our PanCancer analysis showed two clusters of tumors – one with 2N (normal DNA content) and others with 4N (entire genome doubling). Tumors harboring *PTEN* biallelic inactivation showed generally higher levels of ploidy and a higher number of tumors with a genomic contents that approached tetraploidy, as seen in the violin plots (**Figure 6a**). However, when we stratified these samples by tumor type, some tumor types presenting *PTEN* monoallelic inactivation status had higher overall levels of chromosomal instability (**Figure 6b**), such as ACC, BRCA, and SKCM.

The analysis of aneuploidy scores – defined as the presence of large chromosome aberrations, demonstrated that *PTEN*-monoallelic-inactive tumors have a significant increase in general levels of aneuploidy (**Figure 7a**). However, when categorized by tumor type, we observed that the majority of tumors with biallelic *PTEN* inactivation status had higher levels of aneuploidy (**Figure 7b**). Brain tumors (LGG and GBM) showed the lowest aneuploidy levels together with prostate cancer. However, we did not find a similar pattern of *PTEN* inactivation and aneuploidy levels in these malignancies. Moreover, we found a significant association between *PTEN* inactivation and aneuploidy in 27 of the 33 investigated tumor types (**Figure 7b).**

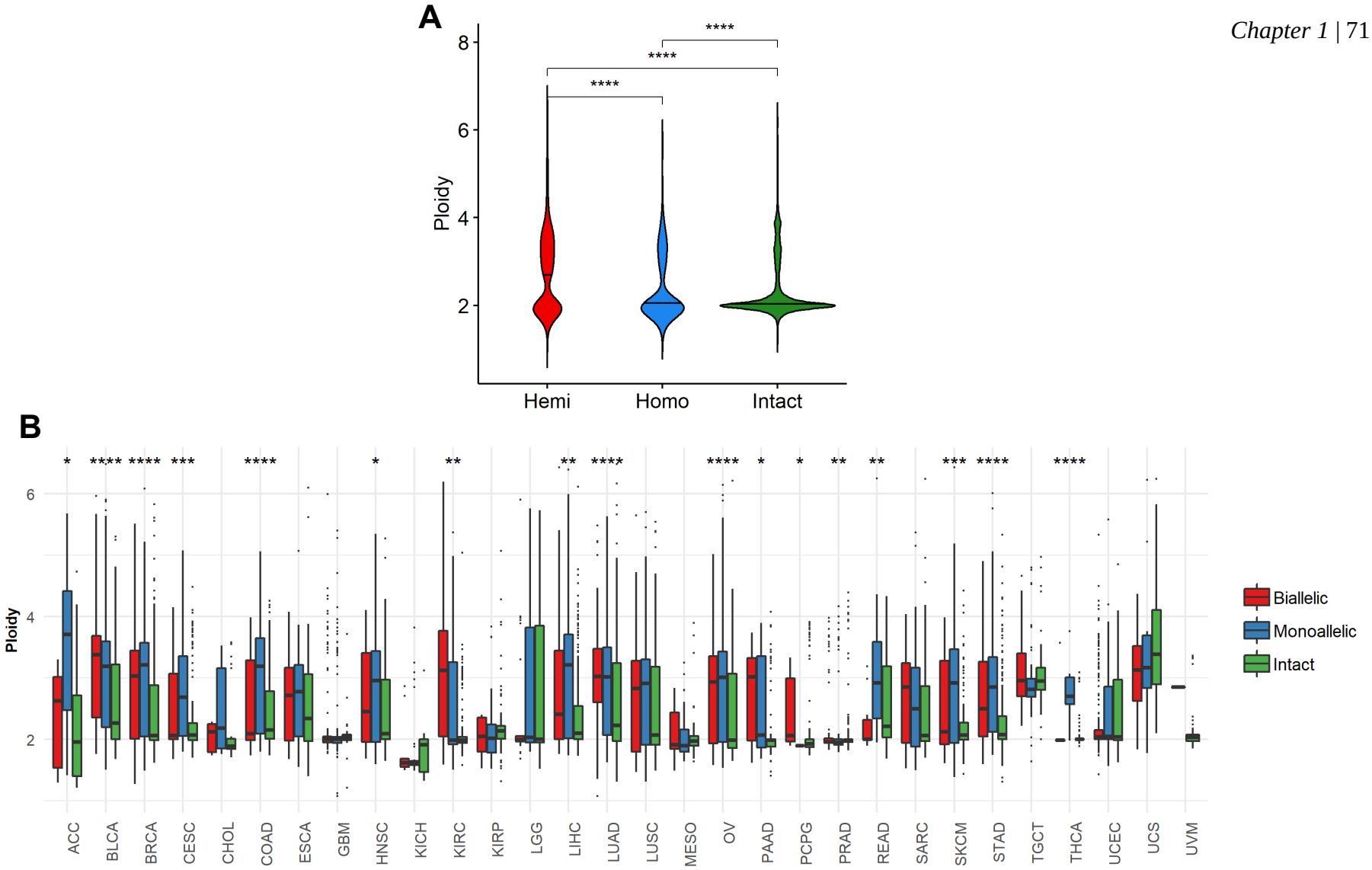

Figure 6. Effect of *PTEN* inactivation on ploidy. Ploidy levels equal to two show normal DNA content, while four shows a complete DNA content duplication. **A** shows the results for all 10,713 tumors and **B** shows results by tumor type. Monoallelic inactivation of *PTEN* was linked to higher levels of ploidy, except in bladder cancer (BLCA), sarcomas (SARC), and testicular tumors (TGCT). Lines in violin plots show the median. Asterisks evidence the P-values derived from Kruskal Wallis test. *P<0.05. **P<0.01. ***P<0.001. ****P<0.0001.

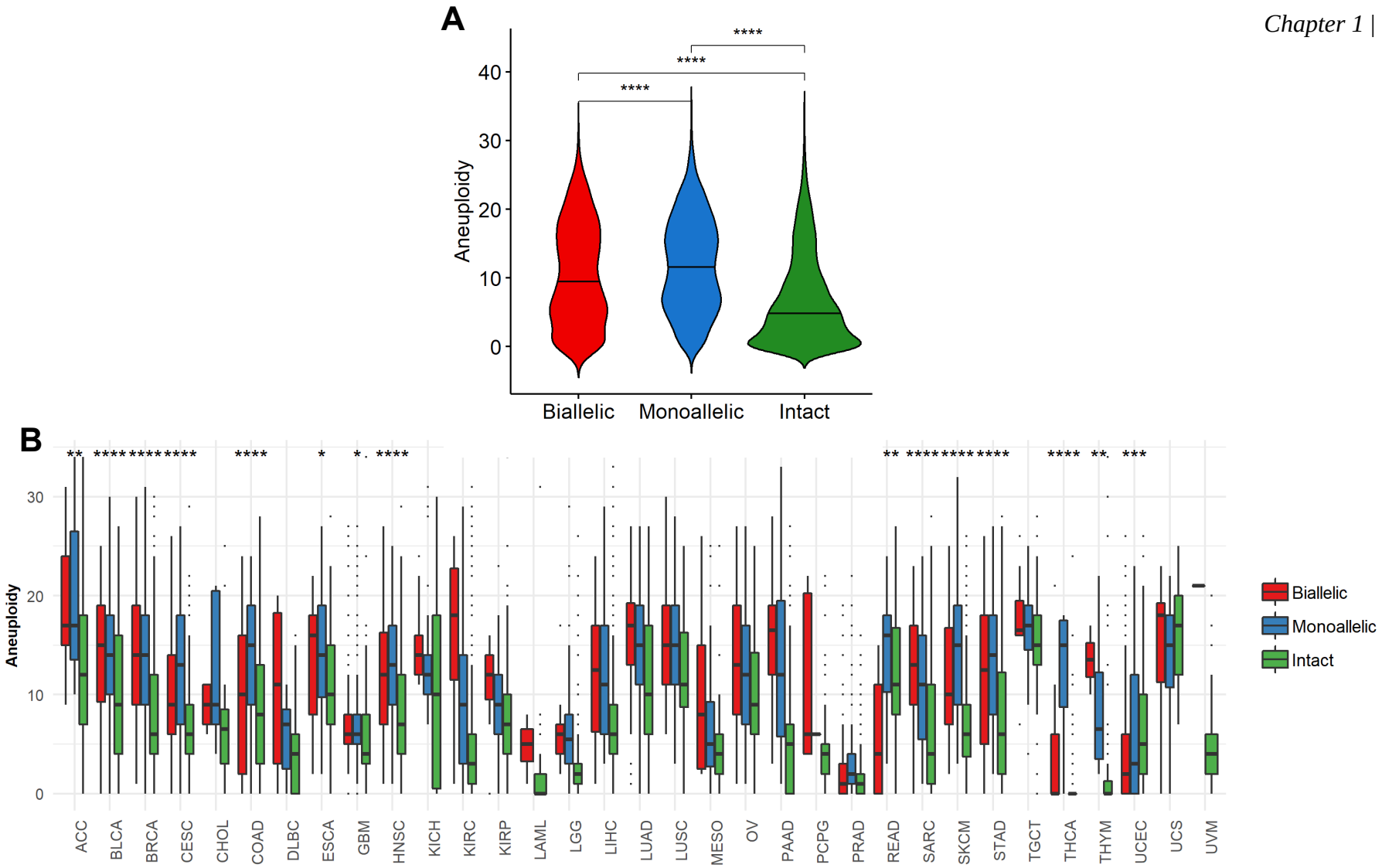

Figure 7. Association between aneuploidy levels and *PTEN* inactivation status. A – *PTEN* inactivation is significantly associated with increased levels of aneuploidy. **B** – Aneuploidy score stratified by tumor type shows that PTEN biallelic inactivation was linked to higher aneuploidy levels in several tumors. Prostate and brain tumors showed the lowest levels of aneuploidy across tumor types. Aneuploidy levels were determined based on the length of copy number alterations and normalized by tumor type. The scores range from 0, which indicates low levels of chromosome aberrations (copy number gains and losses). On the other hand, high levels of aneuploidy indicate that the genome of these tumors are highly altered, with larger chromosome gains and losses occurring. Lines in violin plots show the median. Asterisks show the P-values derived from Kruskal Wallis test. *P<0.05. **P<0.01. ***P<0.001. ****P<0.0001.

Since genomic instability may result from an abnormal chromosome repair and segregation, we investigated the impacts of *PTEN* inactivation status in homologous recombination defects (HDR). Both *PTEN* monoallelic and biallelic status showed increased significant levels of HDR when compared to *PTEN*-intact tumors (**Figure 8**). Twenty-four out of the 33 investigated malignancies showed a significant association between *PTEN* inactivation and HDR levels. In addition, similar patterns of HDR were observed across the 33 studied tumor types.

Our PanCancer analysis revealed that the levels of nonsilent mutations in PTEN-deficient tumors were higher than in *PTEN*-intact tumors (**Figure 9**). When stratified by tumor type, we found that the levels of nonsilent mutations and intratumor heterogeneity were more elevated in tumor samples with monoallelic *PTEN* inactivation (**Figure 9b** and **Figure 10b**). Moreover, we did not observe significant associations when we compared the presence of nonsilent mutations and intratumor heterogeneity across malignancies.

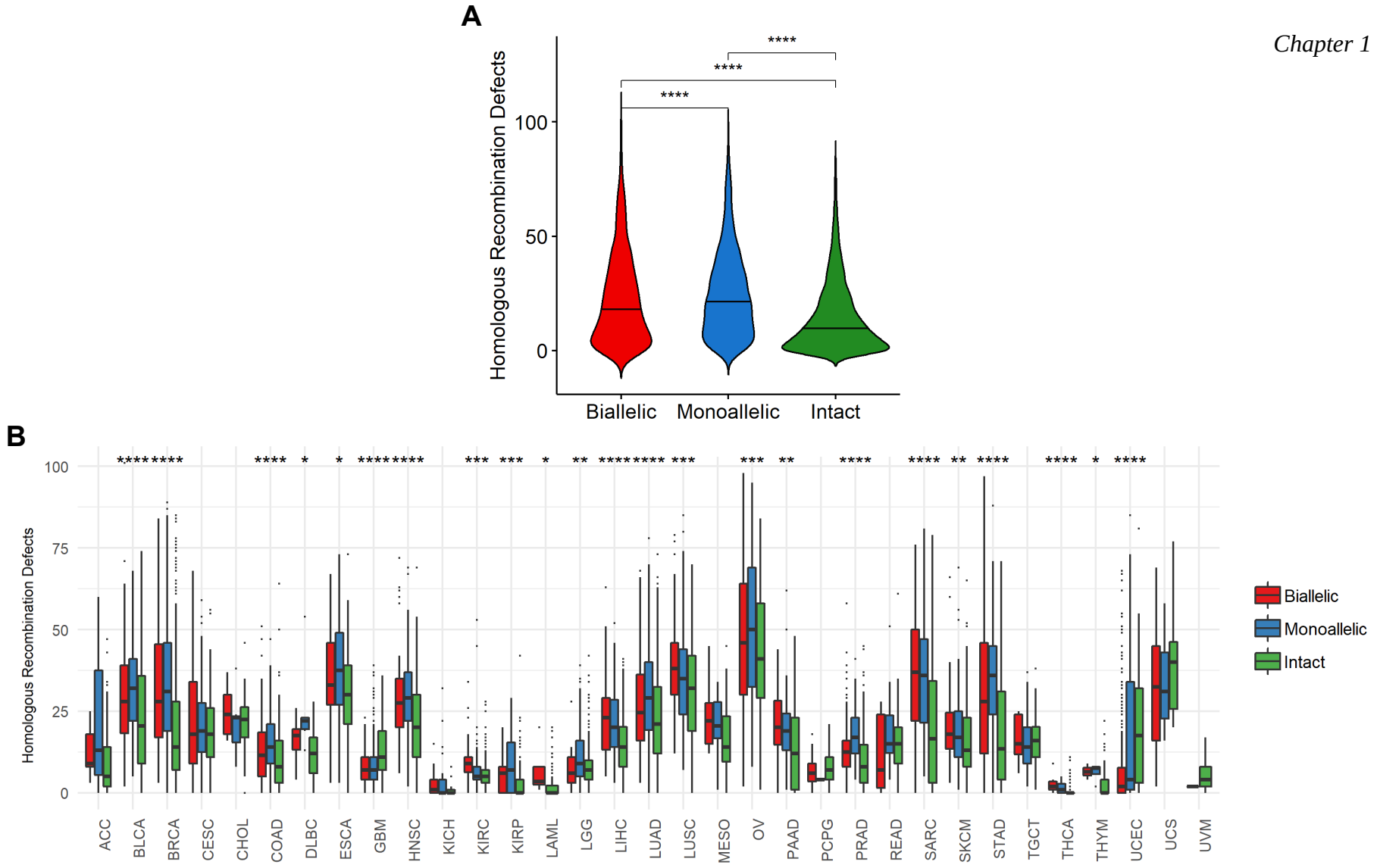

Figure 8. Effect of *PTEN* inactivation on the number of homologous recombination defects (HDR) in the entire TCGA cohort (A) and stratified by malignancy (B). HDR were determined based on copy number alterations through ABSOLUTE algorithm (see methods for more details). As observed in ploidy levels, HRD are more frequently high in tumors with monoallelic *PTEN* inactivation. Lines in violin plots show the median. Asterisks show the P-values derived from Kruskal Wallis test. *P<0.05. **P<0.01. ***P<0.001. ****P<0.0001.

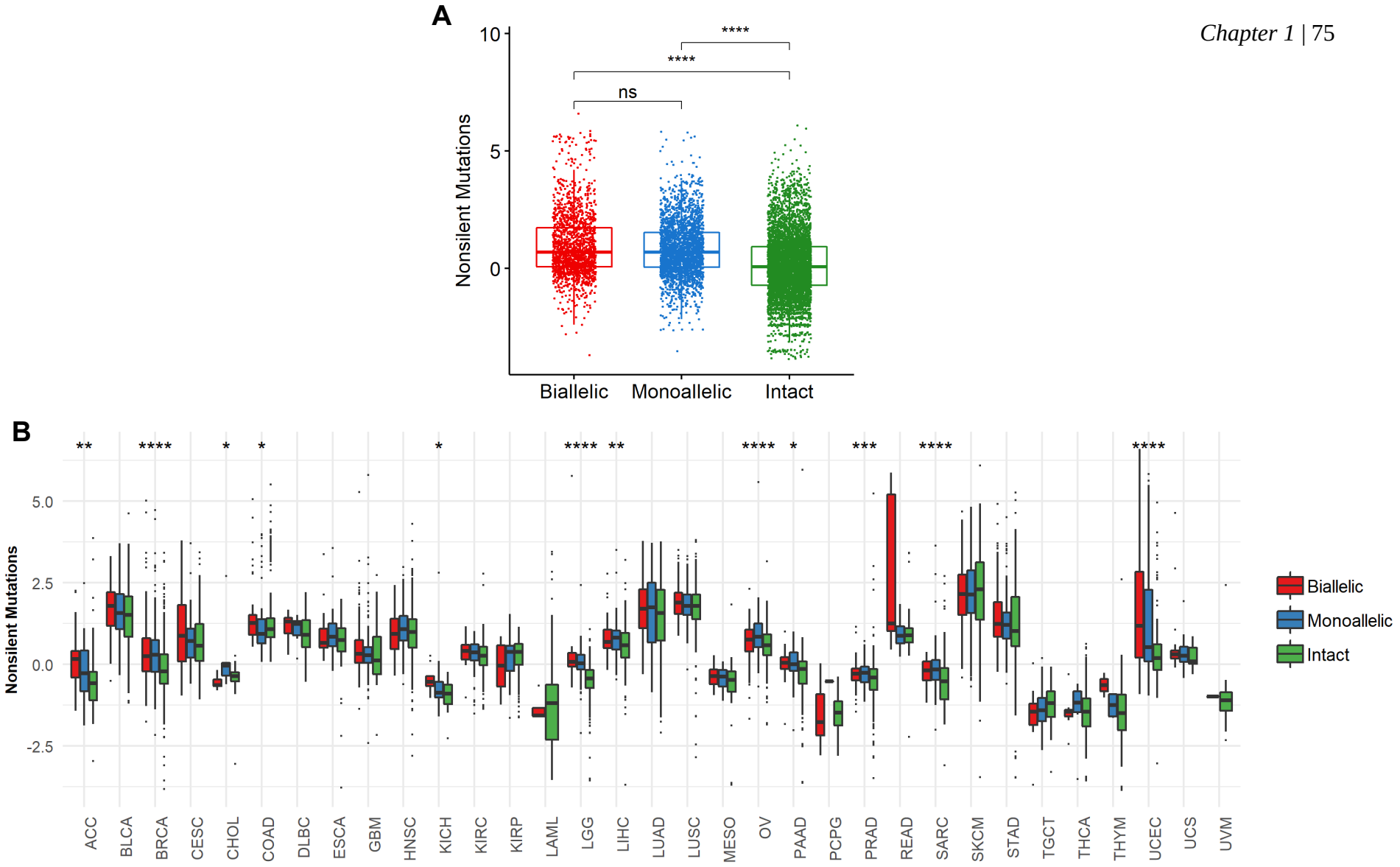

Figure 9. Correlations between *PTEN* inactivation and tumor mutation burden represented by the number of nonsilent mutations. A show the PanCancer results for the associations between *PTEN* inactivation and frequency of nonsilent mutations. **B** shows the nonsilent mutation levels per tumor type. Nonsilent mutations were log-normalized for better visualization. Thus, the scores vary from negative levels to positive values. Asterisks show the P-values derived from Kruskal Wallis test. *P<0.05. **P<0.01. ***P<0.001. ****P<0.0001.

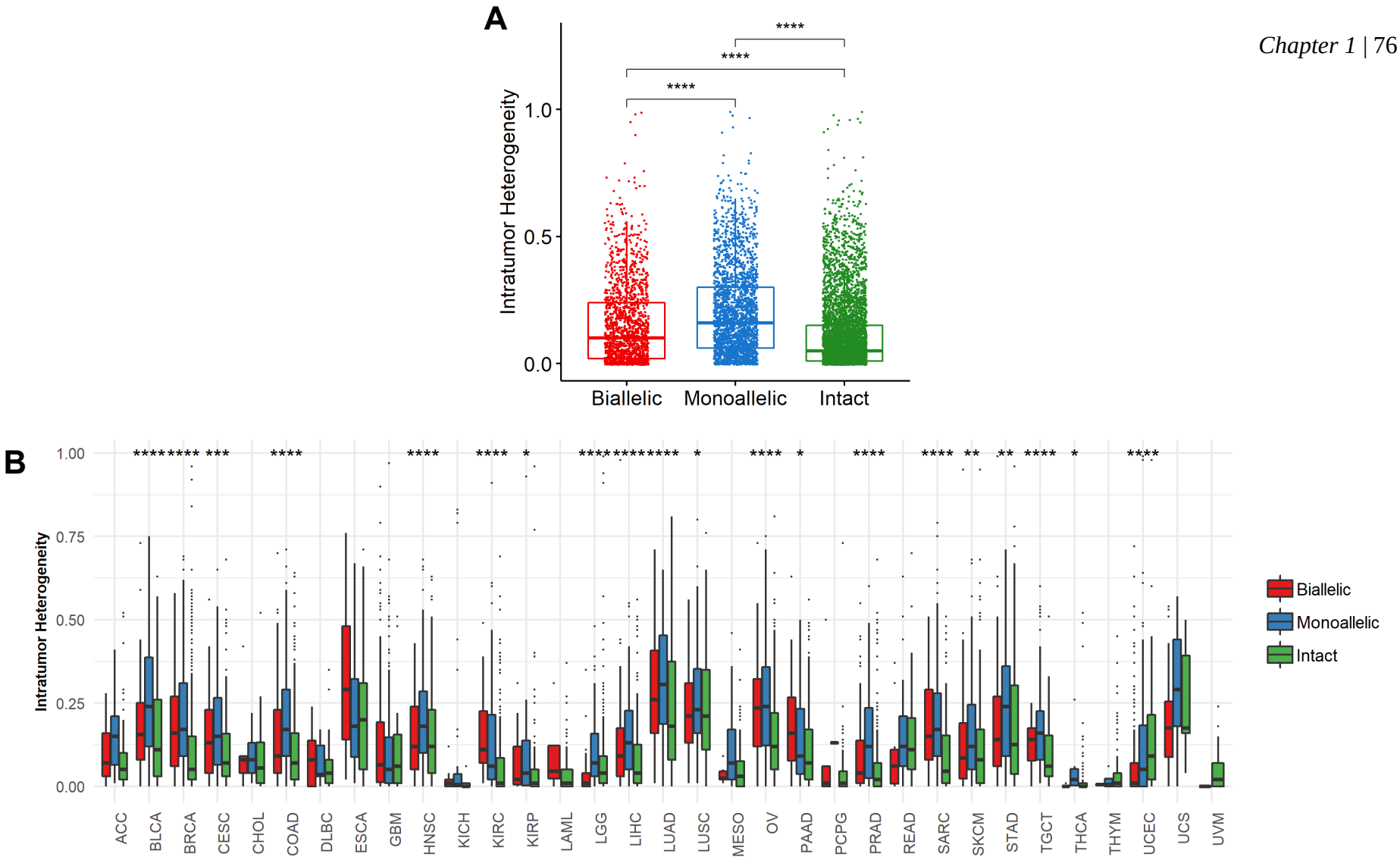

Figure 10. Association between *PTEN* inactivation and tumor heterogeneity. A shows the PanCancer results for the associations between *PTEN* inactivation and intratumoral heterogeneity levels. **B** shows intratumor heterogeneity scores (defined as number the number of copy number alterations and point mutations given by clonal and subclonal components of tumors) per tumor type. Monoallelic tumors showed higher levels of intratumor heterogeneity across most cancer types. Asterisks show the P-values derived from Kruskal Wallis test. *P<0.05. **P<0.01. ***P<0.001. ****P<0.0001.

Considering that tumors with *PTEN* monoallelic inactivation status were remarkably associated with enhanced levels of genomic instability, we investigated whether tumors with hemizygous deletions also exhibit similar patterns of instability across 33 tumor types. By characterizing *PTEN* somatic copy number status, we observed that tumors with *PTEN* hemizygous deletions showed the most significant levels of ploidy, aneuploidy, and intratumoral heterogeneity (**Figure 11a, Figure 11b**, and **Figure 11c**, respectively).

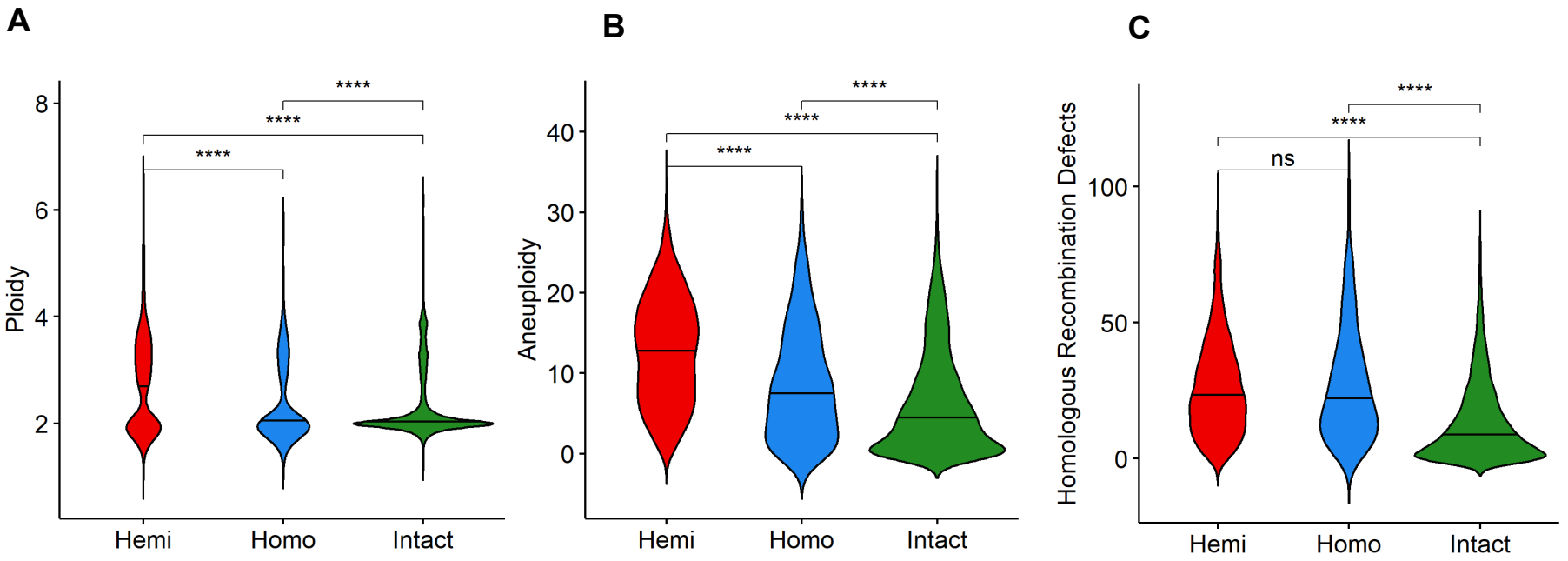

Figure 11. Ploidy, aneuploidy and intratumoral heterogeneity levels by *PTEN* somatic copy number alteration status. A, **B**, and **C** panels show the associations between *PTEN* copy number and ploidy, aneuploidy, and HRD, respectively. We found that tumors harboring *PTEN* duplications or hemizygous deletions are significantly associated with genomic instability features. Asterisks show the P-values derived from Kruskal Wallis test. *P<0.05. **P<0.01. ***P<0.001. ****P<0.0001.

5.3.3 The impact of *PTEN*-deficiency on the immune response across cancers

To identify genes that may be significantly associated with active downstream signaling pathways as a consequence of *PTEN* inactivation, we compared the transcriptome profile of tumors with *PTEN* biallelic and monoallelic inactivation with those with retained *PTEN* expression. This analysis is still ongoing. An enrichment analysis will be performed with the top differentially expressed genes through the GSEA algorithm.

Since *PTEN* plays a primary role in activating the IFN response and cytokine secretion, we performed a combined parallel study of the genomics of tumor cells and associated immune cells to investigate whether the type of *PTEN* inactivation (monallelic vs biallelic) correlated with specific immunogenomic features of tumors. Tumors with *PTEN* biallelic inactivation status had higher rates of SNV neoantigens (**Figure 12a**). Thus, it is expected that more immunogenic tumors – characterized by increased levels of neoantigens – may exhibit more immune cells in the tumor microenvironment[27,130].

We did not identify significant associations between *PTEN* inactivation status and leukocyte fractions when all tumor samples were grouped (**Figure 13a**). However, the stratification by tumor type showed that *PTEN* intact tumors exhibited the most significant leukocyte fraction levels for adrenocortical (ACC), head and neck (HNSC), lung (LUAD and LUSC), pancreas (PAAD), and stomach (STAD) cancers (**Figure 13b**). In contrast, brain tumors showed high leukocyte density when *PTEN* underwent biallelic inactivation events (**Figure 13b**).

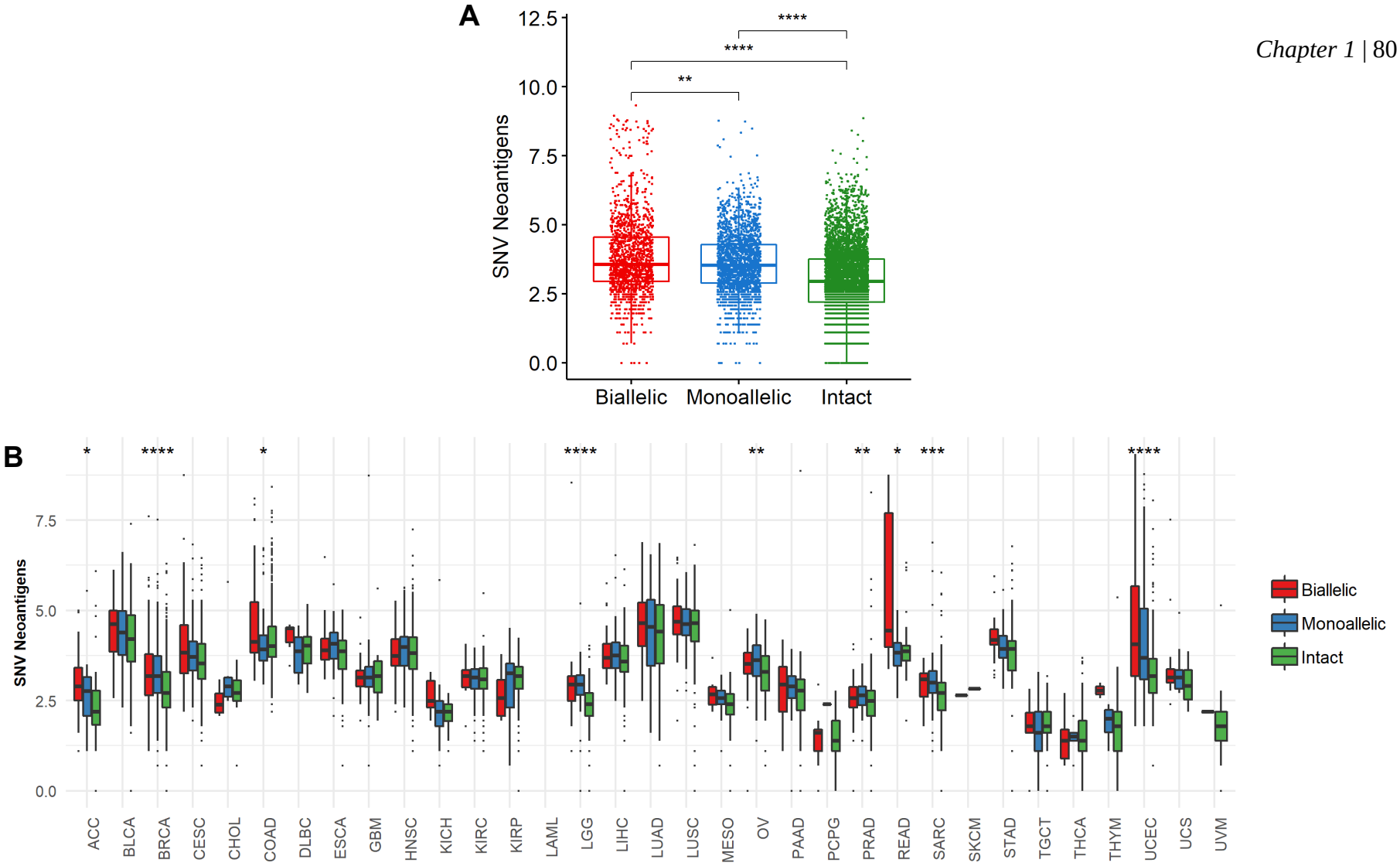

Figure 12. Effect of *PTEN* inactivation on the number of single nucleotide variation (SNV) neoantigens in the whole cohort and stratified by tumor type. A – PanCancer results for SNV neoantigens levels. **B** – Neoantigen burden levels stratified by tumor type. SNV neoantigens were determined based on mutated and expressed peptides with potential scores to acting as antigens derived from NetMHCpan v3.0. SNV neoantigens levels are shown in log scale. Tumors with any *PTEN* inactivation status presented higher number of SNV neoantigens. Note the similarities between low grade gliomas (LGG) and prostate cancer (PRAD). Asterisks show the P-values derived from Kruskal Wallis test. *P<0.05. **P<0.01. ***P<0.001. ****P<0.0001.

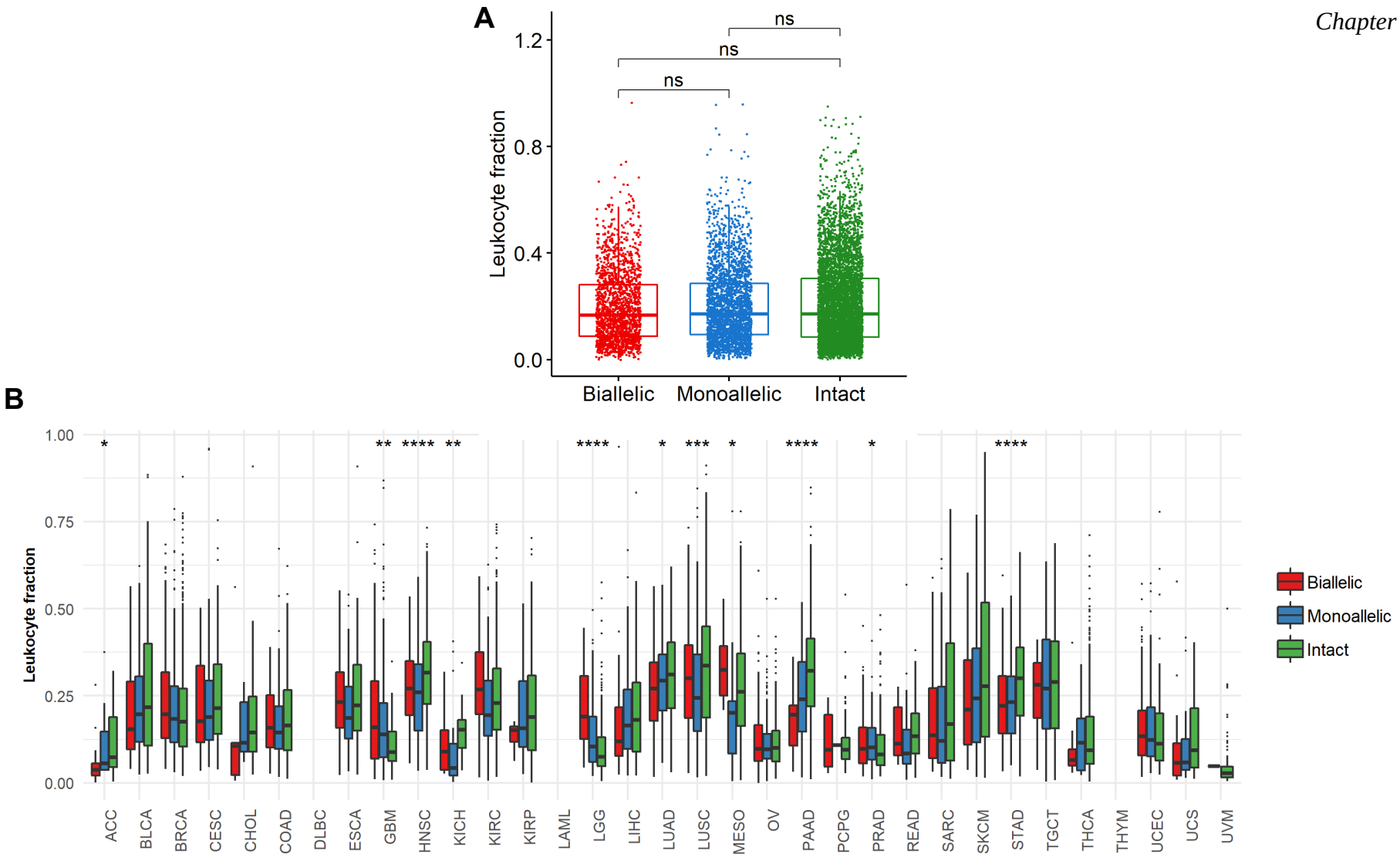

Figure 13. Leukocyte fractions in the PanCancer cohort (A) and by malignancy (B). Leukocyte fraction is a measurement of tumor purity. Higher scores of leukocyte fraction is indicative of high quantity of leukocyte within sampled tumor lesions. By grouping all tumor types, we did not observe a significant effect of *PTEN* inactivation in leukocyte fraction. Interestingly, brain tumors (GBM and LGG) presented high levels of leukocyte fraction when both *PTEN* alleles were inactive. Asterisks show the P-values derived from Kruskal Wallis test. *P<0.05. **P<0.01. ***P<0.001. ****P<0.0001.

The analysis of the immune cell composition of tumors showed that tumors with biallelic *PTEN* inactivation had a higher abundance of regulatory T cells (Treg) (**Figure 14a**). However, by separately analyzing each tumor type, we found that significant associations were only observed for a subset of tumors (**Figure 14b**). For CD8+ T cell abundance, we found that thyroid tumors (THDA) with biallelic *PTEN* inactivation exhibited an enhanced abundance of CD8+ T cells across tumor types (**Figure 15a-b**). Other tumors exhibited an unclear difference regarding CD8+ T cell abundance on *PTEN* deficient vs. intact cancers. Moreover, head and neck tumors harboring *PTEN* monoallelic inactivation showed a significant decrease in CD8+ T cell abundance.

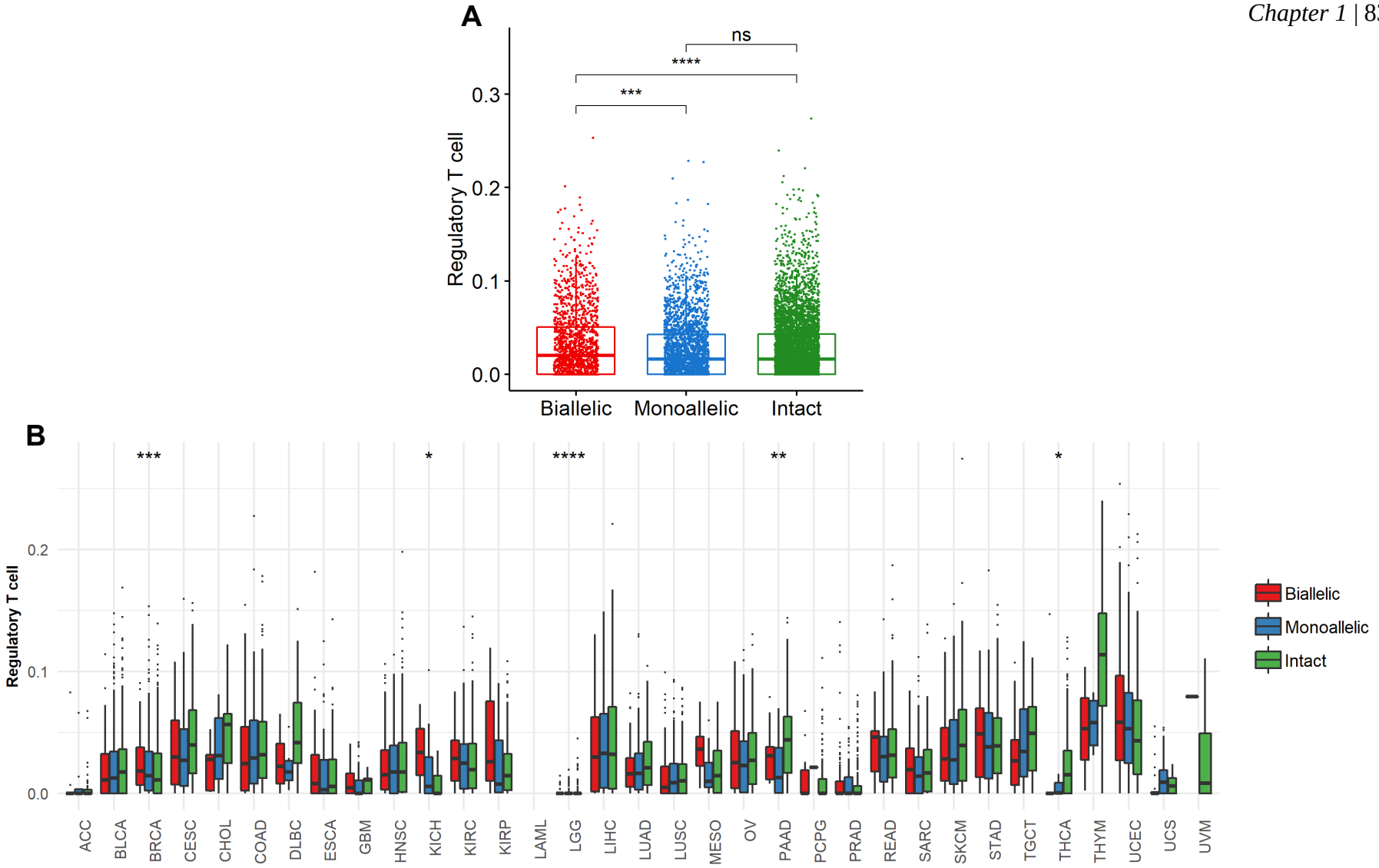

Figure 14. CIBERSORT-derived regulatory T cell (Treg) abundance ratios. A – PanCancer analysis shows that *PTEN* biallelic inactivation is linked to high levels of Treg abundance. When stratified by tumor type (**B**), *PTEN* biallelic inactivation was linked to high Treg density in breast (BRCA) and kidney (KICH) tumors. Y-axis shows the relative CIBERSORT scores for Treg abundance. Asterisks show the P-values derived from Kruskal Wallis test. *P<0.05. **P<0.01. ***P<0.001. ****P<0.0001.

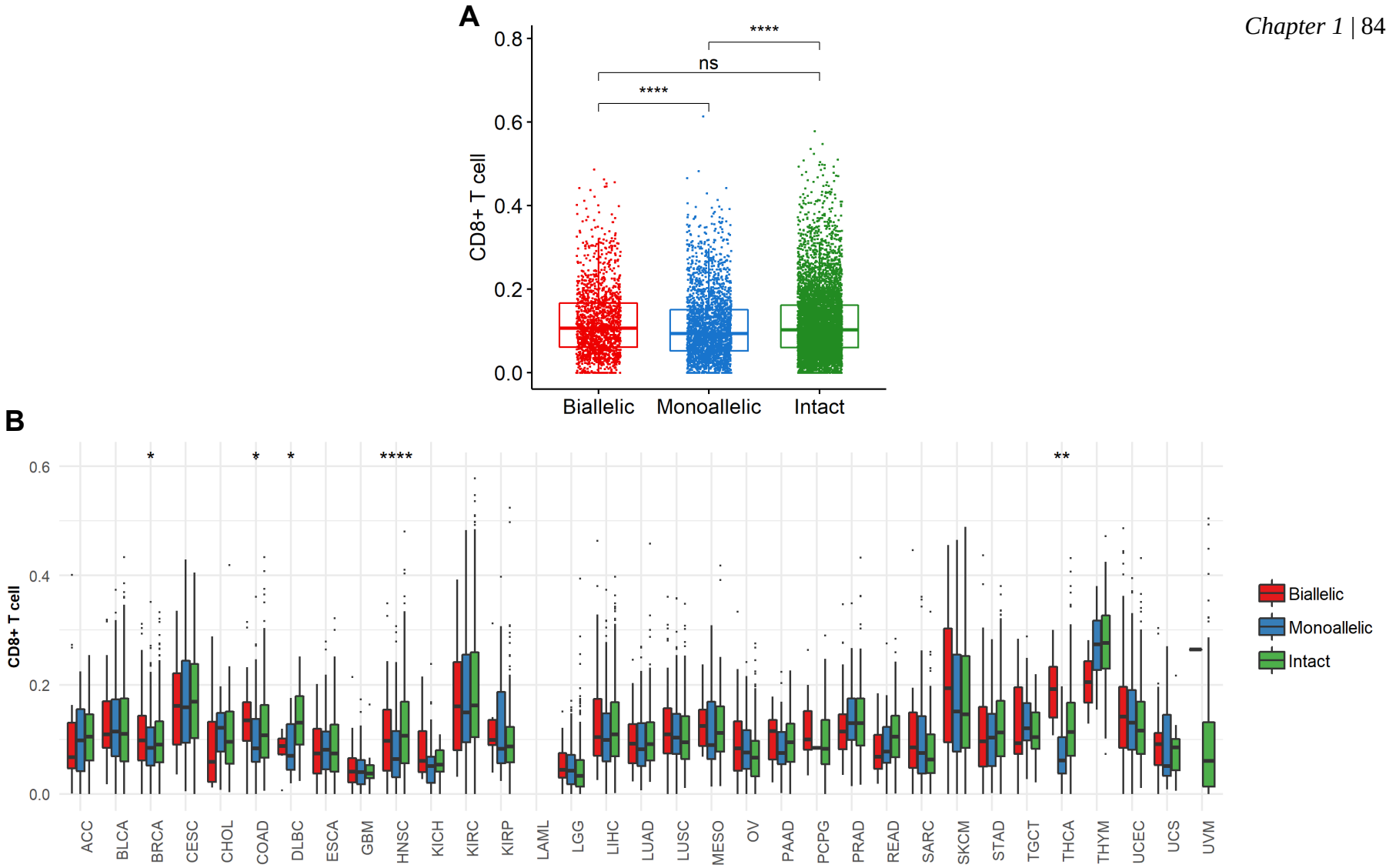

Figure 15. CIBERSORT-derived CD8+ T-cell abundance ratios. A – CD8+ T-cell abundance is decreased in tumors harboring *PTEN* monoallelic inactivation. **B** – The stratification by tumor type shows that all tumors with significant associations between *PTEN* inactivation and CD8+ T-cell abundance have low levels of these cells when *PTEN* underwent monoallelic inactivation. Y-axis shows relative CIBERSORT CD8+ T-cell abundance scores. Asterisks show the P-values derived from Kruskal Wallis test. *P<0.05. **P<0.01. ***P<0.001. ****P<0.0001.

Since *PTEN* is linked to the activation of the type I interferon (IFNI) signaling pathway[11], we investigated the associations between *PTEN* inactivation and downstream IFNI proteins, such as *JAK1*, *JAK2*, *IFNG*, *IFNB*, and the transcription factors *STAT1* and *STAT3*. RNA expression of the molecules mentioned earlier was investigated since protein data for these targets is unavailable through TCGA data portal. Our PanCancer analysis showed that *PTEN* biallelic inactivation was linked to increased *IRF3*, *IFNG*, *IFNB*, *STAT1*, and *STAT3* mRNA expression (**Figure 16**). Conversely, *JAK1* and *JAK2* were downregulated in cancers presenting *PTEN* biallelic inactivation. When stratified by tumor type, gliomas and prostate cancer showed highly distinct opposite profiles of *IRF3* expression, with tumors with biallelic inactivation presenting high vs. low *IRF3* expression in glioma and prostate, respectively (**Figure 17a**). Moreover, head and neck tumors harboring *PTEN* monoallelic inactivation exhibited significantly reduced expression levels of *IRF3*, *STAT1*, and *STAT3*.

In the same way, *STAT1* and *STAT3* expression showed opposite patterns for gliomas and prostate tumors (**Figure 17b-c**). *JAK1* downregulation was consistently observed in *PTEN*-biallelic-inactive tumors in the majority of cancer types, similarly to *JAK2* expression (**Figure 17d-e**).

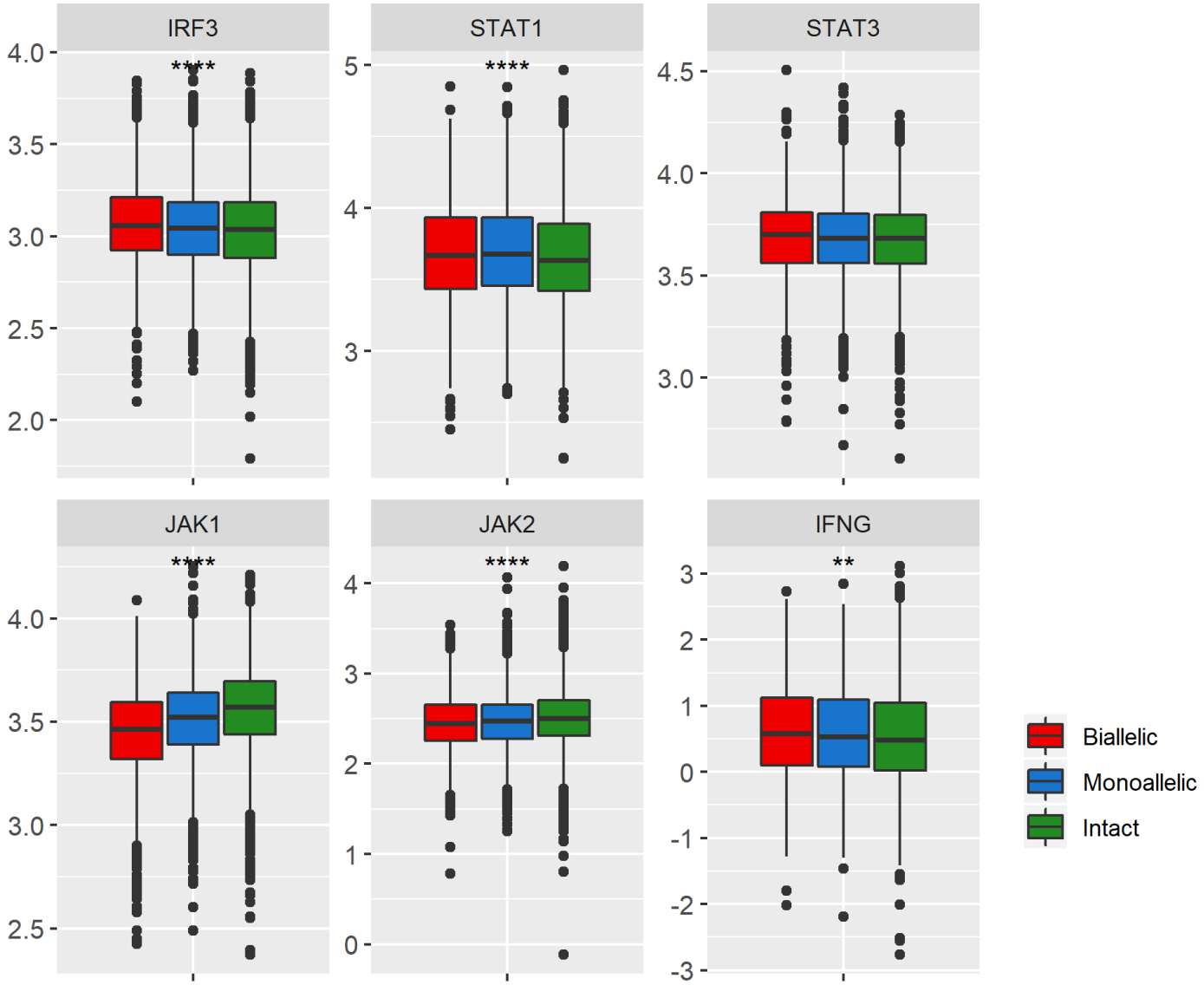

Figure 16. Effect of *PTEN* inactivation status on the expression of interferon response-related genes. Asterisks show the P-values derived from Kruskal Wallis test. *P<0.05. **P<0.01. ***P<0.001. ****P<0.0001. Y-axis shows RSEM-normalized RNAseq gene expression levels. Log-normalization was used for better visualization of results.

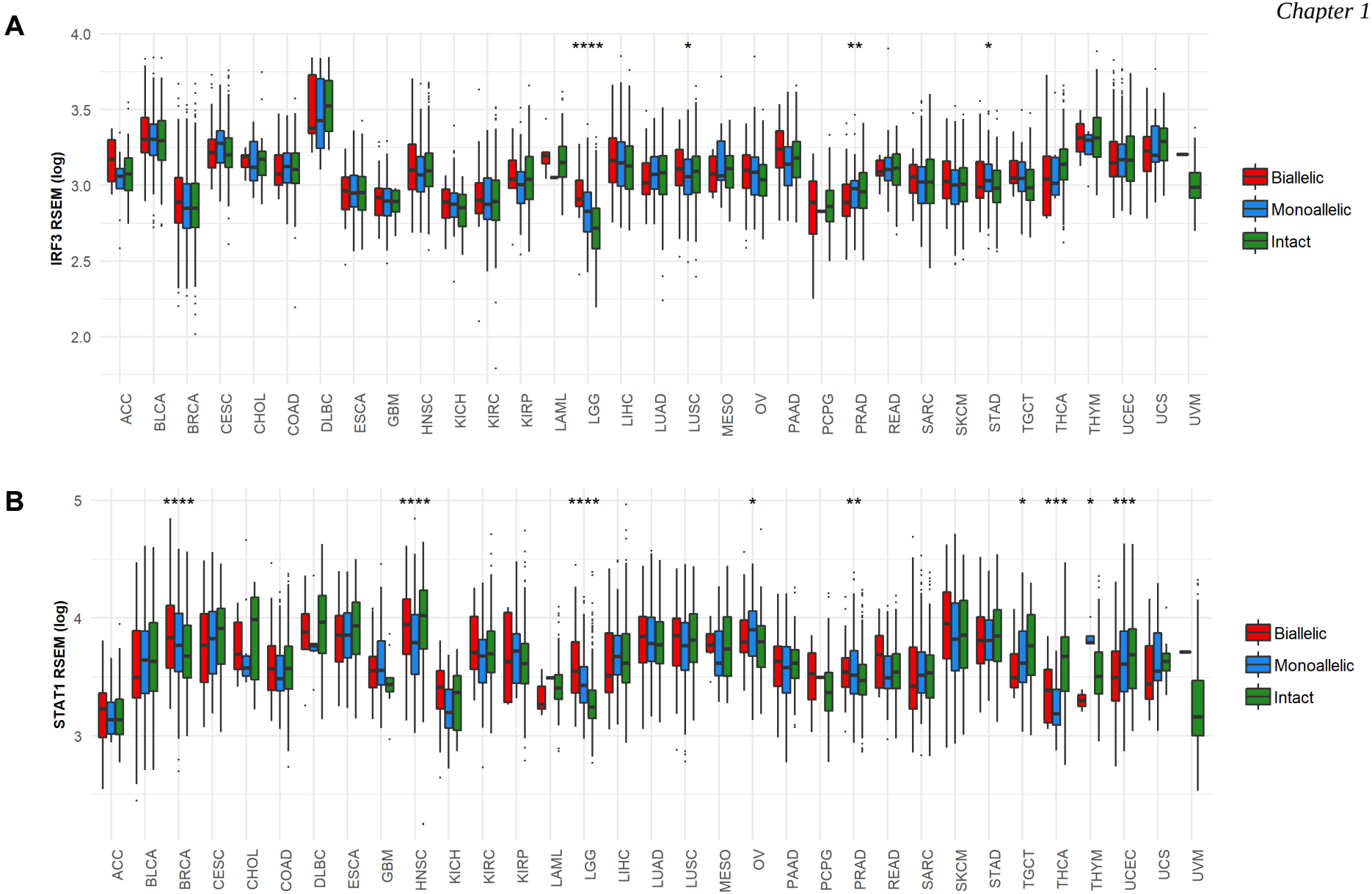

Figure 17. Expression of interferon-related genes in *PTEN* inactive and intact tumors stratified by cancer type. We observed that *PTEN* biallelic inactivation was significantly associated with increased *IRF3* (**A**), *STAT1* (**B**), and *STAT3* (**C**) expression. *JAK1* (**D**) and *JAK2* (**E**) expression was reduced in tumors harboring biallelic inactivation of *PTEN*. *IFNG* expression (**F**) was not consistent among cancer types. Y-axis shows RSEM-normalized RNAseq gene expression levels. Log-normalization was used for better visualization of results. Asterisks show the P-values derived from Kruskal Wallis test. *P<0.05. **P<0.01. ***P<0.001. ****P<0.0001. Continues.

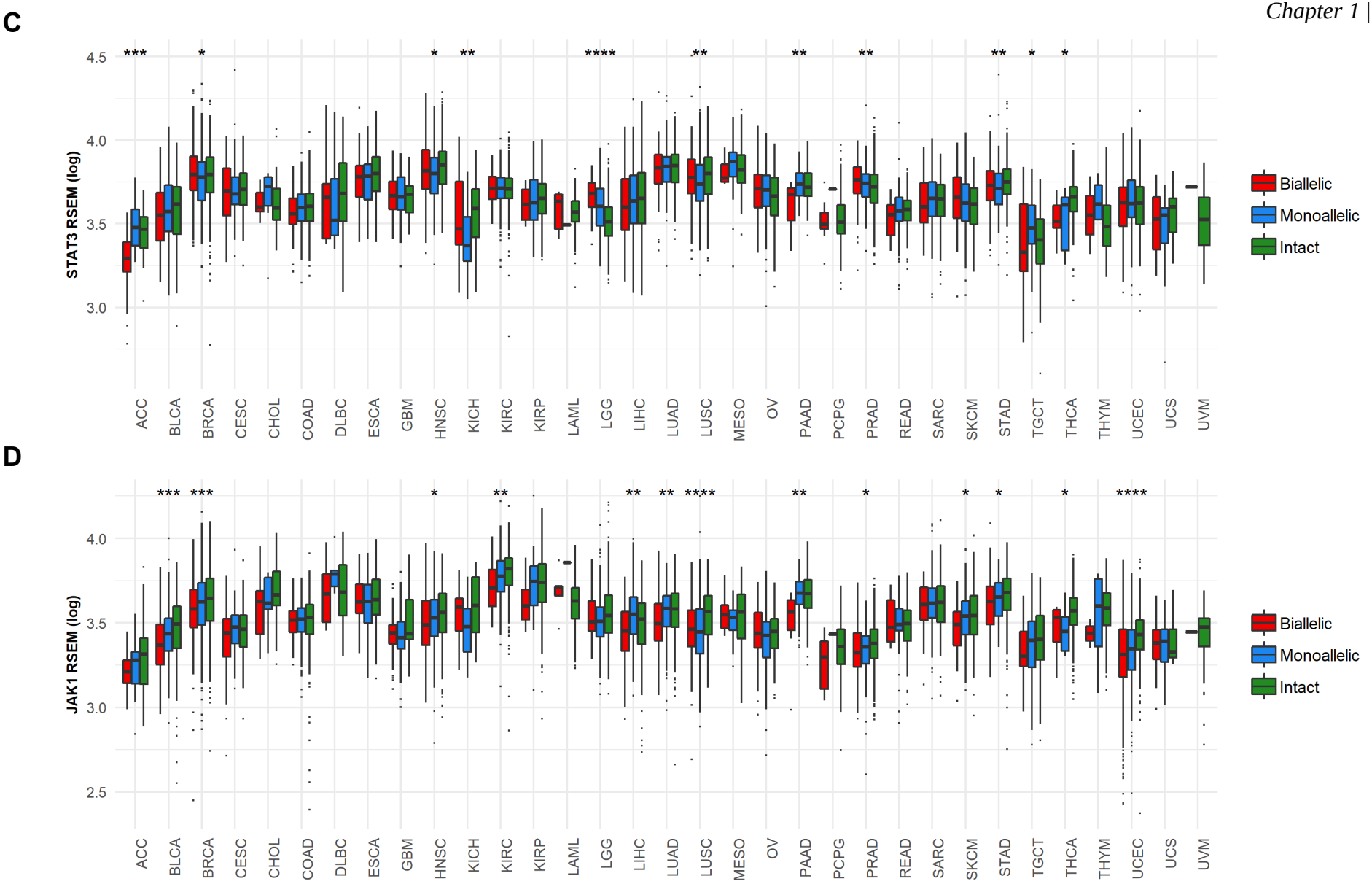

Figure 17. Expression of interferon-related genes in *PTEN* inactive and intact tumors stratified by cancer type. Continues.

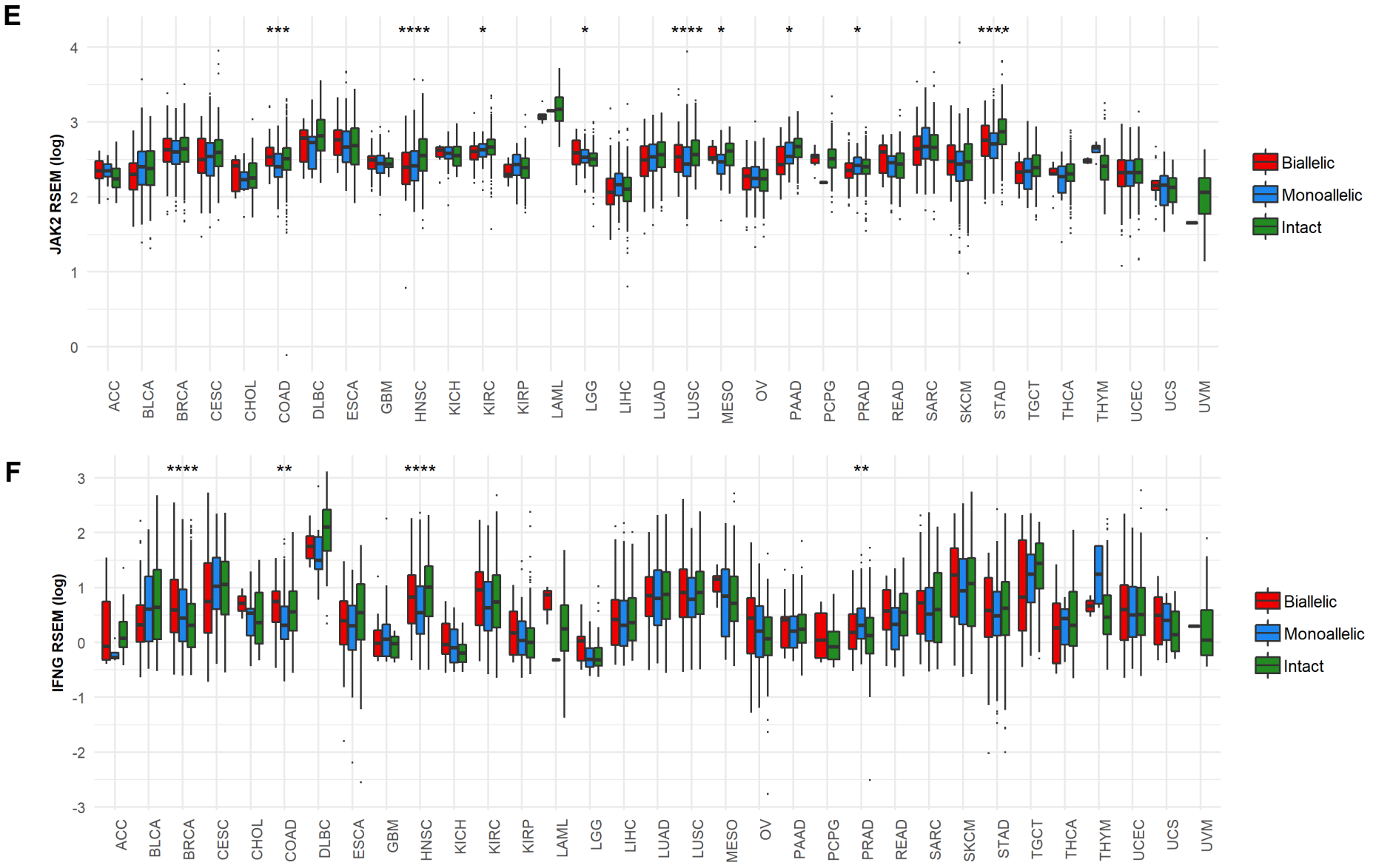

Figure 17. Expression of interferon-related genes in *PTEN* inactive and intact tumors stratified by cancer type.

Since *PTEN* loss has been linked to the expression of immune checkpoint genes, we investigated if *PTEN* inactivation was associated with the expression of *PD1*, *PDL1*, *CTLA4* and *IDO1*. We observed that biallelic *PTEN* inactivation was associated with high *PD1*, *CTLA4*, and *IDO1* mRNA expression (**Figure 18**). *PDL1* expression was significantly reduced in tumors with biallelic *PTEN* inactivation. When stratified by tumor type, we found that a few cancer types exhibited a significant increase in immune checkpoint expression when *PTEN* underwent biallelic inactivation (**Figure 19a-d**). We also found that HNSC tumors harboring *PTEN* monoallelic inactivation status presented a highly distinct pattern of low expression of *PD1, PDL1, CTLA4,* and *IDO1*. Moreover, similar findings were observed for lung tumors. Conversely, breast tumors and gliomas with biallelic inactivation had high expression of the four investigated checkpoints.

Correlation analysis of the PanCancer cohort showed that the expression of the majority of IFN-related genes was positively associated with immune checkpoint expression (**Figure 20a**). Moreover, we stratified our correlation analysis to breast and gliomas since a distinct expression of checkpoints was observed in these cancer types (**Figure 20b** and **20c,** respectively). Interestingly, *IFR3* was the only gene with a differential correlation, showing a negative association with *STAT1* and *JAK* proteins between breast cancer and gliomas.

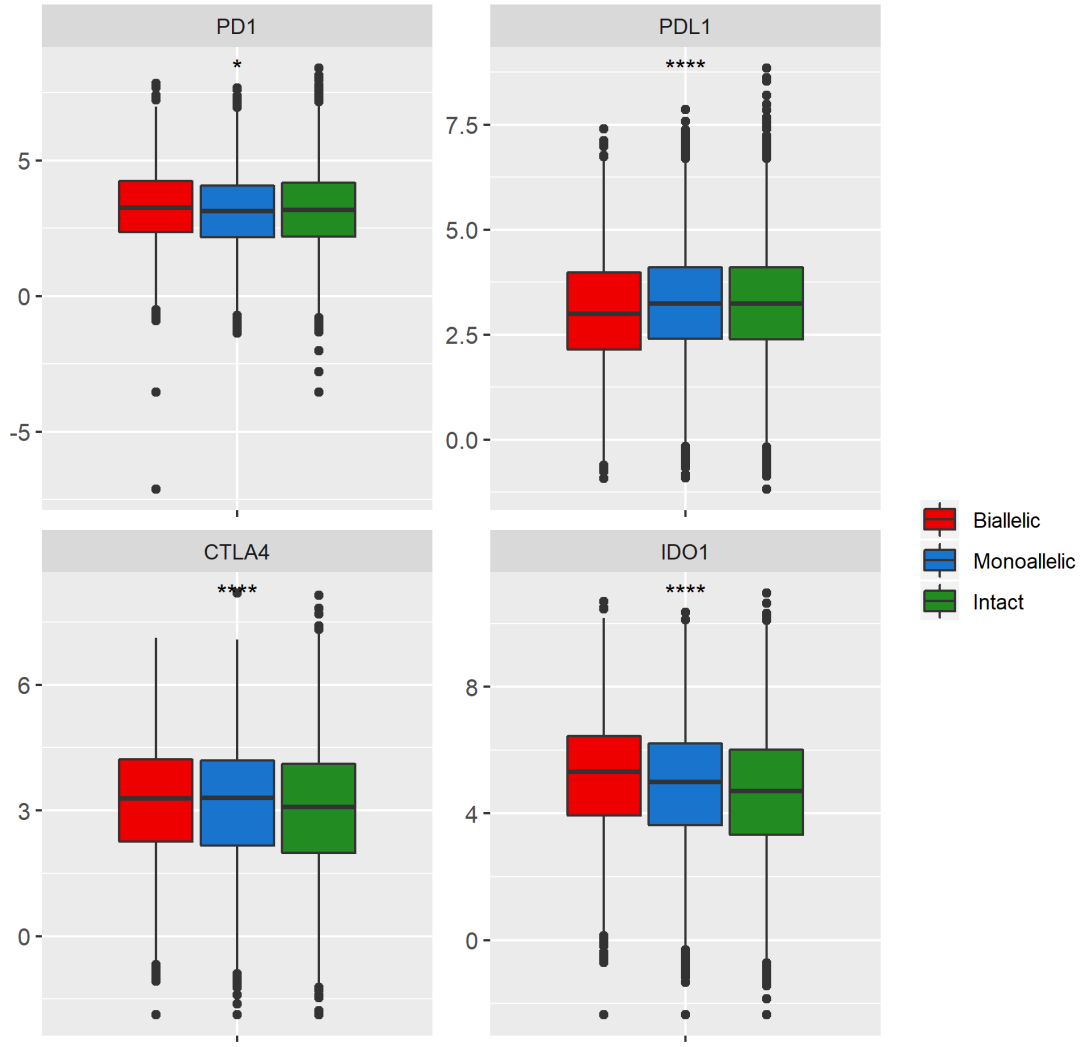

Figure 18. PanCancer analysis of the effect of *PTEN* inactivation in the expression of immune checkpoints. We found significant associations for all four investigated checkpoints. Y-axis shows RSEM-normalized RNAseq gene expression levels. Log-normalization was used for better visualization of results. Asterisks show the P-values derived from Kruskal Wallis test. *P<0.05. **P<0.01. ***P<0.001. ****P<0.0001.

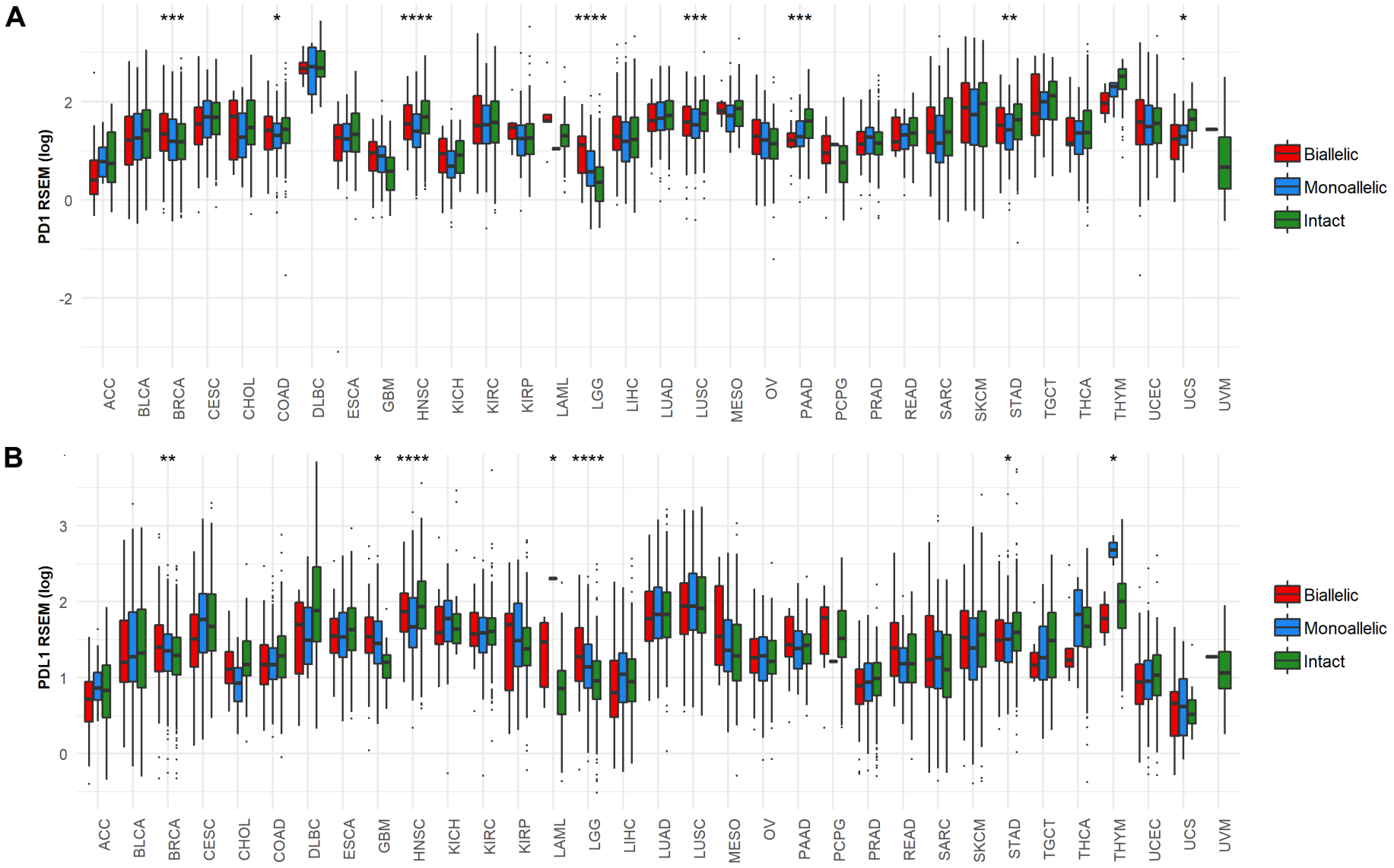

Figure 19. Effect of *PTEN* inactivation in the expression of immune checkpoints by tumor type. A, **B**, **C**, and **D** show tumor type-specific associations with *PTEN* inactivation status for *PD1*, *PDL1*, *CTLA4*, and *IDO1* expression, respectively. Asterisks show the P-values derived from Kruskal Wallis test. Y-axis shows RSEM-normalized RNAseq gene expression levels. Log-normalization was used for better visualization of results. *P<0.05. **P<0.01. ***P<0.001. ****P<0.0001. Continues.

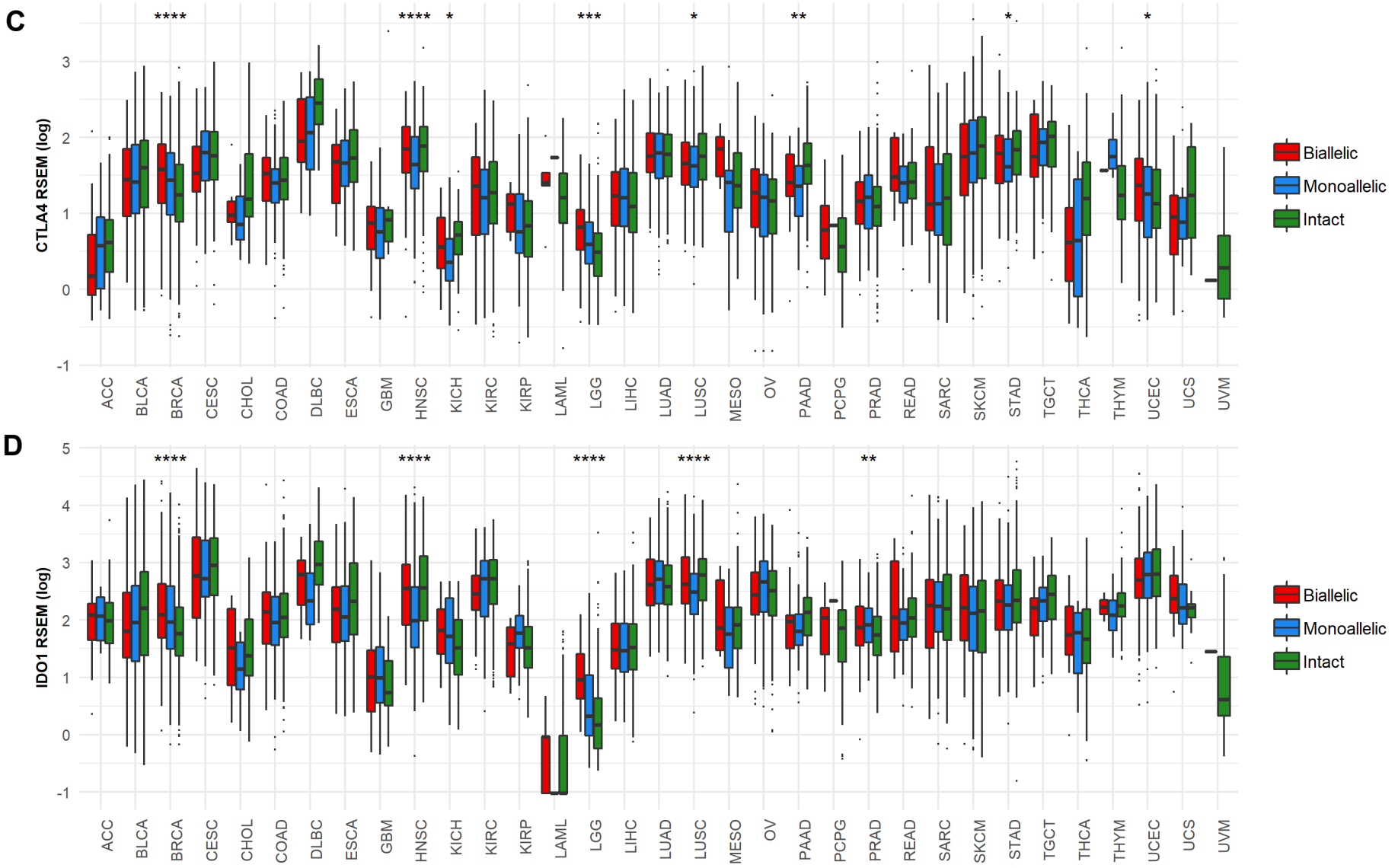

Figure 19. Effect of *PTEN* inactivation in the expression of immune checkpoints by tumor type. Continued.

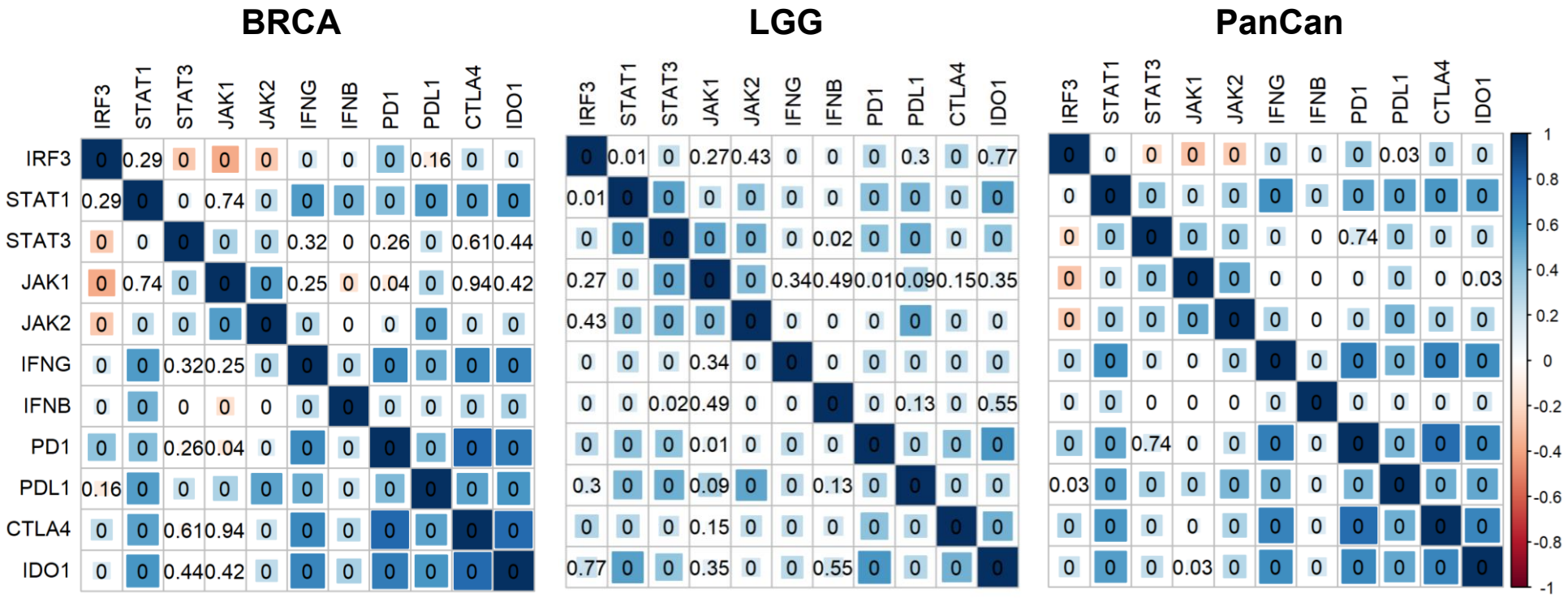

Figure 20. Correlation analysis between immune checkpoint and interferon-related genes for breast cancer (BRCA), low-grade gliomas (LGG), and for all tumors grouped (PanCancer). *IRF3* expression is negatively correlated with *STAT3*, *JAK1*, and *JAK2* in breast tumors and in the PanCancer analysis. However, in LGG, *IRF3* positively correlates with *STAT1*. Blue and red shows positive and negative correlations, respectively. P-values are shown inside each correlation score boxes.

Correlation between immunogenic features and immune-cell abundance

By stratifying tumors based on their *PTEN* inactivation status, we compared the associations between genomic features, immune-cells, and immune gene expression through Spearman correlation. We observed that, in *PTEN* biallelic inactive cancers, aneuploidy was not significantly associated with the expression of immune genes and immune-cell abundance (**Figure 21a**). The opposite was observed when *PTEN* was intact (**Figure 21b**). Moreover, immune cell abundance, such as M2 macrophages and naïve CD4+ T cells, showed a stronger negative correlation with immune-gene expression in *PTEN*-intact tumors when compared to *PTEN*-inactive tumors.

We also observed that the expression of the majority of IFNI-related and immune checkpoint genes was positively associated. In contrast, *IRF3* expression was negatively correlated with *STAT1* and *STAT3* expression, as observed in the correlations for each tumor type in **Figure 19**.

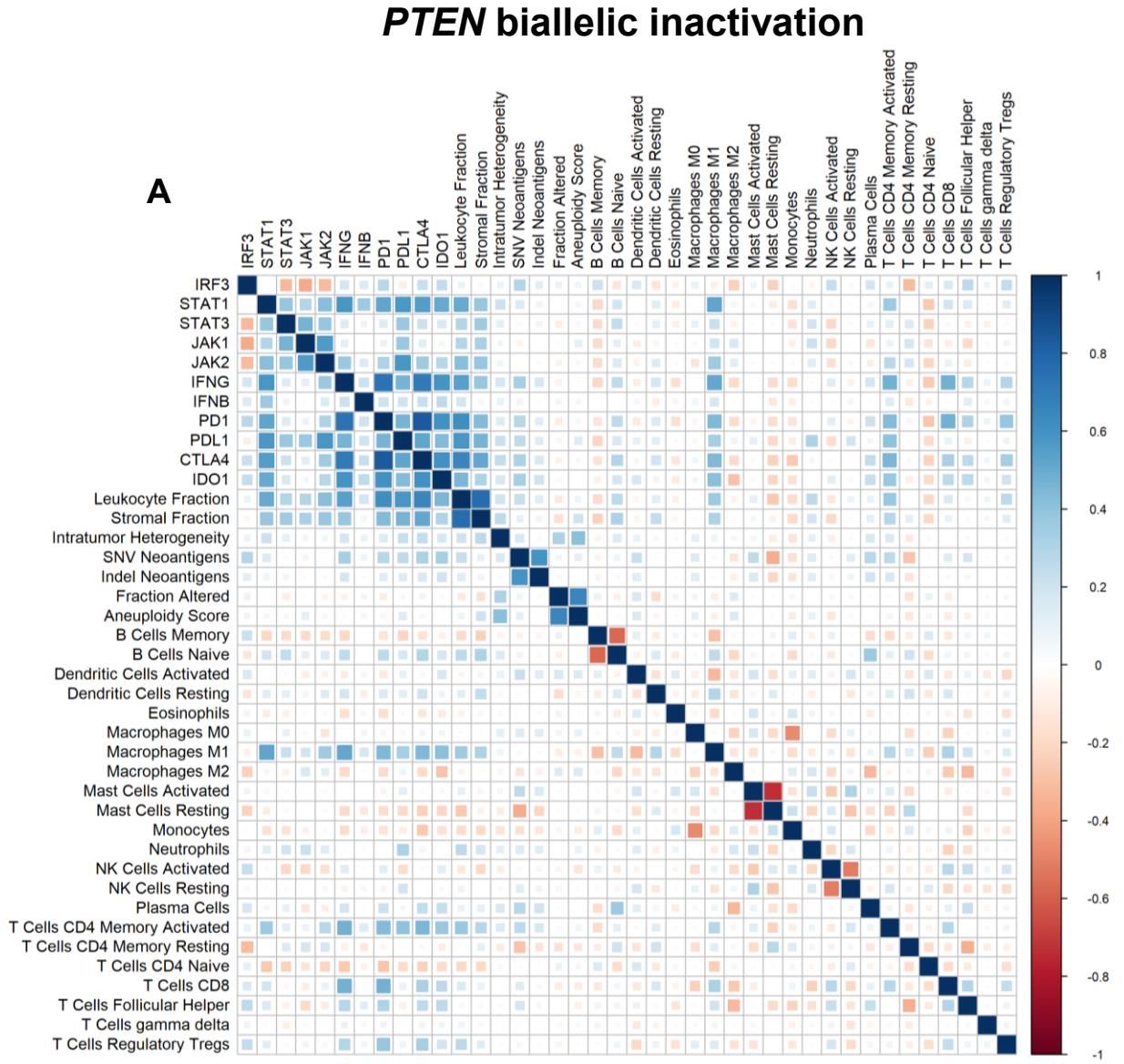

Figure 21. Spearman correlation of immune gene expression, immune-cell abundance, and genomic changes. Blue and red shows positive and negative correlation scores. **A**, **B**, and **C** show correlation plots for *PTEN* biallelic, monoallelic, and intact status, respectively. Continues.

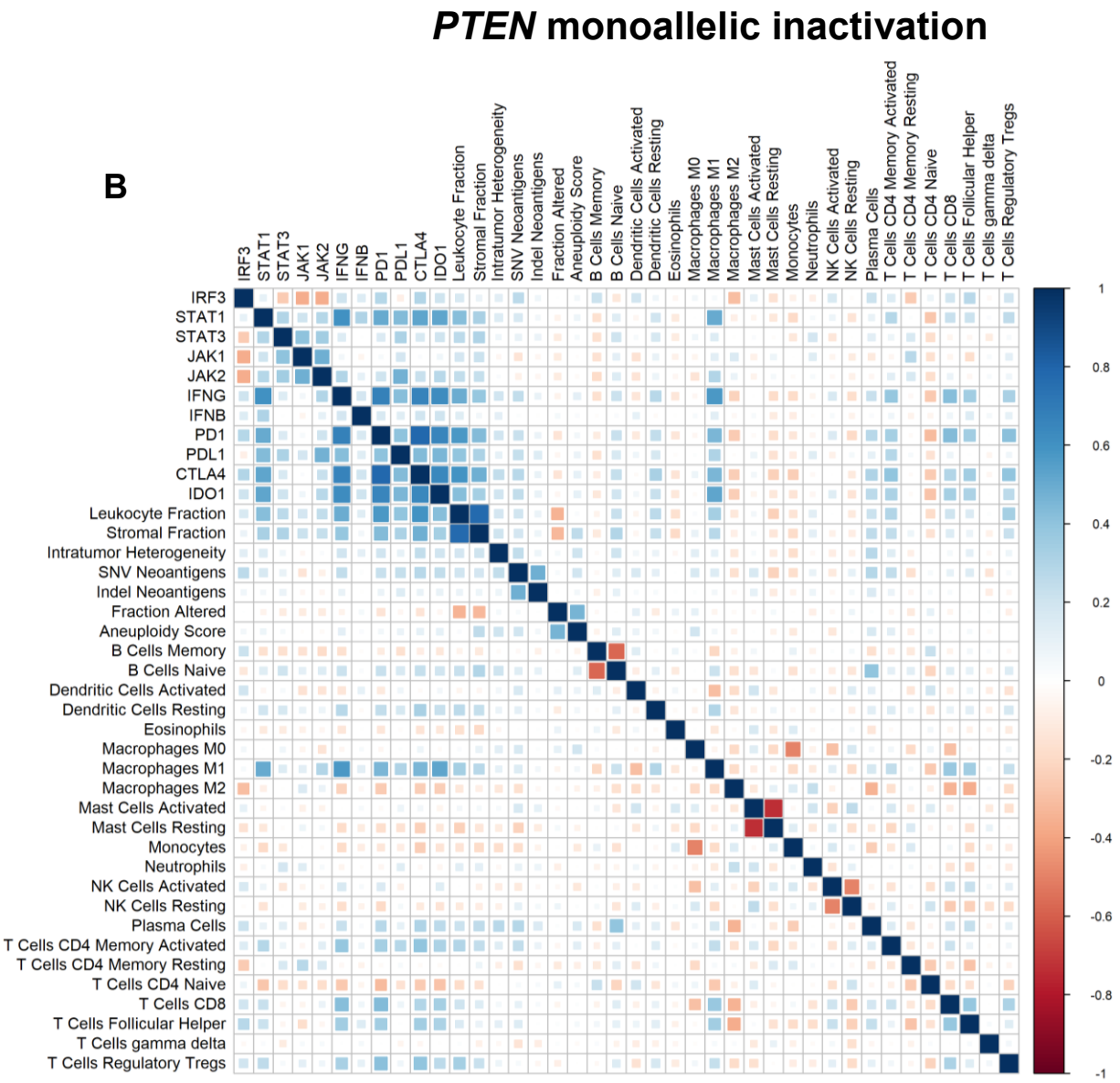

Figure 21. Spearman correlation of immune gene expression, immune-cell abundance, and genomic changes. Continues.

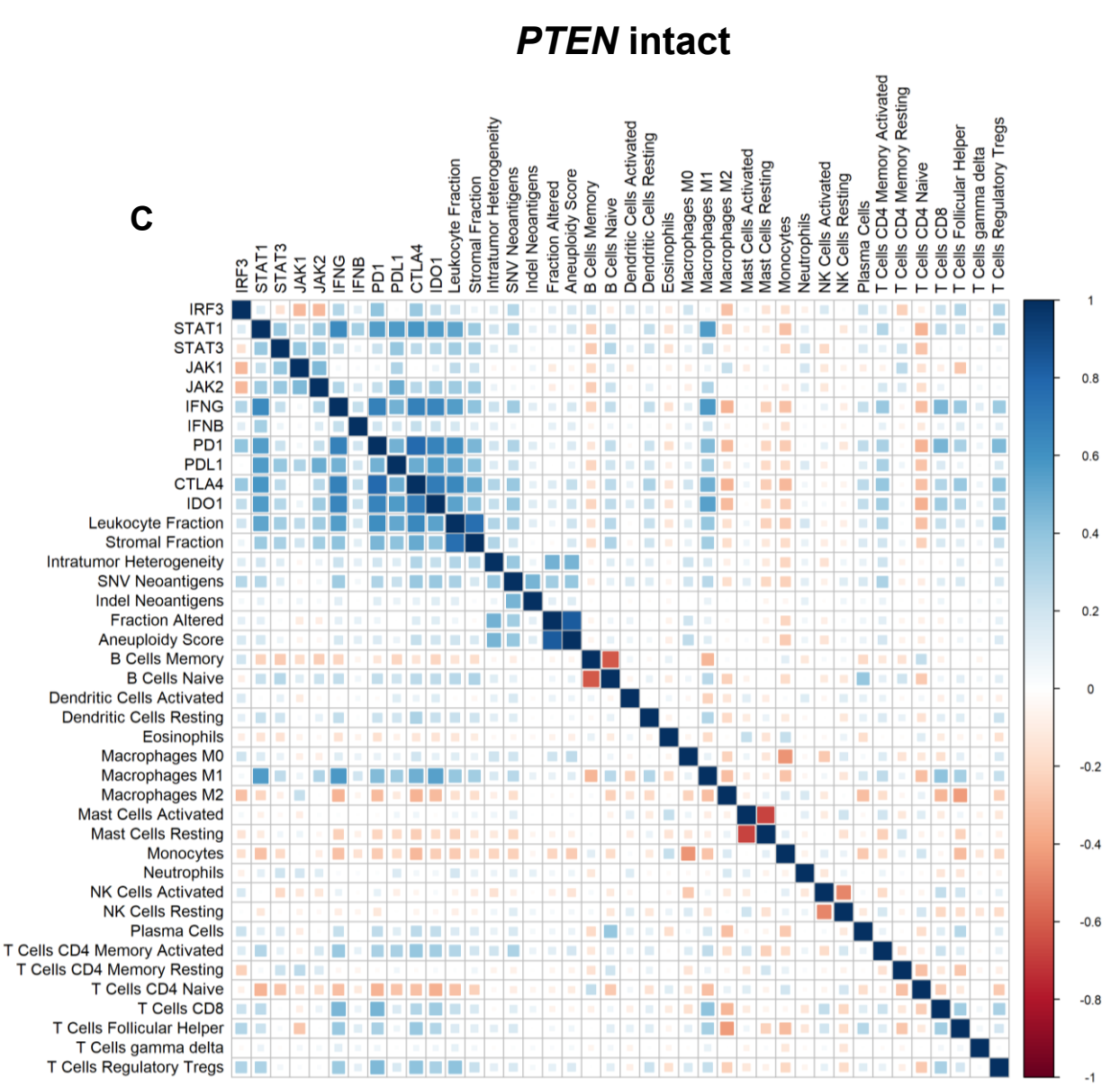

Figure 21. Spearman correlation of immune gene expression, immune-cell abundance, and genomic changes.

5.3.4 *PTEN* inactivation is linked to poor outcome across tumor types

PTEN homozygous deletions have been associated with worse outcome in several tumors, including prostate and melanoma[101,131]. Our PanCancer survival analysis of ~10,000 tumors demonstrated that tumors harboring hemizygous deletions and *PTEN* monoallelic inactivation are linked to earlier recurrence and death events (**Figure 22a-d**). By stratifying per tumor type, however, we found that *PTEN* biallelic inactivation was predictive of earlier death events in ACC (Hazard ratio [HR] = 3.11, 95% Confidence Interval [CI] = 1.46-6.62, P=0.003), BLCA (HR=1.54, 95% CI 1.00-2.37, P=0.04), GBM (HR=1.98, 95% CI 1.38-2.84, P=0.0001), LGG (HR=6.10, 95% CI 3.49-10.65, P=<0.0001), SARC (HR=2.00, 95% CI 1.09-3.67, P=0.02), and STAD (HR=1.55, 95% CI 1.08-2.23, P=0.01).

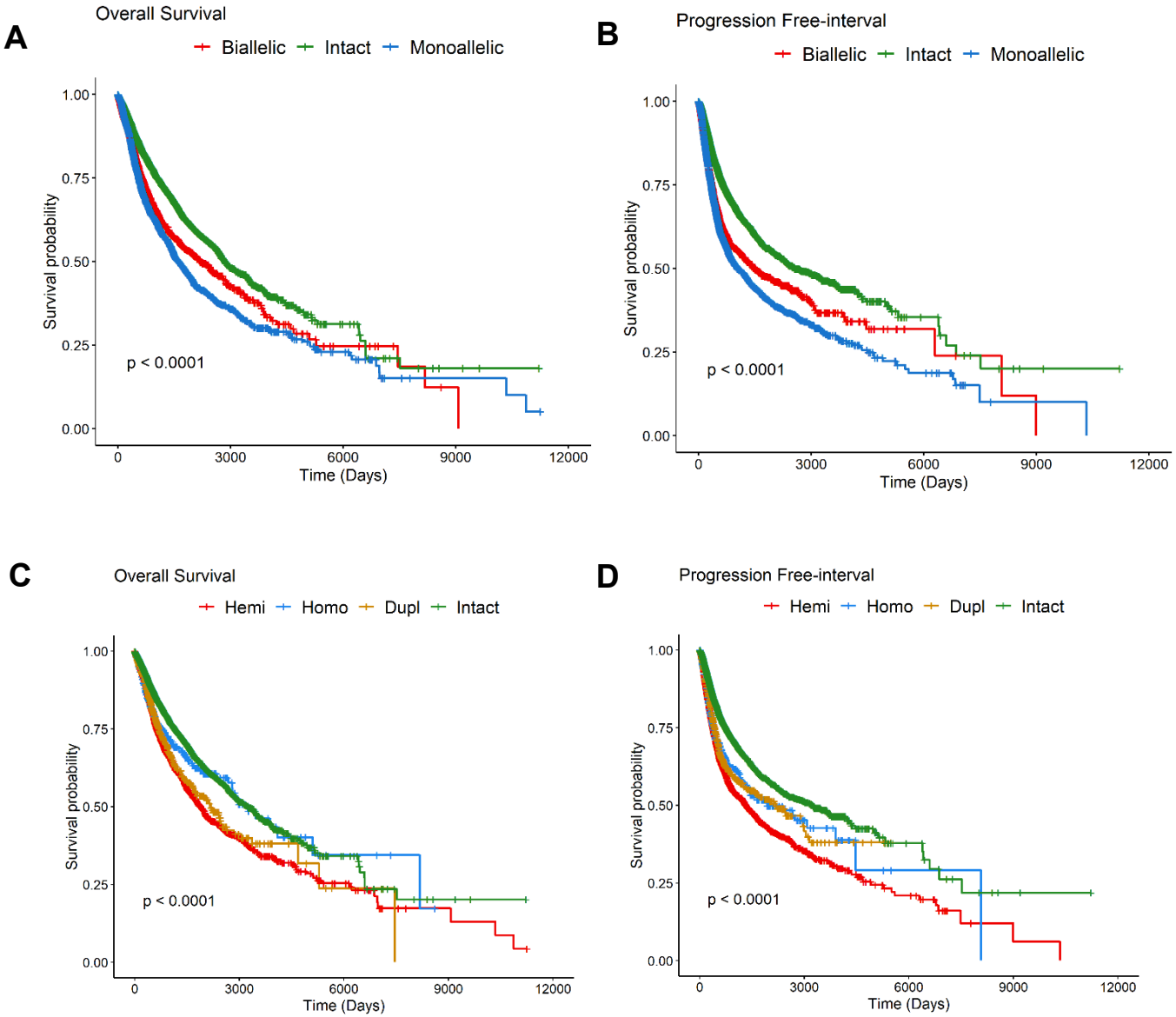

Figure 22. PanCancer prognostic impact of *PTEN* deletions and inactivation on patient outcome. *PTEN* loss by both copy number and inactivation events was significantly associated with overall survival and progression-free interval. **A** and **B** demonstrate the associations between PTEN inactivation and overall survival and progression free-interval, respectively. **C** and **D** show results of PTEN deletions and amplifications on overall survival and progression free-interval. P-values are derived from log-rank scores comparing all conditions simultaneously. Homo – Homozygous deletion, Hemi – Hemizygous deletion, Dupl – *PTEN* amplification.

5.4 Discussion

PTEN inactivation is a recurrent tumor-cell-specific genomic change that impacts several mechanisms in distinct malignancies[37]. Since *PTEN* regulates the activation of the IFNI response[10,11], we speculated on the possibility that *PTEN* loss would be associated with an immunosuppressive TME. On the other hand, since *PTEN* has an established role on genome organization, we hypothesized that *PTEN* inactivation and its associated mutational load and chromosomal aberrations could also indirectly provoke an altered anti-tumor immune response.

Both elements of our hypothesis were supported in our analysis since we found that *PTEN*-biallelic-inactive tumors are genomically unstable and may present, depending on tumor type, strong links with several immunological features of response to cancer. Tumors harboring biallelic inactivation of *PTEN* showed high levels of neoantigens likely as a result of the enhanced levels of nonsilent mutations. However, we found that some tumor types presented an IFNI signaling pattern driven by the high expression of *IRF3*, *STAT1*, and *STAT3*. Moreover, these tumors exhibited high levels of immune checkpoint expression, suggesting that the genomic changes may be provoking an immunosuppressive signature in tumors.

It is known that constitutive expression of *PDL1* in tumor cells may be driven by the activation of IFNI signaling network[64]. Furthermore, a highly unstable genome often associates with the presence of self-DNA in the cytoplasm of tumor cells[125]. Such abnormal presence of DNA in the cytosol triggers the IFNI response by activating the STING-IRF3 axis[132]. In this manner, we speculate that a tumor harboring *PTEN* biallelic inactivation leads to higher probability of having cytosol DNA and, consequently, have an active IFNI response. We observed that *PTEN*-null tumors had high levels of *STAT1* and *STAT3*, which are the two primary transcription factors of IFN-related genes. However, since PTEN is required for IRF3 nuclear migration and consequently activation of the IFNI network, presumably other mechanisms are driven by an unstable genome are occurring.

Gliomas presented the most distinct patterns of genomic changes and immune gene expression signatures when *PTEN* underwent biallelic inactivation. *PTEN* biallelic inactivation in LGG was linked to the overexpression of *PD1*, *PDL1*, *CTLA4*, and *IDO1*, suggesting that these tumors are highly immunosuppressed[17,133–135]. Moreover, *PTEN* loss has been linked to increased *PDL1* expression in gliomas[69]. In addition, *IDO1* expression

was observed in the majority of GBM and LGG tumors and has been related to higher Treg density and poor outcome[136]. Since we found that LGG had the lowest abundance of Tregs when compared to other malignancies, validation using histological sections is required to determine the associations between *PTEN*, *IDO1* and Treg density in gliomas.

Breast tumors showed similar findings as gliomas with regard to immune checkpoint expression. Interestingly, *PTEN* deletions or protein loss have been linked to higher expression of PDL1 in breast tumors[66]. Further, IFNG expression was found to be strongly correlated with *PD1*, *PDL1*, *CTLA4*, and *IDO1* in breast tumors. It is relevant to state that the expression of these checkpoints is obtained from a combination of stromal, neoplastic, and immune cells, which may bias our findings regarding the cell type expressing a particular gene. For instance, *PTEN* and *IDO1* expression in Tregs are linked to their immunosuppressive properties[111,137].

Prostate tumors with *PTEN* biallelic inactivation were linked to high leukocyte fraction, but showed similar genomic instability levels when compared to *PTEN* intact. Interestingly, monoallelic inactivation of *PTEN* in prostate cancer was linked to an overall higher instability. Presumably, *PTEN* heterozygous inactivation may occur in prostate tumors as an earlier event characterized by higher instability. In contrast, *PTEN* biallelic inactivation may occur later during tumor progression, on which cells that present higher genomic changes were killed by immune cells[26]. Low *IRF3* but high *STAT1* and *STAT3* expression was observed in *PTEN*-null prostate cancer. In the same manner, these tumors showed high *IDO1* expression, suggesting that *PTEN*-deficient prostate cancer may be highly immunosuppressive.

Our PanCancer outcome analysis showed that tumors harboring *PTEN* monoallelic inactivation showed earlier relapse and cancer-specific death. However, when stratified by tumor type, we found that *PTEN* biallelic inactivation predicted earlier death-related events through a univariate Cox regression model. *PTEN* homozygous deletions have been linked to worse outcome in several tumors[138–140], which is concordant with our findings. However, the worst outcome that was found for PTEN monoallelic-inactive cancers may be biased by the increased levels of aneuploidy and genomic instability, which are linked to poor survival[65,141].

PTEN has been described as a dosage-sensitive TSG, suggesting that tissue-specific *PTEN* expression levels may trigger differential outcomes in cells. Indeed, complete *PTEN* loss has been linked to cell death and senescence[53,54]. We show that

PTEN monoallelic inactivation, which presumably leads to reduced PTEN protein levels, are associated with worse outcome and a more diverse pattern of genomic instability. This conclusion is in keeping with the observation from other studies that *PTEN* is dosage-sensitive. Allelic serial studies were performed with mice to show the effect of a continuous loss of *Pten* expression[57]. The authors found that tumor incidence and survival was linked to *Pten* expression levels, with tumors expressing 80% of normal *Pten* levels exhibiting a phenotype similar to tumors with monoallelic *Pten* inactivation. Similarly, in a mice astrocytoma model, *Pten* haploinsufficiency was shown to confer *de novo* high-grade tumor development[12].

In a model proposed by Berger and colleagues (2011), *PTEN* suffers quasi-inactivation[56]. In this model, by reducing *PTEN* expression in a context and site-dependent manner, cells might abnormally proliferate and then develop into cancer. The continuous loss of expression influences disease severity until complete loss, where cells undergo *Pten*-associated senescence in a p53-dependent mechanism. In mice prostate cancer models, the complete loss of *Cpb* and the haploinsufficiency of *Pten* induced the development of high-grade prostatic intraepithelial neoplasia[142]. Thus, it is likely that tumors harboring *PTEN* monoallelic inactivation are more aggressive than those with biallelic *PTEN* inactivation – which is presumably under replicative stress, autophagy, and senescence[37].

Considering *PTEN* monoallelic inactivation, we observed that HNSC harboring this genomic change had low immune checkpoints expression levels. In contrast, *PTEN*-intact and *PTEN*-biallelic-inactive HNSC samples had similar patterns of cell-specific immune response and immune checkpoint expression. Presumably, in addition to the genomic changes of *PTEN*-null HNSC (*e.g.* high intratumor heterogeneity and aneuploidy), these tumors may be undergoing PTEN-related-senescence mechanisms, which may explain its proinflammatory state. In this scenario, senescent *PTEN*-null tumor cells are probably driving an anti-tumor immune response through the secretion of proinflammatory chemokines and cytokines[143]. These secreted molecules recruit more immune cells that, in combination with a highly unstable genome, drive their responses to promote tumor-cell death. Reports have linked *PTEN*-deficiency to the development of HNSC[144]; however, the links between PTEN functions and immune response in these tumors are still poorly understood.

Interestingly, we also found that HNSC tumors with monoallelic *PTEN* inactivation had low expression of *STAT1,* which may explain why these tumors are immunologically cold (*i.e.* having low expression of IFN-related genes and low CD8+ T-cell abundance). *PDL1* expression may be upregulated in tumor cells through several mechanisms, one of them being by the activation of the JAK2/STAT1 expression[145]. Thus, partial *PTEN* deficiency in these tumors may promote an immunosuppressive environment that may be unresponsive to current immunotherapeutic approaches. On the other hand, it is expected that HNSC tumors harboring biallelic *PTEN* inactivation may be good responders in immune checkpoint blockade therapies.

In summary, we demonstrate that *PTEN* deficiency have distinct implications on the genome and immune response of different tumor types. Biallelic and monoallelic inactivation of *PTEN* were observed as two entities that might independently influence the TME of certain malignancies. Moreover, particular cancer types may benefit from *PTEN* screening for determining presumable response to immune checkpoint therapies.

Our study has several limitations regarding the localization of immune gene expression and abundance of immune cells. Immune cells may express high levels of immune checkpoint proteins and bias our findings, which were obtained exclusively of tumor-intrinsic genomic changes. In addition, *PTEN* mRNA may be downregulated by other epigenetic mechanisms, such as the presence of miRNAs. Further validation is also required for different cancer types to determine the precise impact of *PTEN* in the genome of tumors and consequently its effects in the anti-tumor immune response.

Lastly, based on the results observed from this PanCancer study, we chose to investigate how PTEN protein loss influences the tumor microenvironment of prostate cancer tumors. Moreover, since metastatic prostate tumors are difficult to treat, we also investigated the tumor microenvironment of these tumors when PTEN was lost.

6. CHAPTER 2

INCREASED FOXP3+ T REGULATORY CELL (TREG) DENSITY AND IDO1 EXPRESSION IN PTEN-DEFICIENT PROSTATE CANCER

6.1 Background

One in seven men in North America is expected to be diagnosed with prostate cancer during their lifetime[146,147]. Genomic aberrations associated with *PTEN* tumor suppressor gene function, are among the most common aberrations in prostate cancer. Inactivation of the *PTEN* gene by deletion or mutation leads to loss of PTEN protein, which occurs in about 25% of primary prostate tumors at radical prostatectomy and as many as 70% of castrate resistant and metastatic prostate cancer[36]. PTEN deficiency in prostate tumors is linked to invasive pathological features and earlier biochemical recurrence after primary therapies[148–150].

Emerging evidence indicates that PTEN may have additional lipid phosphatase independent functions that are independent of PI3K/AKT pathway, including those affecting tumor growth through modulation of the immune response and tumor microenvironment (TME)[10,11]. In immune cells, PTEN is critical for cell maturation and activation[5]. More recently, the secreted PTEN long protein (PTEN-L) was also reported to be key in activating the anti-viral type I interferon (IFNI) response[10]. In addition, PTEN regulates the NF-kB pathway, which underlies several immune response pathways but can be pro-tumorigenic in the TME[45,74]. PTEN may thus influence immune-cell composition in the TME in different ways. However, there is little information on the types of immune changes that take place in the TME when PTEN is lost in prostate cancer.

Methods of enumerating and classifying the immune cell infiltrate of patient tumors using immunohistochemistry or flow cytometry are technically challenging. A recent alternative approach is to computationally characterize high dimensional data from transcriptomes of patient tumors and to subsequently infer the cellular immune components present[87]. This approach has been used to estimate, by inference, the relative abundance of immune cell types from the TME and has been validated using flow cytometry based evaluation[151].

The effect of tumor-intrinsic genomic alterations in the anti-tumor immune response is critical for distinguishing tumors that are more likely to benefit from current immunotherapy approaches[8,16,23]. PTEN and its isoform PTEN-L regulate the IFNI and NF-kB pathways with a substantial impact in the expression of pro-inflammatory cytokines[10,11]. Therefore, PTEN deficiency elicits a distinctive immune-cell landscape in the TME of prostate tumors. In this study, we compared the immune cell types present in the TME of tumors with PTEN loss to those with intact PTEN expression.

As recently reported in some cancers, PTEN deficiency is associated with an immunosuppressive TME state with increased expression of immune checkpoint proteins[16,17]. Indoleamine 2,3-dioxygenase (IDO1) and programmed death-ligand 1 (PDL1) are thought to play significant roles in suppressing anti-tumor immune-cell response in the TME by inducing tolerance to tumor-derived antigens[133,152]. Given the significance of PTEN loss in prostate cancer, our objective was to evaluate potential relationships between PTEN status and levels of the IFN-induced immune checkpoints IDO1 and PDL1 in cancer cells and associated immune cells. Our investigations revealed that PTEN deficiency is associated with higher densities of FoxP3+ T regulatory cells (Treg) and increased expression of IDO1. Furthermore, PTEN-deficient prostate tumors with high FoxP3+ Treg densities demonstrated a higher likelihood of relapse after radical prostatectomy. Collectively, these findings suggest that PTEN-deficient prostate tumors may require immunomodulatory treatment approaches to counter the infiltration of the pro-tumorigenic immune cells in the patient's TME.

6.2 Methods

6.2.1 *In silico* analysis of immune cell abundance in 622 primary and 119 metastatic prostate cancers

The Cancer Genome Atlas (TCGA) prostate cancer profiling dataset (https://portal.gdc.cancer.gov/) was used as the discovery cohort for our study. We downloaded raw and level 3 RNAseq and clinical data of 491 radical prostatectomy-derived tumors from the TCGA cohort. To validate our findings, we further analyzed microarray-based transcriptomic profiling and clinical data from 131 radical prostatectomy specimens from the Memorial Sloan Kettering Cancer Center (MSKCC) resource (Gene Expression Omnibus accession number GSE21032)[153]. We also investigated whole-transcriptome sequencing data from a cohort composed of 96 metastatic castrate resistant prostate cancer (mCRPC) specimens[154]. *PTEN* loss status based on gene expression was defined for tumors that showed *PTEN* expression values equal to or less than the lowest expression quartile value.

To estimate the immune cell landscape in each tumor, we employed the CIBERSORT algorithm (https://cibersort.stanford.edu/) that is an established tool to determine the abundance of immune cells using whole transcriptome data. We separately imputed normalized gene expression data of 491 samples from TCGA, 131 samples from

MSKCC, and 96 mCRPC specimens. For the mCRPC cases, we compared PTEN-deficient vs. PTEN intact tumors from three different locations: bone (n=29), liver (n=17), and lymph nodes (n=50).

We selected the leukocyte signature matrix 22 (LM22) from CIBERSORT and ran the relative mode analysis with 100 permutations. Relative immune cell abundance score was used to estimate the association with PTEN deficiency for tumor samples from all cohorts. Based on previous evidence on PTEN associated immunosuppressed TME across cancers[16,67,84], we also examined the association between expression of *PTEN* with *PDL1* and *IDO1* immune checkpoints in the primary prostate cancer cohorts. For clinical outcome analysis of TCGA and MSKCC cohorts, we employed disease recurrence as an endpoint, which was defined by the presence of PSA-related relapse, local recurrence or metastasis.

6.2.2 Cohort description and TMA design

This study was approved by the Ethics Committee in Research of Hospital of Ribeirão Preto, São Paulo, Brazil (HCRP). This study was approved by the HCRP Ethics Committee (**Attachment 2**). To validate the *in silico* findings, formalin-fixed paraffin-embedded radical prostatectomy derived specimens were collected from 94 patients from the Pathological Archive of the HCRP following informed consent between 2002 and 2015. Clinicopathological and follow-up data from all 94 patients are presented in **Table 3**. Patients had their serum PSA levels monitored every three months after radical prostatectomy, except in cases in which follow-up was lost. During the entire patient follow-up of this cohort, PSA levels >0.2 ng/mL determined the occurrence of biochemical recurrence. An initial evaluation of whole prostate H&E sections was performed by a pathologist (F. P. S.) in two regions with the most prevalent Gleason pattern, one region of the second most prevalent Gleason pattern, and one benign adjacent region for each patient. The tumor blocks were marked, and 1mm needle cores were harvested to build a tissue microarray (TMA) with at least four representative cores per sample. Each core of the TMA slides was independently assessed for tissue identity (cancer vs. benign) and Gleason score by a second pathologist (T. J.) who was blinded to diagnostic and clinical information associated with the cases in the study.

Table 3. Clinicopathological features of 94 prostate tumors from HCRP cohort.

		Frequency	**%**
Follow-up (mean)(median, range)		80 (60, 14-189)	
Age (mean)(median, range)		63 (64.5, 45-77)	
Time to recurrence (mean)(median, range)		59 (41, 1-162)	
Preoperatory PSA (mean)(median, range)		38 (36.5, 0.2-66)	
Biochemical recurrence	Missing	7	7.4
	No	68	72.3
	Yes	19	20.2
Gleason score	Missing	6	6.4
	6	10	10.6
	3+4=7	24	25.5
	4+3=7	25	26.6
	8	16	17
	9	13	13.8
T	Missing	8	8.5
	T2N0	62	66
	T3N0	24	25.5
Extraprostatic extension	Missing	6	6.4
	No	64	68.1
	Yes	24	25.5
Vesicular invasion	Missing	6	6.4
	No	72	76.5
	Yes	16	17.1

Follow-up and time to recurrence are shown in months. Age is shown in years. Preoperatory PSA levels are shown as ng/mL. T and N – pathological staging.

6.2.3 Immunohistochemical staining and scoring

TMA sections were then stained with rabbit anti-human PTEN antibody (1/50 dilution, clone D4.3 XP; Cell Signaling Technologies, Danvers, MA, USA) and anti-human CD8 primary antibody (1/25 dilution, Abcam #ab17147) using the Ventana automated staining platform (Ventana Discovery Ultra, Ventana Medical System, Tucson, AZ, USA). TMA sections were also stained using an immunoenzyme multiple staining method with Intellipath FLX Automated Staining for rabbit anti-human PDL1 (#M4422, Clone SP142, 1/100, Chromogen DAB), mouse anti-human FoxP3 (#14-7979, Clone Ebio7979, 1/100, Chromogen Warp Red), and rabbit anti-human IDO1 (#M5600, Clone SP260, 1/1500, Chromogen Ferangi Blue). All slides were scanned at 20x magnification through Aperio Systems (Leica Microsystems, Buffalo Grove, IL, USA).

PTEN was scored for each TMA core as being lost when at least >10% of the cytoplasm and nucleus of tumor cells presented a negative or remarkably decreased staining compared to control stromal compartment or benign glands[155]. PTEN scoring was performed by a trained pathologist (T. J.). CD8+ T cell was visually enumerated in the epithelial and stromal compartments on 20x scanned TMA sections (Aperio Systems). PDL1, FoxP3, and IDO1 expression status were scored using an automated method. In brief, stained TMA sections were scanned and segmented (stromal and epithelial compartments) in Vectra multispectral imaging system and 20x scanned .im3 files from ten random cores were used to train five independent algorithms in PerkinElmer's InForm software package[156]. InForm software identified positive pixels for each chromogen with the hematoxylin channel removed. Then, the number and intensity of cells stained with the described antibodies in the stromal and epithelial compartments were scored. The five algorithms independently scored each core stained with PDL1, FoxP3, and IDO1 based on the three different associated chromogens. Finally, the score for the stromal and epithelial compartments per core was obtained from the average of the five algorithms (For more details, please refer to **Attachment 3**). Total per TMA core density of FoxP3+ Treg and CD8+ T cells was obtained by the sum of the total number of cells found in the stromal and tumor compartments. Similarly, the overall IDO1 and PDL1 protein expression levels per TMA core were obtained by the sum of the positive signals obtained for the stromal cells and tumor glands from each core. Samples that were exclusively or had only remaining benign cores of the prostate gland were removed from further analyses. Visual validation of the automated scoring was performed for all TMA cores.

To determine the association between PTEN loss and IDO1, PDL1 expression, and FoxP3+ T cell density with prostate cancer recurrence, we defined PTEN loss as those patients with at least one tumor core showing partial or complete negative staining for PTEN protein. All benign adjacent cores were excluded from PTEN scoring and analysis. For log-rank and Cox regression analyses, the expression of IDO1 and PDL1 in addition to FoxP3+ Treg cell density were dichotomized based on tertiles. Values below the top tertile were considered as low, and values above the top tertile were considered as high[81]. FoxP3+ Treg cell density was found to be relatively low (range 0-16, median=1.16) in prostate tumors. Patients classified as having high density of FoxP3+ Treg cells had a minimum of one FoxP3+ Treg per sampled TMA core. The observation that FoxP3+ Treg cell density is low in prostate cancer is in keeping with a recently published study that investigated the clinical impacts of this immune cell in 312 primary prostate tumors[81]. CD8+ T cell enumeration was performed in the present study to underlie the correlation between the immunosuppressive proteins IDO1 and PDL1 in addition to FoxP3+ Treg cell density. Data manipulation, visualization, and statistical analyses were performed in R v.3.4.3.

6.3 Results

6.3.1 FOXP3+ Treg cell abundance is significantly increased in PTEN-deficient primary prostate tumors

We characterized the immune cell landscape and immune checkpoint expression in PTEN-deficient prostate cancer via investigating the transcriptomes of 622 primary prostate specimens from two independent cohorts. *PTEN* loss was present in 19.7% (97/491) and 19.8% (26/131) of patients in the TCGA and MSKCC cohorts, respectively. Supervised clustering analysis based on PTEN status for both TCGA and MSKCC cohorts demonstrated a distinct pattern of increased FoxP3+ Treg cell abundance in PTEN-deficient prostate tumors (**Figure 23a** and **23b**). Mann-Whitney U-test confirmed that increased FoxP3+ Treg abundance was found in PTEN-deficient tumors in both TCGA ($P<0.001$) and MSKCC ($P<0.001$) cohorts (**Figure 23c** and **23d**, respectively). Notably, a comparison between primary vs. metastatic lesions from the MSKCC cohort demonstrated that metastatic tumors exhibit a significant increase in FoxP3+ Treg abundance ($P=0.005$) (**Table 4**). *PDL1* immune checkpoint expression was significantly reduced in tumors harboring *PTEN* loss from the MSKCC cohort ($P<0.01$) (**Figure 23d**).

We did not find any significant association between *PTEN* status and *IDO1* expression in either cohort.

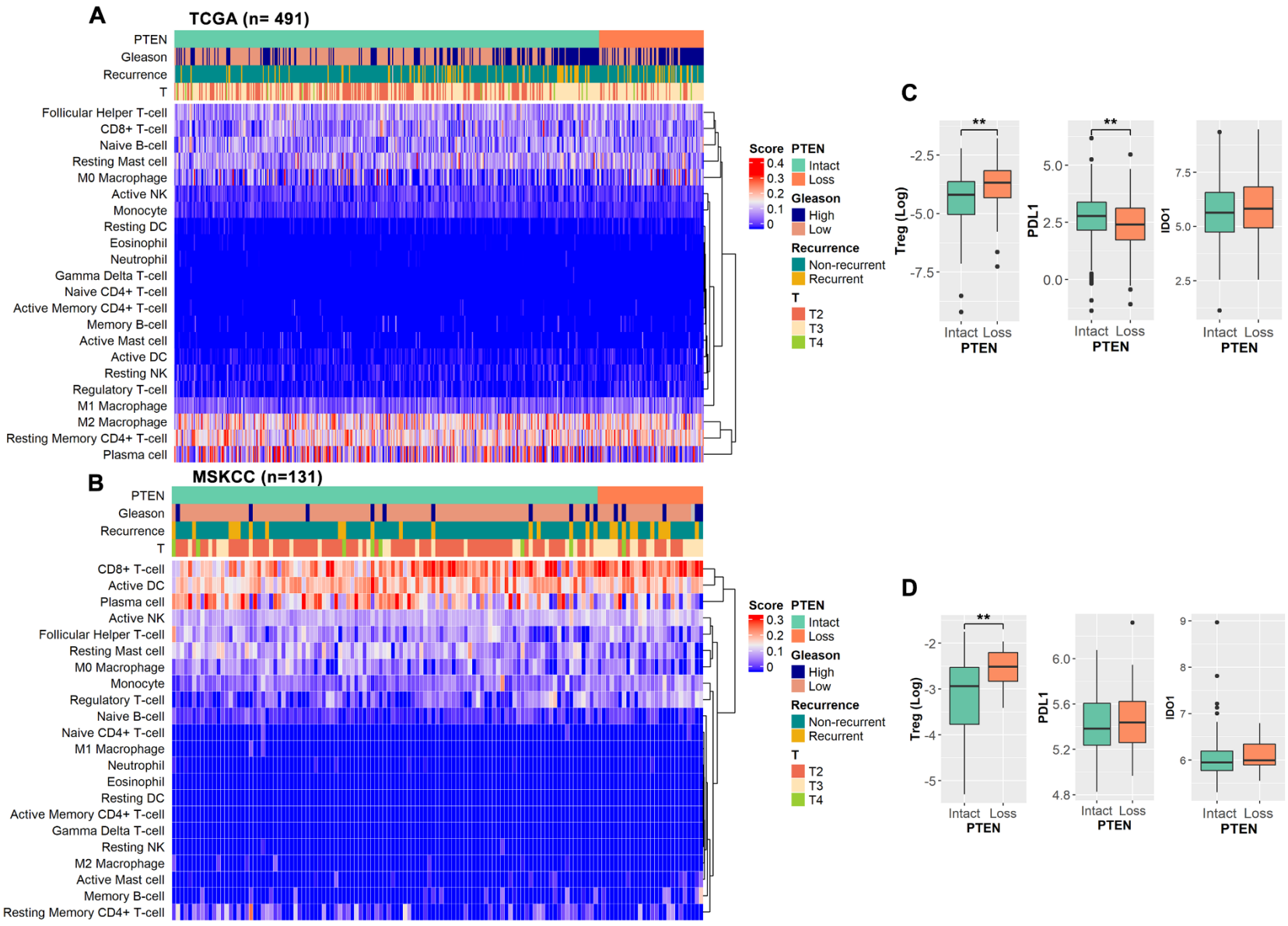
A
TCGA (n= 491)
PTEN
Gleason
Recurrence
T
Follicular Helper T-cell
CD8+ T-cell
Naive B-cell
Resting Mast cell
M0 Macrophage
Active NK
Monocyte
Resting DC
Eosinophil
Neutrophil
Gamma Delta T-cell
Naive CD4+ T-cell
Active Memory CD4+ T-cell
Memory B-cell
Active Mast cell
Active DC
Resting NK
Regulatory T-cell
M1 Macrophage
M2 Macrophage
Resting Memory CD4+ T-cell
Plasma cell
Score
0.4
0.3
0.2
0.1
0
PTEN
Intact
Loss
Gleason
High
Low
Recurrence
Non-recurrent
Recurrent
T
T2
T3
T4
B
MSKCC (n=131)
PTEN
Gleason
Recurrence
T
CD8+ T-cell
Active DC
Plasma cell
Active NK
Follicular Helper T-cell
Resting Mast cell
M0 Macrophage
Monocyte
Regulatory T-cell
Naive B-cell
Naive CD4+ T-cell
M1 Macrophage
Neutrophil
Eosinophil
Resting DC
Active Memory CD4+ T-cell
Gamma Delta T-cell
Resting NK
M2 Macrophage
Active Mast cell
Memory B-cell
Resting Memory CD4+ T-cell
Score
0.3
0.2
0.1
0
PTEN
Intact
Loss
Gleason
High
Low
Recurrence
Non-recurrent
Recurrent
T
T2
T3
T4
C
Treg (Log)
-2.5
-5.0
-7.5
**
Intact Loss
PTEN
PDL1
5.0
2.5
0.0
**
Intact Loss
PTEN
IDO1
7.5
5.0
2.5
Intact Loss
PTEN
D
Treg (Log)
-2
-3
-4
-5
**
Intact Loss
PTEN
PDL1
6.0
5.6
5.2
4.8
Intact Loss
PTEN
IDO1
9
8
7
6
Intact Loss
PTEN

Figure 23. In silico sorting of 22 immune cell types in two independent prostate cancer cohorts. By considering the two primary prostate cancer cohorts, the tumors exhibit a moderate to high abundance with follicular T-cells, CD8+ T-cells, naïve B-cells, resting mast cells, M0 macrophages, resting memory CD4+ T-cells, and plasma cells. Identical immune cell clustering was not observed for the two cohorts likely because of different sample size and different gene expression data origin (**A** and **B**). Tumors harboring PTEN loss exhibit a significant increase in the abundance of FoxP3+ Tregs in both cohorts (**A** and **B**). Indeed, FoxP3+ Treg abundance was found to be relatively low when compared to other immune cell types. We did not identify significant associations between PTEN loss and *IDO1* RNA expression for both cohorts (**C** and **D**). However, PTEN-deficient tumors from MSKCC cohort showed a significantly reduced expression of *PDL1* (**C**). Mann-Whitney U-test was employed to determine significant differences between the groups. Heatmaps show the relative immune scores per tumor. Gleason score was dichotomized as low-to-intermediate risk (3+3 and 3+4) and high risk (4+3, 4+4, ≥4+5). T – Pathological staging, *P<0.05; **P<0.01.

Table 4. Immune-cell deconvolution results for TCGA and MSKCC cohorts demonstrated a differential cell content for PTEN-deficient tumors.

	TCGA			**MSKCC**			**MSKCC**		
	PTEN			**PTEN**			**Tumor lesion**		
	Intact	**Loss**	**P**	**Intact**	**Loss**	**P**	**Metastatic**	**Primary**	**P**
Naive B-cell	0.088	0.0793	0.24	0.013	0.015	0.57	0.0109	0.0134	0.93
Memory B-cell	-	-	-	-	-	-	-	-	-
Plasma cell	0.1415	0.0565	**<0.0001**	0.171	0.117	**0.005**	0.0140	0.1474	**<0.0001**
CD8+	0.0716	0.0677	0.54	0.203	0.242	**0.003**	0.2347	0.2123	0.12
Naive CD4+	-	-	-	-	-	-	-	-	-
Resting memory CD4+	0.1529	0.1683	0.**021**	0.002	0	0.061	-	-	-
Active memory CD4+	-	-	-	-	-		-	-	-
Follicular helper T-cell	0.0836	0.0836	0.77	0.07	0.076	0.69	0.0736	0.0736	0.81
Treg	0	0.0007	0.**005**	0.031	0.071	**<0.0001**	0.0771	0.0410	**0.005**
Gamma-delta T-cell	-	-		-	-		-	-	-
Resting NK	0.0004	0.0019	0.56	-	-		-	-	-
Active NK	0.0205	0.0211	0.7	0.093	0.104	**0.008**	0.0854	0.0944	**0.039**
Monocytes	0.0162	0.012	0.**014**	0.05	0.068	**0.002**	0.0620	0.0521	0.27
M0	0.0394	0.062	0.**002**	0.068	0.049	**0.018**	0.0612	0.0643	0.99
M1	0.0403	0.0591	**<0.0001**	-	-	-	-	-	-
M2	0.1602	0.1668	0.66	-	-	-	-	-	-
Resting DC	-	-	-	-	-	-	-	-	-
Active DC	-	-	-	0.174	0.17	0.94	0.2120	0.1720	**0.002**
Resting Mast cell	0.0837	0.0815	0.51	0.089	0.044	**<0.0001**	0.0731	0.0840	0.19
Active Mast cell	-	-	-	-	-		-	-	-
Eosinophils	-	-	-	-	-		-	-	-
Neutrophils	-	-	-	-	-		-	-	-

Comparison between primary and metastatic lesions from MSKCC cohort are also shown. Median values are shown for PTEN loss vs. PTEN intact groups and primary vs. metastatic lesion per each immune-cell type. P-values were obtained from Mann-Whitney U-test. Significant P-values are bolded. Relative scores equal to zero are shown as dashes. DC – dendritic cell, NK – natural-killer cell, Treg – regulatory T-cell, M0 – M0 macrophage, M1 – M1 macrophage, M2 – M2 macrophage.

6.3.2 PTEN-deficient metastatic prostate cancer exhibits site-specific immune differences

By performing CIBERSORT deconvolution analysis in 119 mCRPC specimens, we identified that the locations of PTEN-deficient metastatic lesions have a distinct immune landscape. The comparison between PTEN-null vs. PTEN intact mCRPC lesions showed that PTEN deficiency in bone metastases is associated with lower CD8+ T-cell abundance (p=0.023) (**Figure 24a**). Moreover, we found that PTEN-deficient liver mCRPC is linked to higher FoxP3+ Treg abundance (P=0.05) (**Figure 24b**). Lastly, PTEN-deficient lymph node metastases were strongly associated with high CD8+ T-cell (P=0.01), memory B-cells (P=0.01), follicular helper T-cells (P=0.008) abundances. M2 macrophage abundance was found to be lower in PTEN-deficient lymph node metastases (P=0.02) (**Figure 24c**).

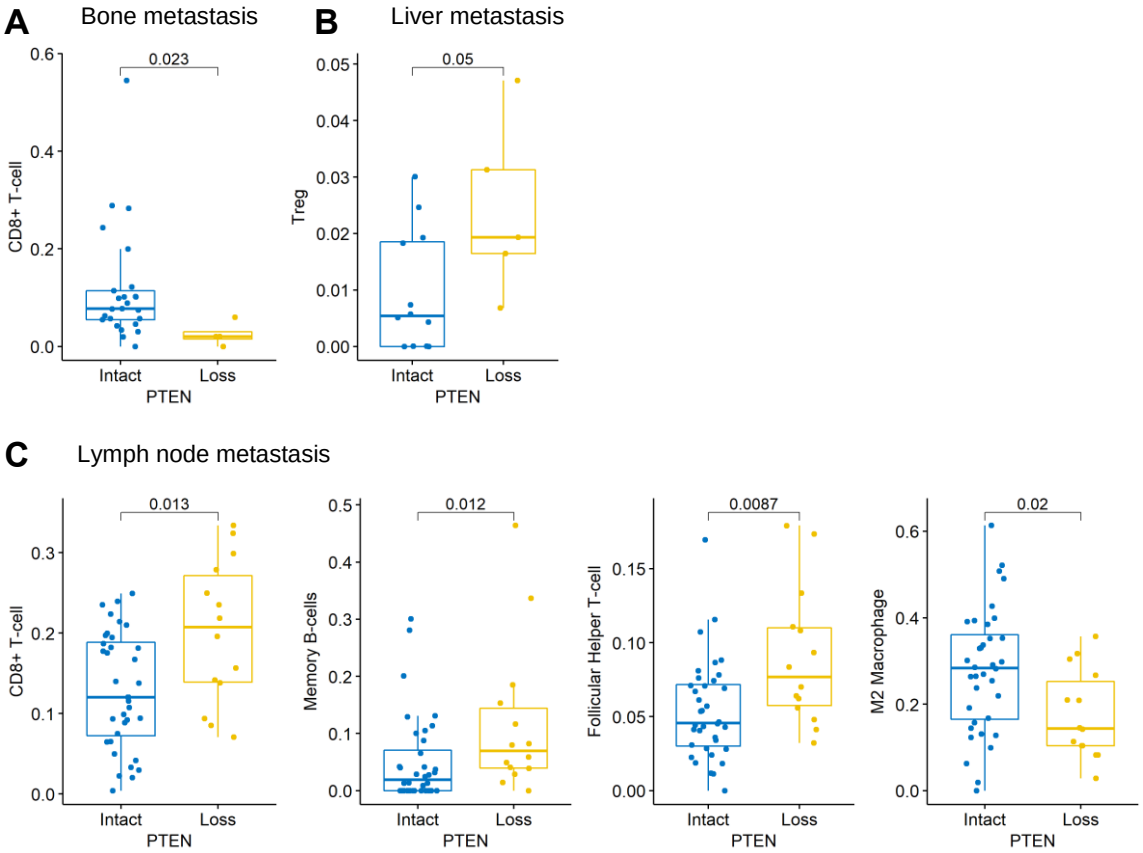

Figure 24. Site-specific PTEN deficiency in prostate cancer metastatic lesions exhibited distinct immune-cell landscapes. PTEN-deficient bone metastases had lower CD8+ T-cell abundance when compared to PTEN intact lesions (**A**). Liver metastases with PTEN loss showed high FoxP3+ Treg abundance (**B**). PTEN-deficient lymph node metastases exhibited high abundance of CD8+ T-cells, memory B-cells, and follicular-helper T-cells. PTEN-deficient lymph node lesions also had low M2 macrophage abundance (**C**).

6.3.3 PTEN-deficient primary prostate tumors exhibit high FoxP3+ Treg density and overexpression of IDO1 protein

Independent validation of findings from *in silico* transcriptomic profiling analysis was performed by interrogating protein expression in a cohort of 94 patients. PTEN protein expression was determined in 76/94 (80%) cases. Protein expression levels of IDO1 and PDL1 and FoxP3+ Treg cell density were measurable in 91% (86/94) cases.

To evaluate whether prostate tumors upregulate expression of IDO1, PDL1, and FoxP3+ Treg cell density, we compared the expression of the three markers in the stroma, tumor, and overall TMA spots between 157 tumor cores to 99 benign adjacent cores. This comparison demonstrated that tumors had increased FoxP3+ Treg cell density in the stroma ($P=0.03$), tumor glands ($P=0.03$), and overall density of cells per core ($P=0.002$) compared to those in benign glandular tissue (**Figure 25a**). IDO1 protein expression was increased in the stroma ($P<0.05$), tumor ($P<0.001$), and overall core ($P<0.0001$) when compared to benign adjacent cores. No significant differences were observed in PDL1 expression levels (**Figure 25a**).

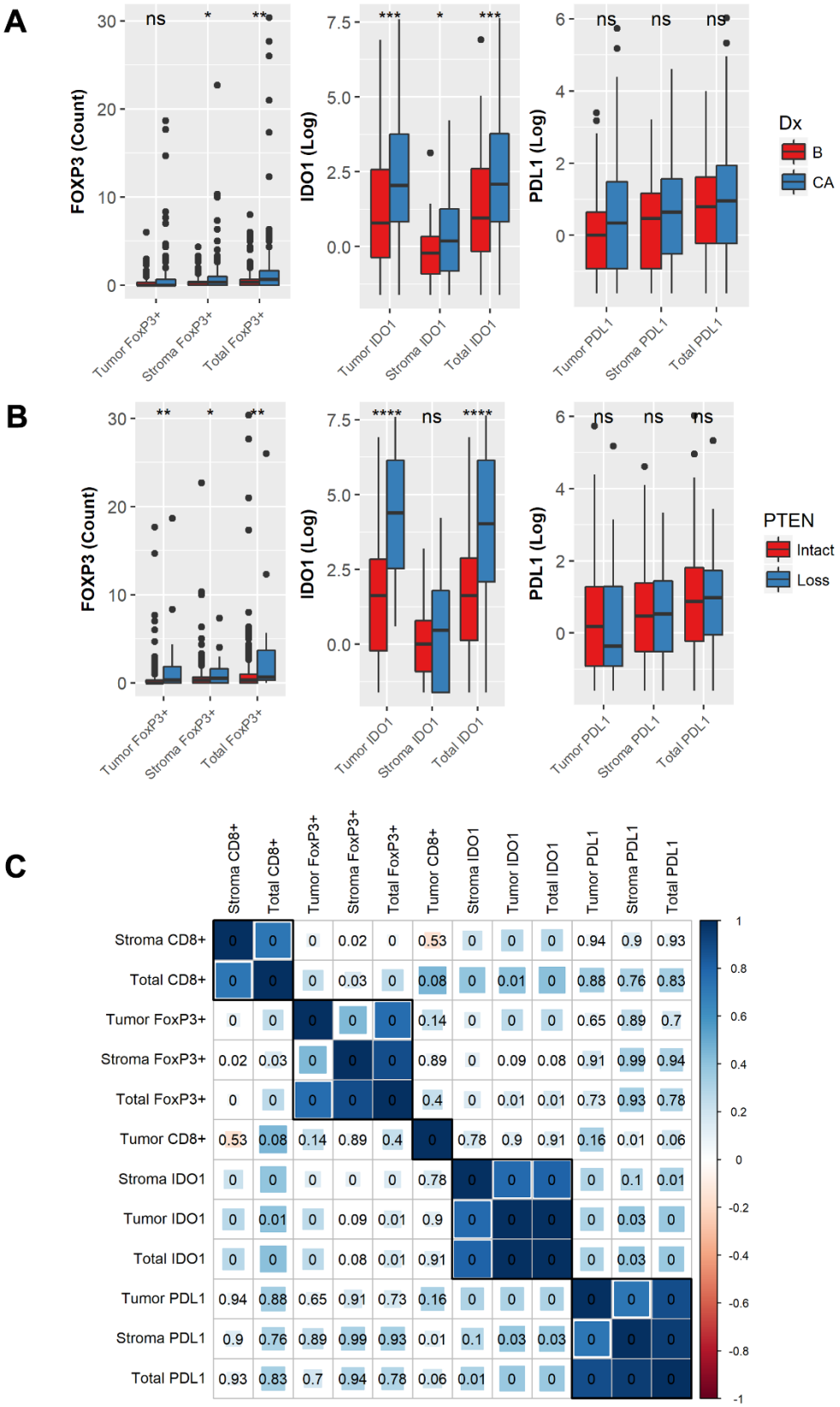
A
FOXP3 (Count)
IDO1 (Log)
PDL1 (Log)
Tumor FoxP3+
Stroma FoxP3+
Total FoxP3+
Tumor IDO1
Stroma IDO1
Total IDO1
Tumor PDL1
Stroma PDL1
Total PDL1
Dx
B
CA
B
PTEN
Intact
Loss
C
Stroma CD8+
Total CD8+
Tumor FoxP3+
Stroma FoxP3+
Total FoxP3+
Tumor CD8+
Stroma IDO1
Tumor IDO1
Total IDO1
Tumor PDL1
Stroma PDL1
Total PDL1

Figure 25. Effect of PTEN deficiency in the expression of IDO1, PDL1 and Treg density. A - Comparison between 157 tumor and 99 benign TMA cores showed that tumor cores have increased stromal FoxP3+ Treg density and increased stromal and epithelial IDO1 expression. **B** - Tumor cores with PTEN loss glands exhibit increased epithelial FoxP3+ Treg density and IDO1 expression. We did not identify significant associations between PTEN loss and PDL1 protein expression. **C** - Spearman correlation analysis between markers showed that stromal and tumor IDO1 expression and FoxP3+ Treg cell density are positively correlated. Moreover, CD8+ T cell density in the stromal compartment was positively correlated with stromal and tumor IDO1 expression and FoxP3+ Treg density. PDL1 and IDO1 are also significantly and positively correlated. Spearman correlation analysis was conducted by using the expression levels of IDO1 and PDL1 in addition to FoxP3+ Treg density defined per patient. P-values are shown for each Spearman correlation test. *P<0.05; **P<0.01; ***P<0.001; ****P<0.0001; ns, not significant. Dx, core diagnosis; B, benign core; CA, tumor core.

Since prostate cancer often presents with multifocal disease and PTEN loss may also be heterogeneous within the tumor[157], we performed a tumor core-by-core comparison, choosing well separated representative areas in the gland. First, we examined levels of PDL1 and IDO1 protein expression and FoxP3+ Treg cell density in the stroma and tumor comparing the tumor cores with PTEN loss to those cores that had retained PTEN protein. PTEN loss was present in 31/157 (19.74%) of the tumor cores. We observed a significantly increased FoxP3+ Treg cell density in the tumor (P=0.006), stromal (P=0.04), and overall core (P=0.008) of PTEN-deficient tumors. Moreover, IDO protein expression was increased in tumor (P<0.0001) and overall core (P<0.0001) of PTEN-deficient prostate tumors (**Figure 25b**). Representative tumor cores with PTEN loss associated FoxP3+ Treg density and IDO1 expression are shown in **Figure 26**.

Spearman correlation analysis showed significant positive correlation between IDO1 protein expression and FoxP3+ Treg density in both stroma and tumor glands. Furthermore, we observed a significant positive correlation between CD8+ T cell density, IDO1 expression, and FoxP3+ Treg cell density (**Figure 25c**; see **Figure 27** for representative TMA core images). PDL1 expression was significantly positively correlated with IDO1 protein expression.

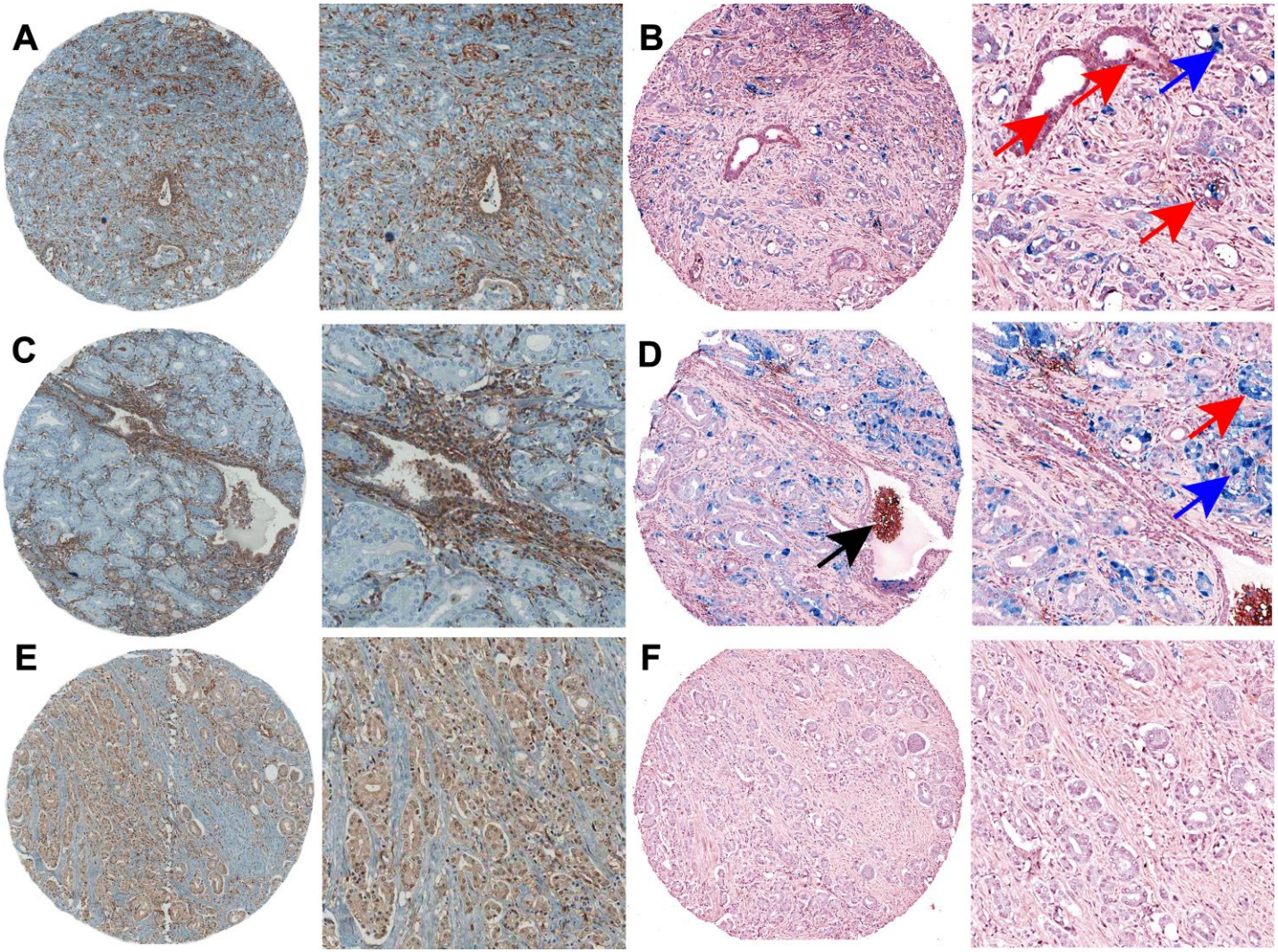

Figure 26. Representative cores showing tumor cores from patients harboring PTEN loss by immunohistochemistry. **A** – Tumor core evidencing complete PTEN loss by immunohistochemistry. Note the presence of control stromal cells that are positively stained with PTEN. **B** – Tumor core stained with anti-IDO1, anti-FoxP3, and anti-PDL1 from the matched sample that harbors PTEN loss demonstrates high total IDO1 expression (blue staining, blue arrow) and high total FoxP3+ Treg cell density (pink staining, red arrow) and foci of PDL1 positive tumor cells

(brown staining). **C** – Core with complete PTEN loss by immunohistochemistry. **D** – Same patient core from **C** showing a total FoxP3+ Treg density (pink staining, red arrow) and IDO1 expression (blue staining, blue arrow). This tumor core also presented increased PDL1 expression (brown staining, black arrow). **E** – Tumor core presenting retained PTEN protein expression. **F** – The same tumor core from **E** demonstrates an absent expression of IDO1 and PDL1 proteins and FoxP3+ Treg density.

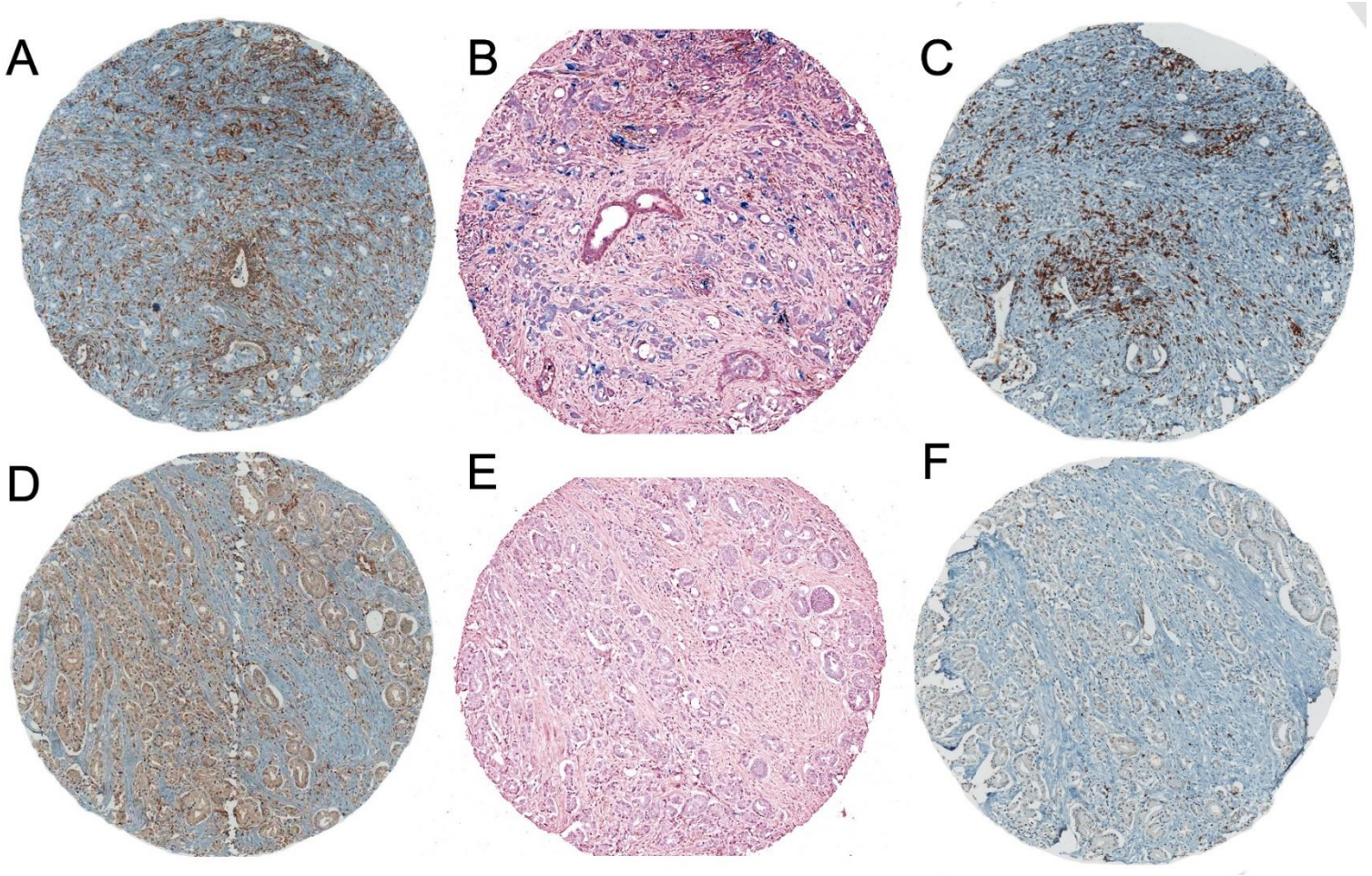

Figure 27. Representative tumor cores showing the association between PTEN and the immune markers. PTEN-deficient tumors (**A**) presented high levels of IDO1 (blue staining), FoxP3+ Treg density (pink staining) (**B**), and CD8+ T cell density (brown staining) (**C**). Conversely, a tumor core with retained PTEN protein expression (**D**) demonstrated low expression of IDO1 and density of FoxP3+ Tregs (**E**). This tumor core also presented low CD8+ T cell density (**F**).

6.3.4 High FoxP3+ Treg cell density is associated with poor outcome in PTEN-deficient prostate cancer

To determine the impact of FoxP3+ Treg cell abundance in the outcome of PTEN-deficient prostate cancer, we investigated tumors with different PTEN status and FoxP3+ Treg densities from TCGA and MSKCC cohorts. We observed that PTEN-deficient tumors with increased FoxP3+ Treg abundance were significantly associated with earlier disease recurrence in TCGA ($P<0.0001$) and MSKCC ($P=0.005$) cohorts (**Figure 28c** and **27d**).

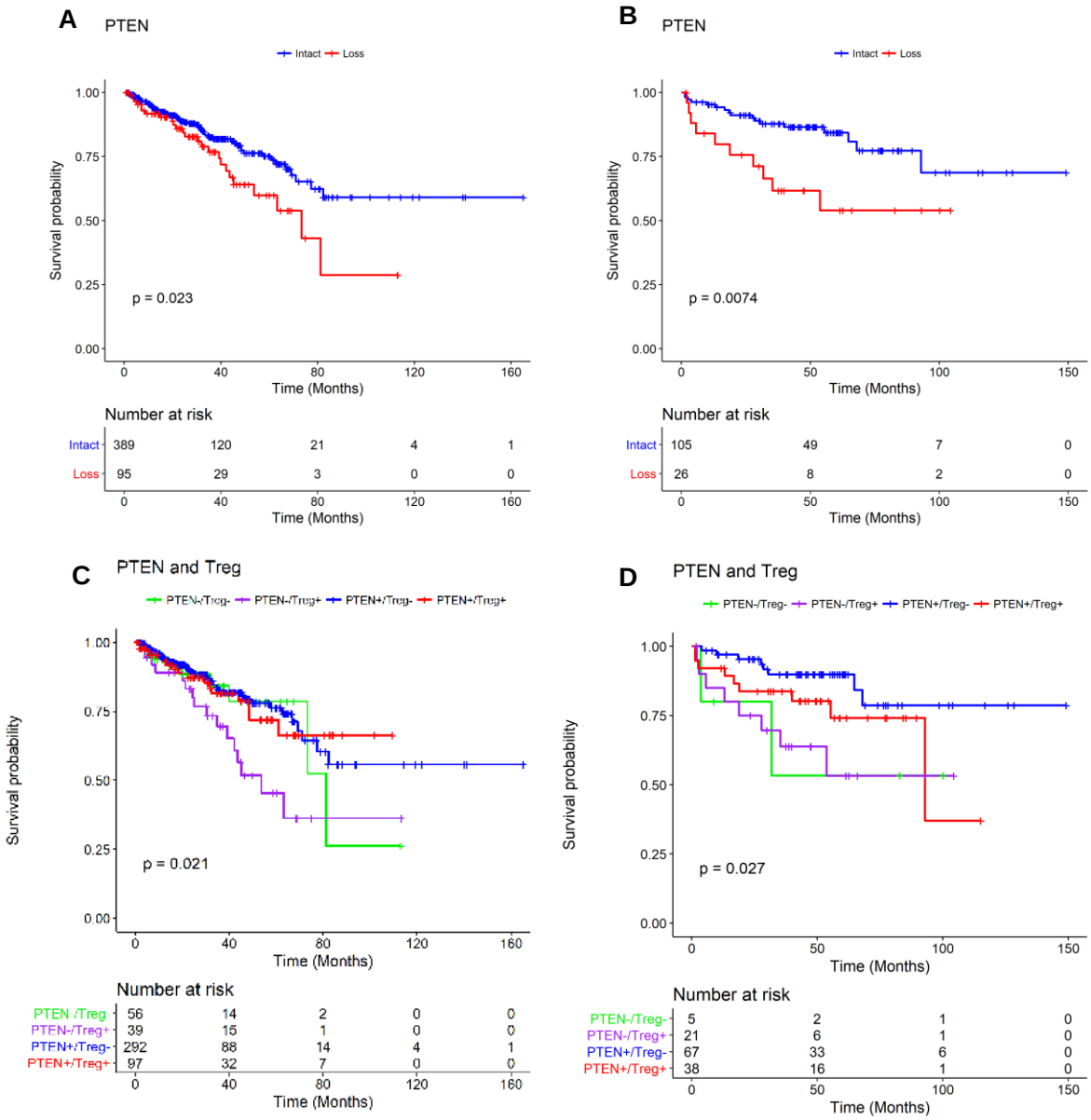

Figure 28. Survival analysis of the in silico cohorts showed that PTEN loss associated with earlier recurrence in both TCGA (A) and MSKCC (B) cohorts. Tumor samples harboring PTEN loss and high FoxP3+ Treg density exhibited earlier disease recurrence in TCGA (**C**) and MSKCC (**D**) cohorts.

The clinical effects of PTEN loss and the overall expression (combined stroma and tumor compartments) of IDO1 and PDL1 proteins and FoxP3+ Treg cell density were then determined for patients from the HCRP cohort. The mean follow-up time for all patients was 80 months, and the average pre-operative PSA level was 38 ng/mL (**Table 5**). From 87 patients with available follow-up data, 19/87 (22%) had biochemical recurrence. From the 76 patients with available PTEN immunohistochemistry data, 16/76 (21%) were PTEN-deficient. Tumors from 30% (26/86) patients had high FoxP3+ Treg cell density (top tertile=1.16), 33% (29/86) had high total IDO1 expression (top tertile=18.6), and 33% (29/86) had high total PDL1 expression (top tertile=5.9).

In the HCRP cohort, high FoxP3+ Treg cell density was significantly associated with high Gleason scores (P=0.01). We did not observe any significant association between IDO1 and PDL1 expression with clinicopathological features in the HCRP cohort (**Table 5**). Outcome analysis showed that high FoxP3+ Treg cell density was significantly associated with earlier biochemical recurrence (P=0.044) (**Figure 29b**). We did not observe any significant association between IDO1 or PDL1 expression with biochemical recurrence (P=0.89 and P=0.63, respectively) (**Figure 30a** and **30b**). In the univariate Cox regression model, we found that patient tumors with high FoxP3+ Treg density were not significantly associated with biochemical recurrence (HR=2.5, CI 95% 0.9-6.6, P=0.052) (**Table 6**). Concordantly, in multivariable analysis adjusted with age, pre-operative PSA, and Gleason score, high FoxP3+ density was not significantly associated with biochemical recurrence (HR=2.59, CI 95% 0.88-7.55, P=0.08).

To validate the *in silico* association between PTEN-deficiency and high FoxP3+ Treg density with earlier recurrence, we combined both biomarkers in the HCRP cohort. These analyses confirmed that PTEN-deficient tumors with high FoxP3+ Treg cell densities present earlier PSA-related relapse, with 50% of patients presenting PSA-related relapse at 50 months after their radical prostatectomy (P=0.003) (**Figure 29c**).

Table 5. Frequency and association of the markers with clinicopathological features of patients from HCRP cohort.

		PTEN			FoxP3+			IDO1			PDL1		
		Intact	**Loss**	**P**	**High**	**Low**	**P**	**High**	**Low**	**P**	**High**	**Low**	**P**
Age (median)		64	66	0.49	63	64	0.36	68	62.5	0.79	63.5	64	0.57
Time to recurrence (median)		76	40	0.20	40.5	77.5	0.51	59.5	40.5	0.38	71.5	40.5	0.38
Preoperative PSA (median)		36	42	0.34	29	45	0.43	42.5	35.5	0.42	44	31	0.42
Biochemical recurrence	Missing	1	0	0.05 *	1	5	0.24	1	5	1	1	5	0.40
	No	48	9		17	45		22	40		20	42	
	Yes	11	7		8	10		6	12		8	10	
Gleason score	Missing	0	0	0.49	1	5	0.01 *	1	5	0.76	1	5	0.47
	6	7	0		1	8		4	5		2	7	
	3+4=7	18	4		2	19		7	14		6	15	
	4+3=7	16	4		10	14		7	17		8	16	
	8	7	4		6	4		5	5		6	4	
	9	12	4		6	10		5	11		6	10	
T	Missing	2	0	0.22	2	6	0.78	1	7	0.60	1	7	0.43
	T2N0	44	9		19	6		19	39		22	36	
	T3N0	16	7		39	16		9	13		6	16	
Extraprostatic extension	Missing	0	0	0.12	1	5	0.58	1	5	0.10	1	5	0.78
	No	46	9		20	40		19	41		22	38	
	Yes	14	7		5	15		9	11		6	14	
Vesicular invasion	Missing	2	0	0.06	1	5	1	1	5	0.48	1	5	0.71
	No	50	10		22	49		26	45		24	47	
	Yes	8	6		3	6		2	7		4	5	

Continuous and categorical variables were compared through Mann-Whitney U-test and Fisher exact test, respectively. Missing values were not included for the analyses. *P-value below or equal to 0.05.

Table 6. Univariate and multivariate Cox regression models show that total FoxP3+ Treg density points towards significance to predict biochemical recurrence events in prostate cancer specimens from HCRP cohort.

	Univariate				Multivariate			
	HR	95% CI		P	HR	95% CI		P
		Lower	Upper			Lower	Upper	
PTEN	3.48	1.32	9.15	0.011*	3.38	1.00	9.674	0.03*
FoxP3+ Treg	2.56	0.99	6.61	0.052	2.59	0.88	7.55	0.08
PSA	1	0.98	1.02	0.87	0.99	0.98	1.02	0.84
Gleason score	2.68	1.07	6.67	0.003*	1.74	0.85	7.75	0.09
Age	1.00	0.94	1.06	0.95	0.94	0.89	1.01	0.14

FoxP3+ Treg density in the tumor was defined as high x low based on the tertiles of the total density of cells in a tumor, with low being set as baseline. PSA levels and age were employed in the model as continuous variables. Gleason score was dichotomized as low-to-intermediate risk (3+3 and 3+4) and high risk (4+3, 4+4, ≥4+5). Low-to-intermediate risk Gleason score was set as baseline. *P-value<0.05. HR – hazard ratio, CI – confidence interval, PSA – preoperative serum PSA levels, T – pathological staging.

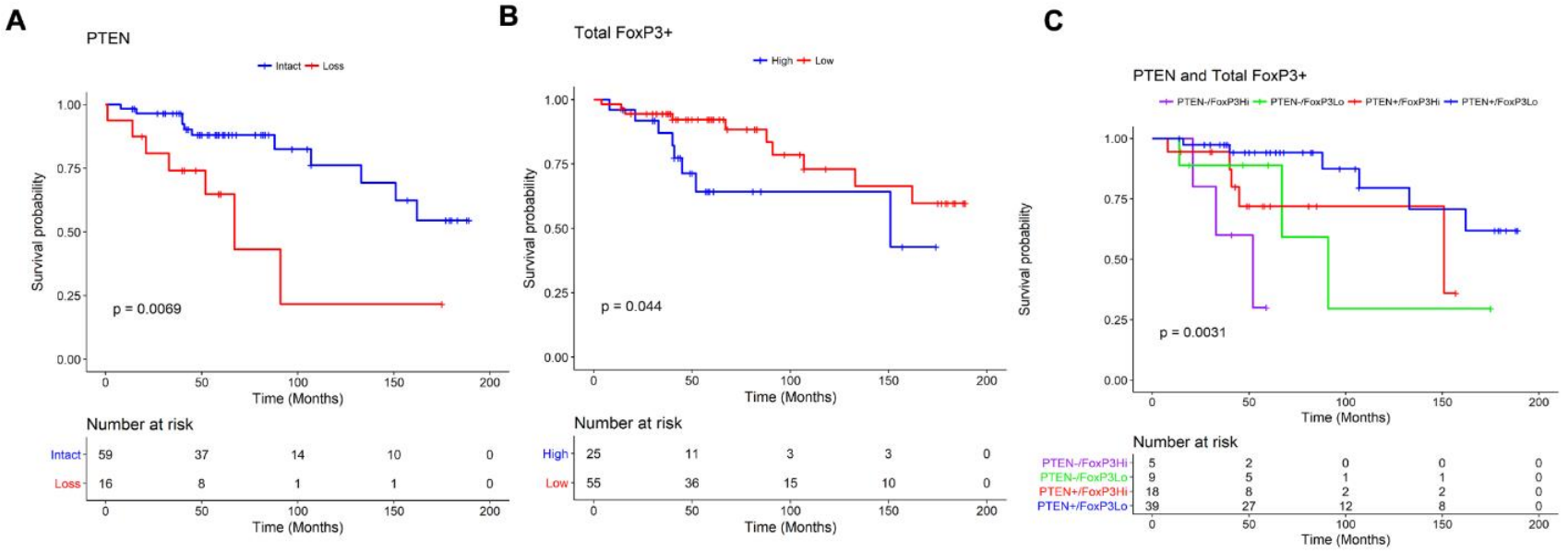

Figure 29. Kaplan Meier curves and log-rank analysis from HCRP cohort showed that PTEN loss and FoxP3+ Treg cell density are significantly associated with biochemical recurrence. A – PTEN deficiency determined by immunohistochemistry was significantly associated with earlier biochemical recurrence. **B** – Increased FoxP3+ Treg cell density was associated with earlier biochemical recurrence in a subset of 80 patients with available data. **C** – Combined PTEN and FoxP3+ Treg density in tumor are strong predictors of earlier biochemical recurrence. Moreover, the comparison between PTEN intact tumors that presented high vs. low FoxP3+ Treg demonstrated that high FoxP3+ Treg density is strongly affects the outcome of patients. FoxP3+ Treg cell density shown was defined based on the overall density in TMA cores (stromal and tumor compartments). P-values shown are derived from log-rank tests.

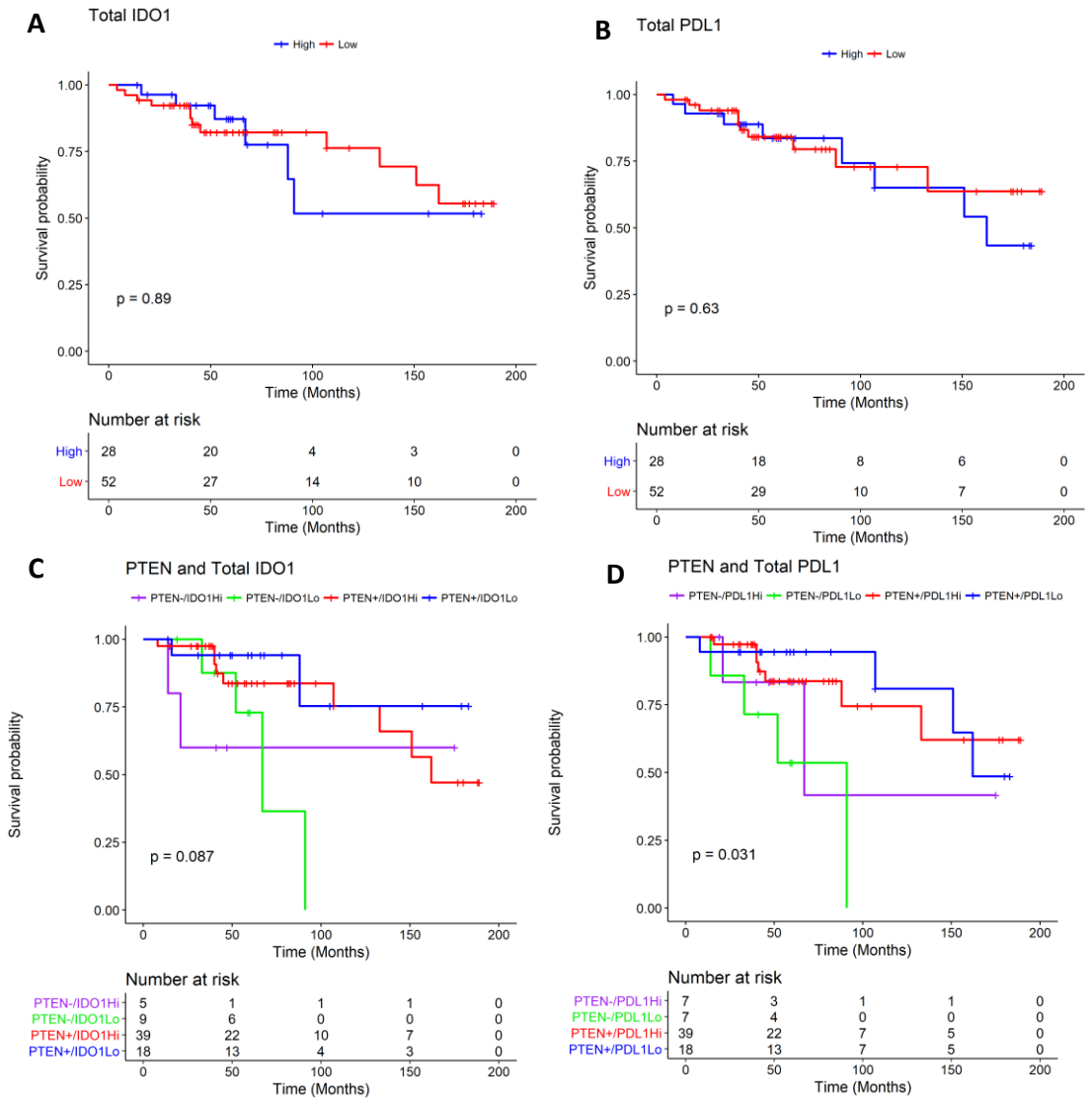

Figure 30. Prognostic impact of immune markers in combination with PTEN status. A – Total IDO1 protein expression was not significantly associated with earlier biochemical recurrence of prostate cancer. **B** – PDL1 was not associated with biochemical recurrence. **C** – PTEN-deficient tumors with high IDO1 protein expression are more likely to have earlier biochemical recurrence. **D** – PTEN deficiency tumors with high PDL1 protein expression were not significantly associated with biochemical recurrence. FoxP3+ Treg cell density and IDO1 and PDL1 protein.

6.4 Discussion

PTEN loss has evolved as a major prognostic biomarker for prostate cancer[36] and has been recently demonstrated to influence the immune response in a PI3K/AKT-independent manner[10,11,45]. Given that tumor-intrinsic changes may contribute to a dysregulated anti-tumor immune response[8,158], our objective was to study the impact of PTEN loss on the TME of prostate tumors. By employing *in silico* tools in a total of 622 primary prostate tumors, 96 mCRPC lesions, and immunohistochemistry in 94 radical prostatectomy specimens, we characterized the PTEN loss associated immune alterations in prostate cancer.

The most novel finding from this study is that PTEN-deficient prostate tumors exhibited increased IDO1 protein expression and had higher FoxP3+ Treg density, suggesting expansion of immunosuppressive factors in PTEN-deficient prostate cancer [159,160]. Although mechanistic studies are needed to assign causal associations, it can be speculated that an immunosuppressed microenvironment in tumors with loss of PTEN and PTEN-L could result from upregulation of IDO1 expression leading to immunosuppression with increased FoxP3+ Treg cells, which in combination could be permissive to tumor growth and invasion.

This study also extended findings of in silico analyses of radical prostatectomy specimens from 94 patients with a prolonged follow-up period. Log-rank analysis revealed that patients with increased FoxP3+ Treg cells are more likely to develop biochemical recurrence. Concordantly, log-rank analysis demonstrated that 50% of patients with PTEN-deficient tumors and high FoxP3+ Treg cell density had PSA-related relapse after 50 months. However, on Cox regression models, there was a trend towards a higher risk of PSA-related relapse for patients with high FoxP3+ Treg density, although statistical significance was not reached in both uni- and multivariable models. Interestingly, high FoxP3+ Treg cell density was defined as the presence of at least one cell per tumor core, which is in concordance with a recent study, suggesting that FoxP3+ cells may have a strong regulatory effect in the TME of prostate tumors[161]. However, due to the limited size of our study cohort, further studies are required to determine the precise impact of FoxP3+ Treg cell in prostate cancer prognosis.

A study conducted on 312 primary prostate cancer specimens showed that high FoxP3+ Treg cell density was not associated with clinicopathological features but was significantly associated with earlier biochemical recurrence and prostate cancer metastasis[81].

In addition, the authors observed that PTEN loss was associated with increased FoxP3+ Treg density. In line with these findings, the evaluation of tumors from 22 patients treated with salvage radiotherapy after radical prostatectomy showed that reduced density of FoxP3+ Tregs was significantly associated with better outcome[162]. Studies conducted in other cancers have confirmed the associations between high FoxP3+ density in breast[108], melanoma[109,110], ovarian[163], and pancreatic[164] tumors and poor outcome.

In prostate cancer, the lack of response to immune checkpoint blockade therapies can be partially attributed to a poorly immune infiltrated TME[165] and a low tumor mutational burden[166–168]. Interestingly, we found that tumors with high IDO1 expression and FoxP3+ Treg cell density also have high density of CD8+ T cells. IDO1 can be expressed on both cancer and immune cells and leads to immunosuppression via degrading tryptophan into kynurenine, which negatively modulates local immune-cell activation[160,169]. Thus, IDO1 suppresses effector T-cell activity and promotes FoxP3+ Treg differentiation[170]. Previous studies have demonstrated that increased expression of *IDO1* in tumors is often associated with poor clinical outcomes including poor response to systemic therapies[134,171]. This finding suggests potentially inactive or dysfunctional state of CD8+ T cells in prostate tumors[134].

It has been previously shown that IFN-γ stimulation of prostate cancer cell lines resulted in the overexpression of IDO1 in PC3 cell lines, which harbor PTEN homozygous deletion[172]. In the same study, the investigation of the prognostic impact of IDO1 expression in 87 prostate cancer cases showed that tumors with high IDO1 expression are more likely to develop biochemical recurrence. A recently published study that investigated 281 primary and metastatic breast tumors demonstrated that IDO1 expression was increased in high-grade triple-negative breast cancers[171]. Given the recent reports on the co-expression of IDO1 and PDL1 immune checkpoints, it has been proposed that combined immunotherapeutic approaches may benefit a subset of breast cancer patients. Since we observed that high IDO1 expression is present in PTEN-deficient tumors, it is possible to speculate that patients with PTEN loss tumors may be more likely to benefit from the currently IDO1-inhibition trials.

Recent reports have shown that the immune checkpoint protein PDL1 is overexpressed in PTEN-deficient lung[115], breast[101] and brain tumors[69]. In metastatic melanoma, PTEN-deficient tumors are less likely to respond to treatment with PD-1 blocking antibodies[84]. Given that PDL1 expression in cancer cells is often induced following

stimulation by IFN-γ produced by activated T cells[173], it can be speculated that lack of IFN-γ in immune excluded tumors is a factor in the reduced expression of PDL1 in prostate cancer tumors. In our study, we did not find any significant correlations between PTEN and PDL1 expression. It has been previously reported that primary prostate tumors usually do not express high levels of PDL1[174] and that PTEN loss does not associate with PDL1 expression[102]. Interestingly, a phase II clinical trial conducted with a patient with metastatic uterine leiomyosarcoma demonstrated that PTEN loss was associated with response to anti-PD1 immune checkpoint blockade therapy[16]. A clear understanding of PDL1 independent immune evasion mechanisms in PTEN-deficient prostate cancer is thus urgently needed for the use of alternate immunomodulatory treatment strategies.

In summary, this study suggests that the TME of PTEN-deficient prostate cancer tumors is immunosuppressed, which is reflected by the presence of factors such as FoxP3+ Treg cells and overexpression of IDO1 protein. Furthermore, these findings may provide insights into future immune checkpoint blockade trials in prostate cancer in which PTEN status has been defined. Further validation in larger independent cohorts and needle-core biopsies are required to precisely determine the prognostic impact of FoxP3+ Treg cells in prostate cancer in the clinical setting. Likewise, mechanistic studies are also needed to define the causal associations between PTEN, IDO1 and FoxP3+ Treg cells.

7. CONCLUSIONS AND FUTURE DIRECTIONS

In this thesis, we performed an extensive review of PTEN functions and investigated how its inactivation is linked to the anti-tumor immune response. *PTEN* loss by mutation and copy number alteration was highly variable among tumor types. Interestingly, gynecological, brain, and prostate tumors exhibited the highest frequencies of *PTEN* inactivation. Our initial hypothesis was that *PTEN*-null tumors would harbor higher aneuploidy and mutational levels compared to tumors with *PTEN* intact or monoallelic inactivation. In fact, we found that *PTEN* monoallelic inactivation was linked to higher genomic instability features in some cancer types.

We also observed that *PTEN*-deficient tumors presented a distinct immune-cell composition depending on tumor type. Moreover, we found that some *PTEN*-null cancers expressed high levels of *IRF3* and other interferon related genes. Thus, we reject our initial hypothesis that *PTEN*-deficient tumors were more likely to exhibit a downregulation of the interferon response.

Immune checkpoint expression was highly heterogeneous among tumors harboring *PTEN* inactivation, suggesting that *PTEN* is a promising biomarker for determining patient response to immunotherapy depending on tumor type. Head and neck, gliomas, glioblastomas, and breast tumors presented the most distinct and significant changes regarding immune checkpoint expression when *PTEN* was lost. Concordantly, in our cohort study of 94 prostate specimens, we found that PTEN protein loss was linked to a highly immunosuppressive TME that presumably favors disease progression. Furthermore, we showed that prostate tumors presenting PTEN protein loss and high Treg density are more likely to be aggressive.

Lastly, we hypothesized that patients whose tumors harbored *PTEN* biallelic inactivation or homozygous deletions would present a worse outcome than those with intact *PTEN*. However, we found that *PTEN* monoallelic inactivation and hemizygous deletions were strongly associated with a shorter recurrence-free survival and cancer-death intervals. Based on these findings, we propose that one allele loss of *PTEN* is linked to a more aggressive disease as a result of haploinsufficiency mechanisms. Thus, when PTEN undergoes biallelic inactivation, tumor cells are presumably under senescence or autophagy-related death mechanisms.

Our PanCancer study is still under development and might thus provide new insights on how PTEN affects the genome and the transcriptome of cancers. Moreover, our study requires several validation experiments, including cohort-derived studies and functional analyses. PTEN silencing in tumor cells followed by functional genomic instability assays may answer questions on how the inactivation of this tumor suppressor influences the TME. In addition, since PTEN loss rates are high depending on tumor type, clinical trials investigating its inactivation status will likely provide insights on how patients respond to therapy.

8. REFERENCES

1. Hanahan D, Weinberg RA. Hallmarks of cancer: The next generation. *Cell* 2011;144:646–74.
2. Schvartzman J-M, Sotillo R, Benezra R. Mitotic chromosomal instability and cancer: mouse modelling of the human disease. *Nat Rev Cancer* 2010;10:102–15.
3. Negrini S, Gorgoulis VG, Halazonetis TD. Genomic instability--an evolving hallmark of cancer. *Nat Rev Mol Cell Biol* 2010;11:220–8.
4. Inoue K, Fry EA. Haploinsufficient tumor suppressor genes. *Adv Med Biol* 118:83–122.
5. Brandmaier A, Hou S-Q, Demaria S, Formenti SC, Shen WH. PTEN at the interface of immune tolerance and tumor suppression. *Front Biol (Beijing)* 2017;12:163–74.
6. Ungefroren H, Sebens S, Seidl D, Lehnert H, Hass R. Interaction of tumor cells with the microenvironment. *Cell Commun Signal* 2011;9:18.
7. Yang Y, Bai Y, He Y, Zhao Y, Chen J, Ma L, Pan Y, Hinten M, Zhang J, Karnes RJ, Kohli M, Westendorf JJ, et al. PTEN Loss Promotes Intratumoral Androgen Synthesis and Tumor Microenvironment Remodeling via Aberrant Activation of RUNX2 in Castration-Resistant Prostate Cancer. *Clin Cancer Res* 2018;24:834–46.
8. Wellenstein MD, de Visser KE. Cancer-Cell-Intrinsic Mechanisms Shaping the Tumor Immune Landscape. *Immunity* 2018;48:399–416.
9. Song MS, Salmena L, Pandolfi PP. The functions and regulation of the PTEN tumour suppressor. *Nat Rev Mol Cell Biol* 2012;13:283–96.
10. Cao Y, Wang H, Yang L, Zhang Z, Li CC-M, Yuan X, Bu L, Chen L, Chen Y, Li CC-M, Guo D. PTEN-L promotes type I interferon responses and antiviral immunity. *Cell Mol Immunol* 2018;15:48–57.
11. Li S, Zhu M, Pan R, Fang T, Cao Y-Y, Chen S, Zhao X, Lei C-Q, Guo L, Chen Y, Li C-M, Jokitalo E, et al. The tumor suppressor PTEN has a critical role in antiviral innate immunity. *Nat Immunol* 2015;17:241–9.
12. Kwon C-H, Zhao D, Chen J, Alcantara S, Li Y, Burns DK, Mason RP, Lee EY-HP, Wu H, Parada LF. Pten Haploinsufficiency Accelerates Formation of High-Grade Astrocytomas. *Cancer Res* 2008;68:3286–94.
13. Snyder A, Makarov V, Merghoub T, Yuan J, Zaretsky JM, Desrichard A, Walsh LA, Postow MA, Wong P, Ho TS, Hollmann TJ, Bruggeman C, et al. Genetic Basis for

Clinical Response to CTLA-4 Blockade in Melanoma. *N Engl J Med* 2014;371:2189–99.

14. Sharma P, Hu-Lieskovan S, Wargo JAJA, Ribas A. Primary, Adaptive, and Acquired Resistance to Cancer Immunotherapy. *Cell* 2017;168:707–23.
15. Goodman AM, Kato S, Bazhenova L, Patel SP, Frampton GM, Miller V, Stephens PJ, Daniels GA, Kurzrock R. Tumor Mutational Burden as an Independent Predictor of Response to Immunotherapy in Diverse Cancers. *Mol Cancer Ther* 2017;16:2598–608.
16. George S, Miao D, Demetri GD, Adeegbe D, Rodig SJ, Shukla S, Lipschitz M, Amin-Mansour A, Raut CP, Carter SL, Hammerman P, Freeman GJ, et al. Loss of PTEN Is Associated with Resistance to Anti-PD-1 Checkpoint Blockade Therapy in Metastatic Uterine Leiomyosarcoma. *Immunity* 2017;46:197–204.
17. Peng W, Chen JQ, Liu C, Malu S, Creasy C, Tetzlaff MT, Xu C, McKenzie JA, Zhang C, Liang X, Williams LJ, Deng W, et al. Loss of PTEN Promotes Resistance to T Cell-Mediated Immunotherapy. *Cancer Discov* 2016;6:202–16.
18. Kryczek I, Lange A, Mottram P, Alvarez X, Cheng P, Hogan M, Moons L, Wei S, Zou L, Machelon V, Emilie D, Terrassa M, et al. CXCL12 and vascular endothelial growth factor synergistically induce neoangiogenesis in human ovarian cancers. *Cancer Res* 2005;65:465–72.
19. Tanaka A, Sakaguchi S. Regulatory T cells in cancer immunotherapy. *Cell Res* 2017;27:109–18.
20. Blankenstein T, Coulie PG, Gilboa E, Jaffee EM. The determinants of tumour immunogenicity. *Nat Rev Cancer* 2012;12:307–13.
21. Turajlic S, Litchfield K, Xu H, Rosenthal R, McGranahan N, Reading JL, Wong YNS, Rowan A, Kanu N, Al Bakir M, Chambers T, Salgado R, et al. Insertion-and-deletion-derived tumour-specific neoantigens and the immunogenic phenotype: a pan-cancer analysis. *Lancet Oncol* 2017;18:1009–21.
22. Dudley JC, Lin M-T, Le DT, Eshleman JR. Microsatellite Instability as a Biomarker for PD-1 Blockade. *Clin Cancer Res* 2016;22:813–20.
23. Jiménez-Sánchez A, Memon D, Pourpe S, Veeraraghavan H, Li Y, Vargas HA, Gill MB, Park KJ, Zivanovic O, Konner J, Ricca J, Zamarin D, et al. Heterogeneous

Tumor-Immune Microenvironments among Differentially Growing Metastases in an Ovarian Cancer Patient. *Cell* 2017;170:927–38.

24. Rosenbaum MW, Bledsoe JR, Morales-Oyarvide V, Huynh TG, Mino-Kenudson M. PD-L1 expression in colorectal cancer is associated with microsatellite instability, BRAF mutation, medullary morphology and cytotoxic tumor-infiltrating lymphocytes. *Mod Pathol* 2016;29:1104–12.
25. Davoli T, Uno H, Wooten EC, Elledge SJ. Tumor aneuploidy correlates with markers of immune evasion and with reduced response to immunotherapy. *Science (80-)* 2017;355:1–14.
26. Taylor AM, Shih J, Ha G, Gao GF, Zhang X, Berger AC, Schumacher SE, Wang C, Hu H, Liu J, Lazar AJ, Cherniack AD, et al. Genomic and Functional Approaches to Understanding Cancer Aneuploidy. *Cancer Cell* 2018;33:676–89.
27. Verdegaal EME, de Miranda NFCC, Visser M, Harryvan T, van Buuren MM, Andersen RS, Hadrup SR, van der Minne CE, Schotte R, Spits H, Haanen JBAG, Kapiteijn EHW, et al. Neoantigen landscape dynamics during human melanoma–T cell interactions. *Nature* 2016;536:91–5.
28. Dong Z-Y, Zhong W-Z, Zhang X-C, Su J, Xie Z, Liu S-Y, Tu H-Y, Chen H-J, Sun Y-L, Zhou Q, Yang J-J, Yang X-N, et al. Potential Predictive Value of TP53 and KRAS Mutation Status for Response to PD-1 Blockade Immunotherapy in Lung Adenocarcinoma. *Clin Cancer Res* 2017;23:3012–24.
29. Ecke TH, Schlechte HH, Schiemenz K, Sachs MD, Lenk S V., Rudolph BD, Loening SA. TP53 gene mutations in prostate cancer progression. *Anticancer Res* 2010;30:1579–86.
30. Davoli T, Xu AW, Mengwasser KE, Sack LM, Yoon JC, Park PJ, Elledge SJ. Cumulative haploinsufficiency and triplosensitivity drive aneuploidy patterns and shape the cancer genome. *Cell* 2013;155:948–62.
31. Muñoz-Fontela C, Mandinova A, Aaronson SA, Lee SW. Emerging roles of p53 and other tumour-suppressor genes in immune regulation. *Nat Rev Immunol* 2016;16:741–50.
32. Yoshimoto M, Cutz JC, Nuin PAS, Joshua AM, Bayani J, Evans AJ, Zielenska M, Squire JA. Interphase FISH analysis of PTEN in histologic sections shows genomic

deletions in 68% of primary prostate cancer and 23% of high-grade prostatic intra-epithelial neoplasias. *Cancer Genet Cytogenet* 2006;169:128–37.

33. Bismar TA, Yoshimoto M, Vollmer RT, Duan Q, Firszt M, Corcos J, Squire JA. PTEN genomic deletion is an early event associated with ERG gene rearrangements in prostate cancer. *BJU Int* 2011;107:477–85.
34. Abate-Shen C. Molecular genetics of prostate cancer. *Genes Dev* 2000;14:2410–34.
35. Nowak DG, Cho H, Herzka T, Watrud K, Demarco D V., Wang VMY, Senturk S, Fellmann C, Ding D, Beinortas T, Kleinman D, Chen M, et al. MYC drives Pten/Trp53-deficient proliferation and metastasis due to IL6 secretion and AKT suppression via PHLPP2. *Cancer Discov* 2015;5:637–51.
36. Jamaspishvili T, Berman DM, Ross AE, Scher HI, De Marzo AM, Squire JA, Lotan TL. Clinical implications of PTEN loss in prostate cancer. *Nat Rev Urol* 2018;15:222–34.
37. Lee Y-R, Chen M, Pandolfi PP. The functions and regulation of the PTEN tumour suppressor: new modes and prospects. *Nat Rev Mol Cell Biol* 2018;19:547–62.
38. Bermúdez Brito M. Focus on PTEN regulation. *Front Oncol* 2015;5:1–15.
39. Maehama T, Dixon JE. The tumor suppressor, PTEN/MMAC1, dephosphorylates the lipid second messenger, phosphatidylinositol 3,4,5-trisphosphate. *J Biol Chem* 1998;273:13375–8.
40. Lee JO, Yang H, Georgescu MM, Cristofano A Di, Maehama T, Shi Y, Dixon JE, Pandolfi P, Pavletich NP. Crystal structure of the PTEN tumor suppressor: Implications for its phosphoinositide phosphatase activity and membrane association. *Cell* 1999;99:323–34.
41. Chen M, Wan L, Zhang J, Zhang J, Mendez L, Clohessy JG, Berry K, Victor J, Yin Q, Zhu Y, Wei W, Pandolfi PP. Deregulated PP1α phosphatase activity towards MAPK activation is antagonized by a tumor suppressive failsafe mechanism. *Nat Commun* 2018;9:159–68.
42. Bassi C, Ho J, Srikumar T, Dowling RJO, Gorrini C, Miller SJ, Mak TW, Neel BG, Raught B, Stambolic V. Nuclear PTEN controls DNA repair and sensitivity to genotoxic stress. *Science* 2013;341:395–9.
43. Shen WH, Balajee AS, Wang J, Wu H, Eng C, Pandolfi PP, Yin Y. Essential Role for

Nuclear PTEN in Maintaining Chromosomal Integrity. *Cell* 2007;128:157–70.

44. Kass EM, Moynahan ME, Jasin M. When Genome Maintenance Goes Badly Awry. *Mol Cell* 2016;62:777–87.
45. Zhao D, Lu X, Wang G, Lan Z, Liao W, Li J, Liang X, Chen JR, Shah S, Shang X, Tang M, Deng P, et al. Synthetic essentiality of chromatin remodelling factor CHD1 in PTEN-deficient cancer. *Nature* 2017;542:484–8.
46. Parisotto M, Grelet E, El Bizri R, Dai Y, Terzic J, Eckert D, Gargowitsch L, Bornert J-M, Metzger D. PTEN deletion in luminal cells of mature prostate induces replication stress and senescence in vivo. *J Exp Med* 2018;215:1749–63.
47. Ning L, Guo-Chun Z, Sheng-Li A, Xue-Rui L, Kun W, Jian Z, Chong-Yang R, Ling-Zhu W, Hai-Tong L. Inhibition of autophagy induced by PTEN loss promotes intrinsic breast cancer resistance to trastuzumab therapy. *Tumor Biol* 2016;37:5445–54.
48. Rosenfeldt MT, O'Prey J, Flossbach L, Nixon C, Morton JP, Sansom OJ, Ryan KM. PTEN deficiency permits the formation of pancreatic cancer in the absence of autophagy. *Cell Death Differ* 2017;24:1303–4.
49. Errafiy R, Aguado C, Ghislat G, Esteve JM, Gil A, Loutfi M, Knecht E. PTEN Increases Autophagy and Inhibits the Ubiquitin-Proteasome Pathway in Glioma Cells Independently of its Lipid Phosphatase Activity. *PLoS One* 2013;8:1–12.
50. Collado M, Blasco MA, Serrano M. Cellular Senescence in Cancer and Aging. *Cell* 2007;130:223–33.
51. Di Mitri D, Toso A, Chen JJ, Sarti M, Pinton S, Jost TR, D'Antuono R, Montani E, Garcia-Escudero R, Guccini I, Da Silva-Alvarez S, Collado M, et al. Tumour-infiltrating Gr-1+ myeloid cells antagonize senescence in cancer. *Nature* 2014;515:134–7.
52. Butler DE, Marlein C, Walker HF, Frame FM, Mann VM, Simms MS, Davies BR, Collins AT, Maitland NJ. Inhibition of the PI3K/AKT/mTOR pathway activates autophagy and compensatory Ras/Raf/MEK/ERK signalling in prostate cancer. *Oncotarget* 2017;8:1–12.
53. Jung SH, Hwang HJ, Kang D, Park HA, Lee HC, Jeong D, Lee K, Park HJ, Ko Y-G, Lee J-S. mTOR kinase leads to PTEN-loss-induced cellular senescence by phosphorylating p53. *Oncogene* 2018;

54. Chen Z, Trotman LC, Shaffer D, Lin H-K, Dotan ZA, Niki M, Koutcher JA, Scher HI, Ludwig T, Gerald W, Cordon-Cardo C, Paolo Pandolfi P. Crucial role of p53-dependent cellular senescence in suppression of Pten-deficient tumorigenesis. *Nature* 2005;436:725–30.
55. Lee JY, Nakada D, Yilmaz OH, Tothova Z, Joseph NM, Lim MS, Gilliland DG, Morrison SJ. mTOR Activation Induces Tumor Suppressors that Inhibit Leukemogenesis and Deplete Hematopoietic Stem Cells after Pten Deletion. *Cell Stem Cell* 2010;7:593–605.
56. Berger AH, Knudson AG, Pandolfi PP. A continuum model for tumour suppression. *Nature* 2011;476:163–9.
57. Alimonti A, Carracedo A, Clohessy JG, Trotman LC, Nardella C, Egia A, Salmena L, Sampieri K, Haveman WJ, Brogi E, Richardson AL, Zhang J, et al. Subtle variations in Pten dose determine cancer susceptibility. *Nat Genet* 2010;42:454–8.
58. Sun Z, Huang C, He J, Lamb KL, Kang X, Gu T, Shen WH, Yin Y. PTEN C-Terminal Deletion Causes Genomic Instability and Tumor Development. *Cell Rep* 2014;6:844–54.
59. Puc J, Keniry M, Li HS, Pandita TK, Choudhury AD, Memeo L, Mansukhani M, Murty VVVS, Gaciong Z, Meek SEM, Piwnica-Worms H, Hibshoosh H, et al. Lack of PTEN sequesters CHK1 and initiates genetic instability. *Cancer Cell* 2005;7:193–204.
60. Puc J, Parsons R. PTEN Loss Inhibits CHK1 to Cause Double Stranded-DNA Breaks in Cells. *Cell Cycle* 2005;4:927–9.
61. Ock C-Y, Hwang J-E, Keam B, Kim S-B, Shim J-J, Jang H-J, Park S, Sohn BH, Cha M, Ajani JA, Kopetz S, Lee K-W, et al. Genomic landscape associated with potential response to anti-CTLA-4 treatment in cancers. *Nat Commun* 2017;8:1050–62.
62. Santaguida S, Richardson A, Iyer DR, M'Saad O, Zasadil L, Knouse KA, Wong YL, Rhind N, Desai A, Amon A. Chromosome Mis-segregation Generates Cell-Cycle-Arrested Cells with Complex Karyotypes that Are Eliminated by the Immune System. *Dev Cell* 2017;41:638–651.e5.
63. Bakhoum SF, Cantley LC. The Multifaceted Role of Chromosomal Instability in Cancer and Its Microenvironment. *Cell* 2018;174:1347–60.

64. Mouw KW, Goldberg MS, Konstantinopoulos PA, D'Andrea AD. DNA damage and repair biomarkers of immunotherapy response. *Cancer Discov* 2017;7:675–93.
65. Vidotto T, Tiezzi DG, Squire JA. Distinct subtypes of genomic PTEN deletion size influence the landscape of aneuploidy and outcome in prostate cancer. *Mol Cytogenet* 2018;11:1–12.
66. Mittendorf EA, Philips A V., Meric-Bernstam F, Qiao N, Wu Y, Harrington S, Su X, Wang Y, Gonzalez-Angulo AM, Akcakanat A, Chawla A, Curran M, et al. PD-L1 Expression in Triple-Negative Breast Cancer. *Cancer Immunol Res* 2014;2:361–70.
67. Berghoff AS, Kiesel B, Widhalm G, Rajky O, Ricken G, Wohrer A, Dieckmann K, Filipits M, Brandstetter A, Weller M, Kurscheid S, Hegi ME, et al. Programmed death ligand 1 expression and tumor-infiltrating lymphocytes in glioblastoma. *Neuro Oncol* 2015;17:1064–75.
68. Garcia AJ, Ruscetti M, Arenzana TL, Tran LM, Bianci-Frias D, Sybert E, Priceman SJ, Wu L, Nelson PS, Smale ST, Wu H. Pten Null Prostate Epithelium Promotes Localized Myeloid-Derived Suppressor Cell Expansion and Immune Suppression during Tumor Initiation and Progression. *Mol Cell Biol* 2014;34:2017–28.
69. Parsa AT, Waldron JS, Panner A, Crane CA, Parney IF, Barry JJ, Cachola KE, Murray JC, Tihan T, Jensen MC, Mischel PS, Stokoe D, et al. Loss of tumor suppressor PTEN function increases B7-H1 expression and immunoresistance in glioma. *Nat Med* 2007;13:84–8.
70. Fuertes MB, Woo SR, Burnett B, Fu YX, Gajewski TF. Type I interferon response and innate immune sensing of cancer. *Trends Immunol* 2013;34:67–73.
71. Parker BS, Rautela J, Hertzog PJ. Antitumour actions of interferons: implications for cancer therapy. *Nat Rev Cancer* 2016;16:131–44.
72. Shen H, Lentsch AB. Progressive dysregulation of transcription factors NF-κB and STAT1 in prostate cancer cells causes proangiogenic production of CXC chemokines. *Am J Physiol Physiol* 2004;286:840–7.
73. Armstrong CWD, Maxwell PJ, Ong CW, Redmond KM, Mccann C, Neisen J, Ward GA, Chessari G, Johnson C, Crawford NT, Labonte MJ, Prise KM, et al. PTEN deficiency promotes macrophage infiltration and hypersensitivity of prostate cancer to IAP antagonist/radiation combination therapy. *Oncotarget* 2016;7:7885–98.

74. Ying H, Elpek KG, Vinjamoori A, Zimmerman SM, Chu GC, Yan H, Fletcher-Sananikone E, Zhang H, Liu Y, Wang W, Ren X, Zheng H, et al. PTEN is a major tumor suppressor in pancreatic ductal adenocarcinoma and regulates an NF-κB-cytokine network. *Cancer Discov* 2011;1:158–69.
75. Calcinotto A, Spataro C, Zagato E, Di Mitri D, Gil V, Crespo M, De Bernardis G, Losa M, Mirenda M, Pasquini E, Rinaldi A, Sumanasuriya S, et al. IL-23 secreted by myeloid cells drives castration-resistant prostate cancer. *Nature* 2018;559:363–9.
76. Toso A, Revandkar A, DiMitri D, Guccini I, Proietti M, Sarti M, Pinton S, Zhang J, Kalathur M, Civenni G, Jarrossay D, Montani E, et al. Enhancing chemotherapy efficacy in pten-deficient prostate tumors by activating the senescence-associated antitumor immunity. *Cell Rep* 2014;9:75–89.
77. Loveridge CJ, Mui EJ, Patel R, Tan EH, Ahmad I, Welsh M, Galbraith J, Hedley A, Nixon C, Blyth K, Sansom O, Leung HY. Increased T-cell Infiltration Elicited by Erk5 Deletion in a Pten -Deficient Mouse Model of Prostate Carcinogenesis. *Cancer Res* 2017;77:3158–68.
78. Phillips RJ, Mestas J, Gharaee-Kermani M, Burdick MD, Sica A, Belperio JA, Keane MP, Strieter RM. Epidermal Growth Factor and Hypoxia-induced Expression of CXC Chemokine Receptor 4 on Non-small Cell Lung Cancer Cells Is Regulated by the Phosphatidylinositol 3-Kinase/PTEN/AKT/Mammalian Target of Rapamycin Signaling Pathway and Activation of Hypoxia Ind. *J Biol Chem* 2005;280:22473–81.
79. Conley-LaComb M, Saliganan A, Kandagatla P, Chen YQ, Cher ML, Chinni SR. PTEN loss mediated Akt activation promotes prostate tumor growth and metastasis via CXCL12/CXCR4 signaling. *Mol Cancer* 2013;12:85.
80. Maxwell PJ, Neisen J, Messenger J, Waugh DJJ. Tumor-derived CXCL8 signaling augments stroma-derived CCL2-promoted proliferation and CXCL12-mediated invasion of PTEN-deficient prostate cancer cells. *Oncotarget* 2014;5:4895–908.
81. Kaur HB, Guedes LB, Lu J, Maldonado L, Reitz L, Barber JR, De Marzo AM, Tosoian JJ, Tomlins SA, Schaeffer EM, Joshu CE, Sfanos KS, et al. Association of tumor-infiltrating T-cell density with molecular subtype, racial ancestry and clinical outcomes in prostate cancer. *Mod Pathol* 2018;1–7.
82. Bian Y, Hall B, Sun Z-J, Molinolo A, Chen W, Gutkind JS, Waes C V, Kulkarni AB.

Loss of TGF-β signaling and PTEN promotes head and neck squamous cell carcinoma through cellular senescence evasion and cancer-related inflammation. *Oncogene* 2012;31:3322–32.

83. Shabaneh TB, Molodtsov AK, Steinberg SM, Zhang P, Torres GM, Mohamed GA, Boni A, Curiel TJ, Angeles C V., Turk MJ. Oncogenic BRAFV600E Governs Regulatory T-cell Recruitment during melanoma tumorigenesis. *Cancer Res* 2018;78:5038–49.
84. Peng W, Chen JQ, Liu C, Malu S, Creasy C, Tetzlaff MT, Xu C, McKenzie JA, Zhang C, Liang X, Williams LJ, Deng W, et al. Loss of PTEN promotes resistance to T cell–mediated immunotherapy. *Cancer Discov* 2016;6:202–16.
85. Mahmoud SMA, Paish EC, Powe DG, Macmillan RD, Grainge MJ, Lee AHS, Ellis IO, Green AR. Tumor-Infiltrating CD8 + Lymphocytes Predict Clinical Outcome in Breast Cancer. *J Clin Oncol* 2011;29:1949–55.
86. Pagès F, Kirilovsky A, Mlecnik B, Asslaber M, Tosolini M, Bindea G, Lagorce C, Wind P, Marliot F, Bruneval P, Zatloukal K, Trajanoski Z, et al. In Situ Cytotoxic and Memory T Cells Predict Outcome in Patients With Early-Stage Colorectal Cancer. *J Clin Oncol* 2009;27:5944–51.
87. Gentles AJ, Newman AM, Liu CL, Bratman S V, Feng W, Kim D, Nair VS, Xu Y, Khuong A, Hoang CD, Diehn M, West RB, et al. The prognostic landscape of genes and infiltrating immune cells across human cancers. *Nat Med* 2015;21:938–45.
88. Sica A, Schioppa T, Mantovani A, Allavena P. Tumour-associated macrophages are a distinct M2 polarised population promoting tumour progression: Potential targets of anti-cancer therapy. *Eur J Cancer* 2006;42:717–27.
89. Zhang M, He Y, Sun X, Li Q, Wang W, Zhao A, Di W. A high M1/M2 ratio of tumor-associated macrophages is associated with extended survival in ovarian cancer patients. *J Ovarian Res* 2014;7:19.
90. Song M, Chen D, Lu B, Wang C, Zhang J, Huang L, Wang X, Timmons CL, Hu J, Liu B, Wu X, Wang L, et al. PTEN Loss Increases PD-L1 Protein Expression and Affects the Correlation between PD-L1 Expression and Clinical Parameters in Colorectal Cancer. *PLoS One* 2013;8:e65821.
91. Crumley S, Kurnit K, Hudgens C, Fellman B, Tetzlaff MT, Broaddus R. Identification

of a subset of microsatellite-stable endometrial carcinoma with high PD-L1 and CD8+ lymphocytes. *Mod Pathol* 2018;In Press.

92. Liang X, Daikoku T, Terakawa J, Ogawa Y, Joshi AR, Ellenson LH, Sun X, Dey SK. The uterine epithelial loss of Pten is inefficient to induce endometrial cancer with intact stromal Pten. *PLoS Genet* 2018;14:1–19.
93. Waldron JS, Yang I, Han S, Tihan T, Sughrue ME, Mills SA, Pieper RO, Parsa AT. Implications for immunotherapy of tumor-mediated T-cell apoptosis associated with loss of the tumor suppressor PTEN in glioblastoma. *J Clin Neurosci* 2010;17:1543–7.
94. Li N, Qin J, Lan L, Zhang H, Liu F, Wu Z, Ni H, Wang Y. PTEN inhibits macrophage polarization from M1 to M2 through CCL2 and VEGF-A reduction and NHERF-1 synergism. *Cancer Biol Ther* 2015;16:297–306.
95. Kim HS, Lee JH, Nam SJ, Ock CY, Moon JW, Yoo CW, Lee GK, Han JY. Association of PD-L1 Expression with Tumor-Infiltrating Immune Cells and Mutation Burden in High-Grade Neuroendocrine Carcinoma of the Lung. *J Thorac Oncol* 2018;13:636–48.
96. Xu C, Fillmore CM, Koyama S, Wu H, Zhao Y, Chen Z, Herter-Sprie GS, Akbay EA, Tchaicha JH, Altabef A, Reibel JB, Walton Z, et al. Loss of lkb1 and pten leads to lung squamous cell carcinoma with elevated pd-l1 expression. *Cancer Cell* 2014;25:590–604.
97. Hlaing AM, Furusato B, Udo E, Kitamura Y, Souda M, Masutani M, Fukuoka J. Expression of phosphatase and tensin homolog and programmed cell death ligand 1 in adenosquamous carcinoma of the lung. *Biochem Biophys Res Commun* 2018;503:2764–9.
98. Lastwika KJ, Wilson W, Li QK, Norris J, Xu H, Ghazarian SR, Kitagawa H, Kawabata S, Taube JM, Yao S, Liu LN, Gills JJ, et al. Control of PD-L1 Expression by Oncogenic Activation of the AKT–mTOR Pathway in Non–Small Cell Lung Cancer. *Cancer Res* 2016;76:227–38.
99. Iwanaga K, Yang Y, Raso MG, Ma L, Hanna AE, Thilaganathan N, Moghaddam S, Evans CM, Li H, Cai W-W, Sato M, Minna JD, et al. Pten Inactivation Accelerates Oncogenic K-ras-Initiated Tumorigenesis in a Mouse Model of Lung Cancer. *Cancer Res* 2008;68:1119–27.

100. Homet Moreno B, Zaretsky JM, Garcia-Diaz A, Tsoi J, Parisi G, Robert L, Meeth K, Ndoye A, Bosenberg M, Weeraratna AT, Graeber TG, Comin-Anduix B, et al. Response to Programmed Cell Death-1 Blockade in a Murine Melanoma Syngeneic Model Requires Costimulation, CD4, and CD8 T Cells. *Cancer Immunol Res* 2016;4:845–57.
101. Dong Y, Richards JA, Gupta R, Aung PP, Emley A, Kluger Y, Dogra SK, Mahalingam M, Wajapeyee N. PTEN functions as a melanoma tumor suppressor by promoting host immune response. *Oncogene* 2014;33:4632–42.
102. Martin AM, Nirschl TR, Nirschl CJ, Francica BJ, Kochel CM, van Bokhoven A, Meeker AK, Lucia MS, Anders RA, DeMarzo AM, Drake CG. Paucity of PD-L1 expression in prostate cancer: innate and adaptive immune resistance. *Prostate Cancer Prostatic Dis* 2015;18:325–32.
103. Jolly LA, Massoll N, Franco AT. Immune Suppression Mediated by Myeloid and Lymphoid Derived Immune Cells in the Tumor Microenvironment Facilitates Progression of Thyroid Cancers Driven by HrasG12V and Pten Loss. *J Clin Cell Immunol* 2016;7:1–12.
104. Colombo MP, Piconese S. Regulatory T-cell inhibition versus depletion: the right choice in cancer immunotherapy. *Nat Rev Cancer* 2007;7:880–7.
105. Sato E, Olson SH, Ahn J, Bundy B, Nishikawa H, Qian F, Jungbluth AA, Frosina D, Gnjatic S, Ambrosone C, Kepner J, Odunsi T, et al. Intraepithelial CD8+ tumor-infiltrating lymphocytes and a high CD8+/regulatory T cell ratio are associated with favorable prognosis in ovarian cancer. *Proc Natl Acad Sci* 2005;102:18538–43.
106. Shen Z, Zhou S, Wang Y, Li R, Zhong C, Liang C, Sun Y. Higher intratumoral infiltrated Foxp3+ Treg numbers and Foxp3+/CD8+ ratio are associated with adverse prognosis in resectable gastric cancer. *J Cancer Res Clin Oncol* 2010;136:1585–95.
107. Jordanova ES, Gorter A, Ayachi O, Prins F, Durrant LG, Kenter GG, van der Burg SH, Fleuren GJ. Human Leukocyte Antigen Class I, MHC Class I Chain-Related Molecule A, and CD8+/Regulatory T-Cell Ratio: Which Variable Determines Survival of Cervical Cancer Patients? *Clin Cancer Res* 2008;14:2028–35.
108. Bates GJ, Fox SB, Han C, Leek RD, Garcia JF, Harris AL, Banham AH. Quantification of regulatory T cells enables the identification of high-risk breast

cancer patients and those at risk of late relapse. *J Clin Oncol* 2006;24:5373–80.

109. Miracco C, Mourmouras V, Biagioli M, Rubegni P, Mannucci S, Monciatti I, Cosci E, Tosi P, Luzi P. Utility of tumour-infiltrating CD25+FOXP3+ regulatory T cell evaluation in predicting local recurrence in vertical growth phase cutaneous melanoma. *Oncol Rep* 2007;18:1115–22.
110. Mougiakakos D, Johansson CC, Trocme E, All-Ericsson C, Economou MA, Larsson O, Seregard S, Kiessling R. Intratumoral forkhead box p3-positive regulatory t cells predict poor survival in cyclooxygenase-2-positive uveal melanoma. *Cancer* 2010;116:2224–33.
111. Sharma MD, Shinde R, McGaha TL, Huang L, Holmgaard RB, Wolchok JD, Mautino MR, Celis E, Sharpe AH, Francisco LM, Powell JD, Yagita H, et al. The PTEN pathway in T regs is a critical driver of the suppressive tumor microenvironment. *Sci Adv* 2015;1:1–15.
112. Gabrilovich DI, Nagaraj S. Myeloid-derived suppressor cells as regulators of the immune system. *Nat Rev Immunol* 2009;9:162–74.
113. Limagne E, Euvrard R, Thibaudin M, Rébé C, Derangère V, Chevriaux A, Boidot R, Végran F, Bonnefoy N, Vincent J, Bengrine-Lefevre L, Ladoire S, et al. Accumulation of MDSC and Th17 Cells in Patients with Metastatic Colorectal Cancer Predicts the Efficacy of a FOLFOX–Bevacizumab Drug Treatment Regimen. *Cancer Res* 2016;76:5241–52.
114. Gabitass RF, Annels NE, Stocken DD, Pandha HA, Middleton GW. Elevated myeloid-derived suppressor cells in pancreatic, esophageal and gastric cancer are an independent prognostic factor and are associated with significant elevation of the Th2 cytokine interleukin-13. *Cancer Immunol Immunother* 2011;60:1419–30.
115. Lastwika KJ, Wilson W, Li QK, Norris J, Xu H, Ghazarian SR, Kitagawa H, Kawabata S, Taube JM, Yao S, Liu LN, Gills JJ, et al. Control of PD-L1 expression by oncogenic activation of the AKT-mTOR pathway in non-small cell lung cancer. *Cancer Res* 2016;76:227–38.
116. Zhang X, Zeng Y, Qu Q, Zhu J, Liu Z, Ning W, Zeng H, Zhang N, Du W, Chen C, Huang J. PD-L1 induced by IFN-γ from tumor-associated macrophages via the JAK/STAT3 and PI3K/AKT signaling pathways promoted progression of lung cancer.

Int J Clin Oncol 2017;22:1026–33.

117. Mimura K, Teh JL, Okayama H, Shiraishi K, Kua L-F, Koh V, Smoot DT, Ashktorab H, Oike T, Suzuki Y, Fazreen Z, Asuncion BR, et al. PD-L1 expression is mainly regulated by interferon gamma associated with JAK-STAT pathway in gastric cancer. *Cancer Sci* 2018;109:43–53.
118. Feng S, Cheng X, Zhang L, Lu X, Chaudhary S, Teng R, Frederickson C, Champion MM, Zhao R, Cheng L, Gong Y, Deng H, et al. Myeloid-derived suppressor cells inhibit T cell activation through nitrating LCK in mouse cancers. *Proc Natl Acad Sci* 2018;115:10094–9.
119. Marshall NA, Galvin KC, Corcoran A-MB, Boon L, Higgs R, Mills KHG. Immunotherapy with PI3K Inhibitor and Toll-Like Receptor Agonist Induces IFN-+IL-17+ Polyfunctional T Cells That Mediate Rejection of Murine Tumors. *Cancer Res* 2012;72:581–91.
120. Williams JL, Greer PA, Squire JA. Recurrent copy number alterations in prostate cancer: An in silico meta-analysis of publicly available genomic data. *Cancer Genet* 2014;207:474–88.
121. Endersby R, Baker SJ. PTEN signaling in brain: neuropathology and tumorigenesis. *Oncogene* 2008;27:5416–30.
122. Koh CM, Gurel B, Sutcliffe S, Aryee MJ, Schultz D, Iwata T, Uemura M, Zeller KI, Anele U, Zheng Q, Hicks JL, Nelson WG, et al. Alterations in nucleolar structure and gene expression programs in prostatic neoplasia are driven by the MYC oncogene. *Am J Pathol* 2011;178:1824–34.
123. He J, Zhang Z, Ouyang M, Yang F, Hao H, Lamb KL, Yang J, Yin Y, Shen WH. PTEN regulates EG5 to control spindle architecture and chromosome congression during mitosis. *Nat Commun* 2016;7:12355–7.
124. Planchon SM, Waite K a, Eng C. The nuclear affairs of PTEN. *J Cell Sci* 2008;121:249–53.
125. Chabanon RM, Pedrero M, Lefebvre C, Marabelle A, Soria J-C, Postel-Vinay S, Hodi F, O'Day S, McDermott D, Weber R, Sosman J, Haanen J, et al. Mutational Landscape and Sensitivity to Immune Checkpoint Blockers. *Clin Cancer Res* 2016;22:4309–21.
126. Colaprico A, Silva TC, Olsen C, Garofano L, Cava C, Garolini D, Sabedot TS, Malta

TM, Pagnotta SM, Castiglioni I, Ceccarelli M, Bontempi G, et al. TCGAbiolinks : an R/Bioconductor package for integrative analysis of TCGA data. *Nucleic Acids Res* 2016;44:1–11.

127. Thorsson V, Gibbs DL, Brown SD, Wolf D, Bortone DS, Ou Yang TH, Porta-Pardo E, Gao GF, Plaisier CL, Eddy JA, Ziv E, Culhane AC, et al. The Immune Landscape of Cancer. *Immunity* 2018;48:812–830.e14.
128. Malta TM, Sokolov A, Gentles AJ, Burzykowski T, Poisson L, Weinstein JN, Kamińska B, Huelsken J, Omberg L, Gevaert O, Colaprico A, Czerwińska P, et al. Machine Learning Identifies Stemness Features Associated with Oncogenic Dedifferentiation. *Cell* 2018;173:338–354.e15.
129. Krohn A, Diedler T, Burkhardt L, Mayer PS, De Silva C, Meyer-Kornblum M, Kötschau D, Tennstedt P, Huang J, Gerhäuser C, Mader M, Kurtz S, et al. Genomic deletion of PTEN is associated with tumor progression and early PSA recurrence in ERG fusion-positive and fusion-negative prostate cancer. *Am J Pathol* 2012;181:401–12.
130. Anagnostou V, Smith KN, Forde PM, Niknafs N, Bhattacharya R, White J, Zhang T, Adleff V, Phallen J, Wali N, Hruban C, Guthrie VB, et al. Evolution of neoantigen landscape during immune checkpoint blockade in non-small cell lung cancer. *Cancer Discov* 2017;7:264–76.
131. McMenamin ME, Soung P, Perera S, Kaplan I, Loda M, Sellers WR. Loss of PTEN expression in paraffin-embedded primary prostate cancer correlates with high Gleason score and advanced stage. *Cancer Res* 1999;59:4291–6.
132. Härtlova A, Erttmann SF, Raffi FAM, Schmalz AM, Resch U, Anugula S, Lienenklaus S, Nilsson LM, Kröger A, Nilsson JA, Ek T, Weiss S, et al. DNA Damage Primes the Type I Interferon System via the Cytosolic DNA Sensor STING to Promote Anti-Microbial Innate Immunity. *Immunity* 2015;42:332–43.
133. Li F, Zhang R, Li S, Liu J. IDO1: An important immunotherapy target in cancer treatment. *Int Immunopharmacol* 2017;47:70–7.
134. Kiyozumi Y, Baba Y, Okadome K, Yagi T, Ishimoto T, Iwatsuki M, Miyamoto Y, Yoshida N, Watanabe M, Komohara Y, Baba H. IDO1 Expression Is Associated With Immune Tolerance and Poor Prognosis in Patients With Surgically Resected

Esophageal Cancer. *Ann Surg* 2018;1–8.

135. Rooney MSS, Shukla SAA, Wu CJJ, Getz G, Hacohen N. Molecular and Genetic Properties of Tumors Associated with Local Immune Cytolytic Activity. *Cell* 2015;160:48–61.
136. Wainwright DA, Balyasnikova I V., Chang AL, Ahmed AU, Moon K-S, Auffinger B, Tobias AL, Han Y, Lesniak MS. IDO Expression in Brain Tumors Increases the Recruitment of Regulatory T Cells and Negatively Impacts Survival. *Clin Cancer Res* 2012;18:6110–21.
137. Munn DH, Sharma MD, Johnson TS, Rodriguez P. IDO, PTEN-expressing Tregs and control of antigen-presentation in the murine tumor microenvironment. *Cancer Immunol Immunother* 2017;66:1049–58.
138. Yoshimoto M, Cunha IW, Coudry RA, Fonseca FP, Torres CH, Soares FA, Squire JA. FISH analysis of 107 prostate cancers shows that PTEN genomic deletion is associated with poor clinical outcome. *Br J Cancer* 2007;97:678–85.
139. Millis SZ, Ikeda S, Reddy S, Gatalica Z, Kurzrock R. Landscape of Phosphatidylinositol-3-Kinase Pathway Alterations Across 19 784 Diverse Solid Tumors. *JAMA Oncol* 2016;0658:1–9.
140. Song MS, Salmena L, Pandolfi PP. The functions and regulation of the PTEN tumour suppressor. *Nat Rev Mol Cell Biol* 2012;13:283–96.
141. Holland AJ, Cleveland DW. Boveri revisited: chromosomal instability, aneuploidy and tumorigenesis. *Nat Rev Mol Cell Biol* 2009;10:478–87.
142. Ding L, Chen S, Liu P, Pan Y, Zhong J, Regan KM, Wang L, Yu C, Rizzardi A, Cheng L, Zhang J, Schmechel SC, et al. CBP Loss Cooperates with PTEN Haploinsufficiency to Drive Prostate Cancer: Implications for Epigenetic Therapy. *Cancer Res* 2014;74:2050–61.
143. Greten TF, Eggert T. Cellular senescence associated immune responses in liver cancer. *Hepatic Oncol* 2017;4:123–7.
144. Squarize CH, Castilho RM, Abrahao AC, Molinolo A, Lingen MW, Gutkind JS. PTEN Deficiency Contributes to the Development and Progression of Head and Neck Cancer. *Neoplasia* 2013;15:461–71.
145. Boussiotis VA. Molecular and Biochemical Aspects of the PD-1 Checkpoint Pathway.

N Engl J Med 2016;375:1767–78.

146. Wilt TJTJ, Brawer MK, Jones KM, Barry MJMJ, Aronson WJWJ, Fox S, Gingrich JRJR, Wei JT, Gilhooly P, Grob BM, Nsouli I, Iyer P, et al. Radical prostatectomy versus observation for localized prostate cancer. *N Engl J Med* 2012;367:203–13.
147. Siegel RL, Miller KD, Jemal A. Cancer Statistics, 2017. *CA Cancer J Clin* 2017;67:7–30.
148. Troyer DA, Jamaspishvili T, Wei W, Feng Z, Good J, Hawley S, Fazli L, McKenney JK, Simko J, Hurtado-Coll A, Carroll PR, Gleave M, et al. A multicenter study shows PTEN deletion is strongly associated with seminal vesicle involvement and extracapsular extension in localized prostate cancer. *Prostate* 2015;75:1206–15.
149. Mithal P, Allott E, Gerber L, Reid J, Welbourn W, Tikishvili E, Park J, Younus A, Sangale Z, Lanchbury JS, Stone S, Freedland SJ. PTEN loss in biopsy tissue predicts poor clinical outcomes in prostate cancer. *Int J Urol* 2014;21:1209–14.
150. Picanço-Albuquerque CG, Morais CL, Carvalho FLF, Peskoe SB, Hicks JL, Ludkovski O, Vidotto T, Fedor H, Humphreys E, Han M, Platz EA, De Marzo AM, et al. In prostate cancer needle biopsies, detections of PTEN loss by fluorescence in situ hybridization (FISH) and by immunohistochemistry (IHC) are concordant and show consistent association with upgrading. *Virchows Arch* 2016;468:607–17.
151. Ali HR, Chlon L, Pharoah PDP, Markowetz F, Caldas C. Patterns of Immune Infiltration in Breast Cancer and Their Clinical Implications: A Gene-Expression-Based Retrospective Study. *PLoS Med* 2016;13:1–24.
152. Pardoll DM. The blockade of immune checkpoints in cancer immunotherapy. *Nat Rev Cancer* 2012;12:252–64.
153. Taylor BBS, Schultz N, Hieronymus H, Gopalan A, Xiao Y, Carver BS, Arora VK, Kaushik P, Cerami E, Reva B, Antipin Y, Mitsiades N, et al. Integrative Genomic Profiling of Human Prostate Cancer. *Cancer Cell* 2010;18:11–22.
154. Robinson D, Van Allen EM, Wu YM, Schultz N, Lonigro RJ, Mosquera JM, Montgomery B, Taplin ME, Pritchard CC, Attard G, Beltran H, Abida W, et al. Integrative clinical genomics of advanced prostate cancer. *Cell* 2015;161:1215–28.
155. Lotan TL, Gurel B, Sutcliffe S, Esopi D, Liu W, Xu J, Hicks JL, Park BH, Humphreys E, Partin AW, Han M, Netto GJ, et al. PTEN protein loss by immunostaining: Analytic

validation and prognostic indicator for a high risk surgical cohort of prostate cancer patients. *Clin Cancer Res* 2011;17:6563–73.

156. Kramer AS, Latham B, Diepeveen LA, Mou L, Laurent GJ, Elsegood C, Ochoa-Callejero L, Yeoh GC. InForm software: a semi-automated research tool to identify presumptive human hepatic progenitor cells, and other histological features of pathological significance. *Sci Rep* 2018;8:1–10.
157. Yoshimoto M, Ding K, Sweet JM, Ludkovski O, Trottier G, Song KS, Joshua AM, E Fleshner N, Squire JA, Evans AJ. PTEN losses exhibit heterogeneity in multifocal prostatic adenocarcinoma and are associated with higher Gleason grade. *Mod Pathol* 2013;26:435–47.
158. Giannakis M, Mu XJ, Shukla SA, Qian ZR, Cohen O, Nishihara R, Bahl S, Cao Y, Amin-Mansour A, Yamauchi M, Sukawa Y, Stewart C, et al. Genomic Correlates of Immune-Cell Infiltrates in Colorectal Carcinoma. *Cell Rep* 2016;15:857–65.
159. Lee SH, Park JS, Byun JK, Jhun J, Jung K, Seo HB, Moon YM, Kim HY, Park SH, Cho M La. PTEN ameliorates autoimmune arthritis through down-regulating STAT3 activation with reciprocal balance of Th17 and Tregs. *Sci Rep* 2016;6:1–11.
160. Curran TA, Jalili RB, Farrokhi A, Ghahary A. IDO expressing fibroblasts promote the expansion of antigen specific regulatory T cells. *Immunobiology* 2014;219:17–24.
161. Xue D, Xia T, Wang J, Chong M, Wang S, Zhang C. Role of regulatory T cells and CD8+ T lymphocytes in the dissemination of circulating tumor cells in primary invasive breast cancer. *Oncol Lett* 2018;16:3045–53.
162. Nardone V, Botta C, Caraglia M, Martino EC, Ambrosio MR, Carfagno T, Tini P, Semeraro L, Misso G, Grimaldi A, Boccellino M, Facchini G, et al. Tumor infiltrating T lymphocytes expressing FoxP3, CCR7 or PD-1 predict the outcome of prostate cancer patients subjected to salvage radiotherapy after biochemical relapse. *Cancer Biol Ther* 2016;17:1213–20.
163. Curiel TJ, Coukos G, Zou L, Alvarez X, Cheng P, Mottram P, Evdemon-Hogan M, Conejo-Garcia JR, Zhang L, Burow M, Zhu Y, Wei S, et al. Specific recruitment of regulatory T cells in ovarian carcinoma fosters immune privilege and predicts reduced survival. *Nat Med* 2004;10:942–9.
164. Hiraoka N, Onozato K, Kosuge T, Hirohashi S. Prevalence of FOXP3+ regulatory T

cells increases during the progression of pancreatic ductal adenocarcinoma and its premalignant lesions. *Clin Cancer Res* 2006;12:5423–34.

165. Sfanos KS, Yegnasubramanian S, Nelson WG, De Marzo AM. The inflammatory microenvironment and microbiome in prostate cancer development. *Nat Rev Urol* 2017;15:11–24.
166. Troutman SM, Price DK, Figg WD. Prostate cancer genomic signature offers prognostic value. *Cancer Biol Ther* 2010;10:1079–80.
167. Abeshouse A, Ahn J, Akbani R, Ally A, Amin S, Andry CD, Annala M, Aprikian A, Armenia J, Arora A, Auman JT, Balasundaram M, et al. The Molecular Taxonomy of Primary Prostate Cancer. *Cell* 2015;163:1011–25.
168. Alexandrov LB, Nik-Zainal S, Wedge DC, Aparicio SAJRJR, Behjati S, Biankin A V., Bignell GR, Bolli N, Borg A, Børresen-Dale A-LL, Boyault S, Burkhardt B, et al. Signatures of mutational processes in human cancer. *Nature* 2013;500:415–21.
169. Muller AJ, DuHadaway JB, Donover PS, Sutanto-Ward E, Prendergast GC. Inhibition of indoleamine 2,3-dioxygenase, an immunoregulatory target of the cancer suppression gene Bin1, potentiates cancer chemotherapy. *Nat Med* 2005;11:312–9.
170. Spranger S, Spaapen RM, Zha Y, Williams J, Meng Y, Ha TT, Gajewski TF. Up-Regulation of PD-L1, IDO, and Tregs in the Melanoma Tumor Microenvironment Is Driven by CD8+ T Cells. *Sci Transl Med* 2013;5:1–10.
171. Dill EA, Dillon PM, Bullock TN, Mills AM. IDO expression in breast cancer: an assessment of 281 primary and metastatic cases with comparison to PD-L1. *Mod Pathol* 2018;31:1513–22.
172. Banzola I, Mengus C, Wyler S, Hudolin T, Manzella G, Chiarugi A, Boldorini R, Sais G, Schmidli TS, Chiffi G, Bachmann A, Sulser T, et al. Expression of indoleamine 2,3-dioxygenase induced by IFN-γ and TNF-α as potential biomarker of prostate cancer progression. *Front Immunol* 2018;9:1–15.
173. Garcia-Diaz A, Shin DS, Moreno BH, Saco J, Escuin-Ordinas H, Rodriguez GA, Zaretsky JM, Sun L, Hugo W, Wang X, Parisi G, Saus CP, et al. Interferon Receptor Signaling Pathways Regulating PD-L1 and PD-L2 Expression. *Cell Rep* 2017;19:1189–201.
174. Haffner MC, Guner G, Taheri D, Netto GJ, Palsgrove DN, Zheng Q, Guedes LB, Kim

K, Tsai H, Esopi DM, Lotan TL, Sharma R, et al. Comprehensive Evaluation of Programmed Death-Ligand 1 Expression in Primary and Metastatic Prostate Cancer. *Am J Pathol* 2018;188:1478–85.

9. ATTACHMENTS

Attachment 1 - Vidotto et al. 2018 – Distinct subtypes of genomic PTEN deletion size influence the landscape of aneuploidy and outcome in prostate cancer Published in *Molecular Cytogenetics*

Attachment 2 – HCRP Ethics Committee Approval

Attachment 3 - Immunohistochemistry and InForm analysis protocol